J. Int. Financ. Markets Inst. Money 85 (2023) 101767

Contents lists available at ScienceDirect

Journal of International Financial Markets, Institutions & Money

journal homepage: www.elsevier.com/locate/intfin

A multifractal model of asset (in)variances

Klaus Grobys [1]

Finance Research Group, School of Accounting and Finance, University of Vaasa, Wolffintie 34, 65200 Vaasa, Finland
Innovation and Entrepreneurship (InnoLab), University of Vaasa, Wolffintie 34, 65200 Vaasa, Finland

ARTICLE INFO

JEL:
C14
C22
C60
G10
G17

Keywords:
Bitcoin
MMAR
Multifractal model of asset invariances
Long memory
Power laws
Hurst exponents

ABSTRACT

This study extends Mandelbrot's (2008) multifractal model of asset returns to model realized variances across different time frequencies. In a comparative manner, various degrees of time deformations are explored for implementation of the multiplicative cascade. In doing so, this study focuses on two effects: *discontinuity* measured by the specific power-law exponent and *dependency* measured by the Hurst exponent. This study shows that the benchmark model, for which Mandelbrot's (2008) "cartoon" is the foundation, has some remarkable properties as it is capable of explaining the realized variances for the GBP/USD exchange rate and Bitcoin. Notably, the realized variances for crude oil and the S&P 500 require a more extreme time deformation. The invariance hypothesis is confirmed for all realized variances because the power-law exponents for weekly and monthly data coincide with predictions of the multifractal model. Overall, the novel results derived from the proposed multifractal models suggest that some realized variances of otherwise unrelated asset markets are driven by the same underlying "driving force"—a common multifractal cascade.

1. Introduction

Segnon and Lux (2013) highlighted that one of the most important tasks in financial economics is modeling price fluctuations of risky assets. The authors pointed out the following:

> For analysts and policy makers volatility is a key variable for understanding market fluctuations. Analysts need accurate forecasts of volatility as an indispensable input for tasks such as risk management, portfolio allocation, value-at-risk assessment, and option and futures pricing. Asset market volatility also plays an important role in monetary policy. Repercussions from the … financial crisis on the global economy show how important it is to take into account financial market volatility in conducting effective monetary policy. (Segnon and Lux, 2013, p. 2)

A well-known and stylized fact of financial markets is volatility clustering—the empirical observation that periods of high and low volatility alternate in a persistent manner. An early and often-cited study by Engle (1982) was the first to address this phenomenon by introducing the so-called autoregressive conditional heteroscedasticity (ARCH) model, which was generalized to GARCH by Bollerslev (1986). As pointed out by Segnon and Lux (2013), these models are designed to capture the dependency structures of the second

E-mail address: klaus.grobys@uwasa.fi.

[1] This research article was presented at the 2022 Finance Research Seminar of the Chair of Monetary Economics and International Finance, Christian-Albrechts-University (CAU) of Kiel. The author is thankful for having received valuable comments from Thomas Lux, Cristina Sattarhoff, and Lutz Honvehlmann. The author is thankful for having received valuable comments from two anonymous reviewers.

https://doi.org/10.1016/j.intfin.2023.101767
Received 10 January 2023; Accepted 30 March 2023
Available online 13 April 2023

moment in a phenomenological way by modeling returns as a mixture of normals, with the current variance being driven by a deterministic difference equation. Different derivatives of the original GARCH model have been discussed in the literature with the objective to better capture the stylized facts.[2] Despite the GARCH model framework's appealing structure prima facie, Mandelbrot (2008) argued that

> GARCH is, certainly, a handy abacus now used by many option traders and finance directors trying to model risk. But it begs the question of what makes the bell [curve] vibrate. And as you try to work with the model, it becomes increasingly complicated. To say much with little: Such is the goal of good science. But most established financial models say little with much. They input endless data, require many parameters, take long calculation. When they fail by losing money, they are seldom thrown away as a bad start. Rather they are "fixed." They are amended, qualified, particularized, expanded, and complicated … That people still lose money on these models should come as no great surprise. (Mandelbrot, 2008, p. 222)

In view of Mandelbrot's (2008) argument, Segnon and Lux (2013) concluded that

> … one might follow Mandelbrot's frequently voiced methodological premise to model apparently generic features of data by similarly generic models rather than using "fixes" (Mandelbrot, 1997a). Introducing amendments to existing models (e.g., GARCH, SV) to adapt those to new stylized facts might lead to highly parameterized setups that lack robustness when applied to data from different markets, while simple generating mechanisms for multifractal behavior are available that could, in principle, capture the whole spectrum of time series properties highlighted above in a more parsimonious way. In addition, if one wants to account for multi-scaling proper (rather than as a spurious property) no avenue is known so far for equipping GARCH- or SV-type models with this property in a generic way. Hence, adapting in an appropriate way some known generating mechanism for multifractal behavior appears the only avenue available so far to come up with models that generically possess such features, and jointly reproduce all stylized facts of asset returns.

Motivated by this literature, this study proposes a model for the second moment of financial assets based on realized variances. Following Mandelbrot, we use a multifractal framework for modeling the return processes of financial assets. To deform clock time into trading time, we employ binominal bending of time to compound the multiplicative cascade which is the foundation for the multifractal model. The multifractal process is obtained by combining the multifractal cascade and a normally distributed random variable in a multiplicative manner. Interpreting the model's output as an asset return–generating process, we sum the squared returns of 5 and 20 consecutive, nonoverlapping trading days to compute weekly and monthly realized variances. We simulate 1000 time paths to explore the model's statistical properties. For each simulation, we estimate both the power-law exponent and Hurst exponent to assess the tail properties and dependency structure, respectively. This allows us to assess whether the model can capture stylized facts of financial market fluctuations in a parsimonious model framework. As Mandelbrot pointed out that the multiplicative cascade is of fundamental importance for generating multifractality, we explore various types of binominal bending and reassess the model properties.

Moreover, we assess whether the models generate multifractality across time dimensions by studying the weekly and monthly models in a comparative manner. We hypothesize that a correctly specified model should generate tail properties and dependency structures that are stable across time dimensions. Another novelty of this study is that it investigates in more detail the dependency structure for observations governed by a power-law process. Specifically, the power-law null hypothesis per se only suggests that observations exceeding a certain threshold are governed by a power law, but it does not provide any answer concerning how those observations are distributed across the simulated time-series data. Therefore, to investigate the dependency structure of the Paretian tail, we record for all simulated data series the maximum time length of consecutive observations governed by a power-law process and propose a test that assumes independency under the null hypothesis. A rejection of the null hypothesis would suggest a clustering of power-law observations, which would be in line with the stylized, empirical fact of volatility clustering in financial data.

This study contributes to the existing literature in some important ways. First of all, GARCH models are designed to model the variance of assets by parametrizations. However, Segnon and Lux (2013) argued that introducing extensions to existing GARCH-type models might lead to highly parameterized setups that lack robustness when applied to data from different markets. Also, Mandelbrot (2008) criticized the problem of changing parameters obtained from GARCH-type models, arguing that "… many recent models of price variation try to explain the obviously shifting pattern of volatility by inserting parameters that change by the day, hour, and second; such are the GARCH family mentioned earlier." In contrast to GARCH-type models, the multifractal framework works with just a set of a few consistent parameters that remain constant over time and place. We contribute to the literature on modeling uncertainty in financial markets by proposing a multifractal model for asset variances and test the invariance phenomenon across different time scales.

Moreover, in a recent study, Grobys, Junttila, Kolari, and Sapkota (2021) analyzed the volatility processes of so-called "stable cryptocurrencies" or "stablecoins" and their potential stochastic interdependencies with Bitcoin volatility. Using realized volatilities,

[2] Extensions of GARCH with the objective to better capture the stylized facts of financial volatility are, for instance, the exponential GARCH (EGARCH) model proposed by Nelson (1991), which accounts for asymmetric behavior of returns, the threshold GARCH (TGARCH) model of Rabemananjara and Zakoian (1993) addressing leverage effects, the regime-switching GARCH (RS-GARCH) proposed by Cai (1994), and the integrated GARCH (IGARCH) introduced by Engle and Bollerslev (1986), which allows for capturing high-volatility persistence. Moreover, the Itô diffusion or jump-diffusion processes can be retrieved as a continuous time limit of discrete GARCH sequences [see Nelson (1990) and Drost and Werker (1996)].

the authors tested the power-law null hypothesis for both stablecoin and Bitcoin volatilities. The study found strong evidence for Paretian tails in the volatility processes of all tested cryptocurrencies. Another study by Grobys (2021) used the realized variances for five different asset markets to test the power-law null hypothesis. In line with Grobys et al. (2021), Grobys (2021) found strong evidence for Paretian tails across all asset market variances. The novel aspect of this work is that it models the second moment of financial asset markets using a realized-variance approach as opposed to using GARCH-type models. In both studies, the variance of variance did not exist in any of those asset markets. Hence, it should not come as a surprise that parameter estimates retrieved from GARCH-type models are subject to sample specificity, as pointed out by Grobys (2021). The current study extends this research by proposing a model that could generate the underlying process of realized asset market variances. In this regard, Mandelbrot (2008) highlighted that a

> … model must work two ways, forward and backward. Forward means that we should be able to construct artificial price charts from the fractal seeds … Backwards means that we should be able to take raw price data, analyze it on our computers, and estimate the key parameters that the multifractal model requires. Then using those values, we should be able to tell the computer to reconstitute the market – to generate an artificial price series that differs from the real one but follows the same statistical pattern. (Mandelbrot, 2008, p. 220)

While earlier research focused only on revealing the tail properties of the second moment of financial assets (that is, markets), one novel aspect of this study is that it takes both perspectives—forward and backward—and in doing so, it focuses on exploring the key parameters measuring the exposure to extreme events in the realized-variance processes and the long-term dependency structure.

Next, in the wake of Mandelbrot, Fisher, and Calvet's (1997b) study, which laid the foundation for multifractal models, the literature on multifractal models is still in an emerging phase. It is surprising to note that Segnon and Lux (2013) documented that Mandelbrot et al.'s (1997b) paper has not been published in a journal—despite its impact. Furthermore, Segnon and Lux (2013) pointed out that multifractal measures have been adapted to asset-price modeling by employing them as a stochastic clock to transform chronological time into trading time, that is, business time. Whereas Mandelbrot et al. (1997b) proposed binominal bending of time to deform chronological time into trading time, Calvet and Fisher (2002) discussed time deformations derived from lognormal, Poisson, and gamma distributions. Other time transformations have been discussed by Muzy and Bacry (2002), Bacry, Kozhemyak, and Muzy (2008), and Calvet, Fisher, and Wu (2018), for instance. An interesting and detailed overview on the relevant literature was provided by Segnon and Lux (2013). In view of this literature, the current study is the first to extend the multifractal framework to first (*i*) model realized-variance processes of financial assets, second (*ii*) to provide simulation-based evidence for some key metrics, and third (*iii*) to evaluate the model's performance using real-life financial market data. The concept of realized variance or volatility was developed by Andersen, Bollerslev, Diebold, and Labys (2001) as an alternative measure of the variability of asset prices and is considered a consistent and highly efficient nonparametric estimator. Whereas the literature has derived second-moment implications from multifractal models for asset returns, there is no study available that explores the properties of a multifractal model for realized asset variances derived from a simulation-based setting. In view of the recent literature exploring the power-law properties of realized variances/volatilities (Grobys et al., 2021; Grobys, 2021, 2023; Grobys and Kolari, 2022), this is a timely topic that demands further investigation. The current study remedies this gap in the literature.

A minor contribution of this study is that it takes a novel view on the persistence of power laws in variances. The power-law null hypothesis only suggests that observations exceeding a certain threshold are governed by a power law, but it is silent on how the observations are distributed across the data. The observations governed by a power law can be distributed evenly across the data sample observations or they can cluster together. This study derives a test that is valid even in the presence of an infinite variance of variance. In a sense, this test can be considered another approach to test for volatility clustering in financial data. An earlier contribution in this field of research is, for instance, the work of Hsiao and Li (2001), who besides provided an interesting literature review. This body of research studies, however, is based on asset returns as opposed to realized asset variances, and it does not account for documented recent evidence that the variance of variance is infinite (Grobys et al., 2021; Grobys, 2021, 2023; Grobys and Kolari, 2022), thereby rendering *t*-statistics derived from regression model–based tests invalid. The proposed test for dependency in this study is valid even in research environments where the variance of variance does not exist.

The results of the study show that realized variances based on the multifractal model are governed by Paretian tails and exhibit long-term dependencies that vary with respect to the multiplicative cascade chosen. The simulated benchmark model using binominal bending with probabilities $p = 0.60$ and $(1-p) = 0.40$, as proposed by Mandelbrot (2008), produces Paretian tails for the weekly variances exhibiting an average tail exponent of $\alpha = 2.6112$ with standard deviation of 0.3812. Using a more moderate binominal bending employing $p = 0.55$ and $(1-p) = 0.45$ produces Paretian tails for the weekly variances exhibiting an average tail exponent of $\alpha = 3.7216$ with a standard deviation of 0.6658, whereas a more extreme binominal bending using $p = 0.65$ and $(1-p) = 0.35$ produces Paretian tails for the weekly variances exhibiting an average tail exponent of $\alpha = 2.1253$ with a standard deviation of 0.2863. Using monthly variances, we find that the average tail exponents fall into the 95% confidence interval for weekly data, suggesting scale invariance, which strongly supports Grobys' (2021) recent finding of the scale invariance of the S&P 500 realized variances.

The multifractal models show that Hurst exponents do not appear to relate to the power-law exponent given each multifractal cascade. However, taking a coarse-grained perspective, the evidence suggests a strong link between binominal bending and dependency structures: the more extreme the time deformation, the more persistent the realized variance, irrespective of which time frequency (viz., weekly or monthly) is considered. Indeed, using weekly data the estimated correlation between average power-law exponent and average Hurst exponent across different models is -0.9781; that is, the more extreme is the bending of time, the more extreme is the variance's discontinuity and the more extreme is the level of persistence. We interpret this as strong evidence for different multiplicative cascades indeed producing very distinct stochastic processes as defined in terms of their discontinuities and dependency structures.

This strongly supports Mandelbrot's (2008) argument that the power-law exponent and the Hurst exponent are in a dual relationship manifested in a negative correlation between Hurst exponent and power-law exponent. Persistence is also measured by the maximum number of consecutive observations in which a variance process remains in a power-law regime. The findings indicate that there is a clear link between power-law exponent and this measure for persistence: the lower the economic magnitude of the power-law exponent, the longer the observed maximum time length in which some process remains in the power-law regime. This result holds for both *within* each multifractal model itself and *across* different analyzed multifractal models.

Comparing the multifractal models with weekly and monthly realized variances for the GBP/USD exchange rate, Bitcoin, crude oil, and the S&P 500 indicates that the benchmark model used in this study—which is based on a multiplicative cascade proposed by Mandelbrot (2008) using binominal bending with $p = 0.60$ and $(1 - p) = 0.40$—is capable of explaining the asset market variances for the GBP/USD exchange rate and Bitcoin in terms of their tail characteristics and dependency structures as measured by the individual power-law exponent and Hurst exponent, respectively. It also predicts that the variances of variances do not exist for weekly data. Notably, using daily data, the nonexistence of the variance of variance for key financial markets was documented in a recent study (Grobys, 2021). Also, Grobys et al. (2021) found that the variances of daily Bitcoin and stablecoin volatilities are undefined, whereas Grobys (2023) and Grobys and Kolari (2022) found that that variances of variances do not exist for the vast majority of realized G10 currencies, irrespective of the time frequency considered. Further evidence suggests that the asset market variances for crude oil and the S&P 500 are rather explained by a common multifractal model based on a multiplicative cascade derived from binominal bending with $p \approx 0.70$ and $(1 - p) \approx 0.30$ due to their unbounded behavior manifested in Hurst exponents > 1. This result supports Sun and Zhou (2014) who documented that fitted GARCH models to S&P 500 data are Near-IGARCH.

A remarkable commonality of the multifractal variance models explored here is that the average power-law exponents for monthly variances are higher in their economic magnitude than the corresponding figures for weekly data. Still, the average power-law exponents for monthly variances remain clearly in the 95% confidence interval for the power-law exponents based on weekly data. This result lines up with those of Mandelbrot (2008, p. 218), who argued that "the Noah effect is fading, that is, price variability settles down as lower time frequencies are employed." We show that the same patterns are observed for both synthetic and real-life data. Therefore, our multifractal model framework offers a possibility for testing the invariance hypothesis, an important implication being that even though variances appear to be "less wild" at lower time frequencies, the invariance hypothesis cannot necessarily be rejected. Indeed, the results documented in this study provide strong evidence for invariance across asset market variances' time frequencies.

This study is organized as follows: the next section provides a literature review and the third section describes the methodology. The fourth section presents the results, the fifth section presents a discussion, and the last section concludes the study.

2. Literature review

In his seminal paper published in 1982 in the well-recognized journal *Econometrica*, Robert Engle proposed autoregressive conditional heteroscedasticity (ARCH) models to model the time-varying variance process of inflation in the U.K. A simple ARCH-type model is given by,

$$RET_{i,t} = c_i + u_{i,t}$$

$$u_{i,t} = \sigma_{i,t}\epsilon_{i,t}$$

$$\sigma_{i,t} = \sqrt{\delta_0 + \delta_1 u_{i,t-1}^2 + \cdots \delta_p u_{i,t-p}^2}$$

$$\epsilon_{i,t}\ N(0,1)$$

where $RET_{i,t}$ denotes the return of asset i at time t, $\sigma_{i,t}$ denotes the asset's conditional volatility, c_i, δ_0, δ_1, …, δ_p are model parameters, and the innovation process $\epsilon_{i,t}$ is typically assumed to be normally distributed.[3] This ARCH model accounts for a lag-order of p. Generally speaking, a higher lag-order implies a higher level of persistence in the conditional variance process. The ARCH model has been generalized (e.g., GARCH) in a study of Bollerslev (1986) by incorporating a moving average component together with the autoregressive component. As of now, the studies of Engle (1982) and Bollerslev (1986) have been cited more than 32,000 times. In fact, Sornette (2017) and Sun and Zhou (2014, p. 287) argue that the plain GARCH(1,1) model has become the industry standard, respectively "workhorse in both academic and practice due to its simplicity and intuitive interpretation." The original models have been extended in several ways. For instance, an important and often-used extension of the plain GARCH model is the threshold GARCH (e.g., TGARCH) model proposed by Glosten, Jagannathan, and Runkle (1993). Unlike the original GARCH model, the TGARCH model is capable of addressing the empirical fact that bad news has a greater impact on the uncertainty than good news by adding an additional regressor to the variance equation. Similarly, using the exponential GARCH (e.g., EGARCH) model, as proposed by Nelson (1991), one is able to test whether bad news has a greater impact on the conditional variance than good news. Unlike GARCH or TGARCH models, EGARCH models have the advantage that the variance will be positive even if some model parameters were negative. A recent study from Chalissery, Anagreh, Nishad, and Tabash (2022) conducts a comprehensive review on the relevant GARCH model

[3] For instance, Sun and Zhou (2014, p. 288) highlight that "the most often applied GARCH(1,1) model assumes that the innovation term follows a standard normal distribution."

literature using bibliometric analysis to identify the models' key foundations and evolution.

Unsurprisingly, Mandelbrot (2008, p. 222) terms GARCH model extensions "fixes" and argues that these fixes become "increasingly complicated" and "say little with much." Perhaps, the main problem with GARCH-type models is sample-specificity. Depending on the chosen sample period, parameter estimates can vary by a substantial margin. For instance, in an early paper, Chu (1995) tested for parameter constancy in the variance equations of GARCH models. Using S&P 500 data the study's findings indicated that the hypothesis of stable conditional variance parameters could be rejected. The sample-specificity could be a manifestation of non-normality in the innovation process. As pointed out from Lundbergh and Teräsvirta (2002, p. 418), "Very often in applications, the assumption of a normal error distribution of a GARCH process is too restrictive." In this regard, Sun and Zhou (2014) highlight that a well-established stylized fact, documented in the empirical literature on risk management, is that the conditional normality assumption performs poorly in evaluating the downside risk of financial time series.

The establishment and subsequent evolution of econometric models derived under the assumption of normally distributed data is indeed a surprising issue–especially given the well-known empirical fact that financial markets are subject to reoccurring extreme events. Already in his 1963 paper entitled "New methods in statistical economics" published in the *Journal of Political Economy*, Benoit Mandelbrot introduced power laws in an effort to address the problem of extreme events in economic data.[4] Power laws are essentially Pareto type distributions which make large standard deviations from the mean possible though rare. Surprisingly, Vilfredo Pareto formalized his distributional law governing wealth distribution–often referred to as the "Pareto Law" or "80/20 rule"–much earlier in 1897 in the same journal.[5] In a second 1963 paper, Mandelbrot showed that cotton price changes are governed by a power-law process.[6] The evidence strongly suggested that the theoretical variance of cotton price changes is undefined, respectively, infinite. West (2017, p. 142) highlights that Mandelbrot's findings have "stimulated the development of a new transdisciplinary subfield of finance called *econphysics* and motivated investment companies to hire physicists, mathematicians, and computer scientists to use these sorts of ideas to develop novel investment strategies." It is interesting to note that Fama (1963) reviewed Mandelbrot's proposition and commented that:

> … the infinite variance assumption of the stable Paretian model has extreme implications. From a purely statistical standpoint, if the population variance of the distribution of first differences is infinite, the sample variance is probably a meaningless measure of dispersion. Moreover, if the variance is infinite, other statistical tools (e.g., least-squares regression) which are based on the assumption of finite variance will, at best, be considerably weakened and may in fact give very misleading answers. (Fama, 1963, p. 421)

Despite knowing about the problems associated with financial analysis based on Gaussian frameworks, most finance researchers (including Fama who was Mandelbrot's doctoral student) continue to use and propose statistical techniques (including GARCH-type models) based on the assumption that the variance is finite.

On the other hand, and as pointed out by West (2017), another branch of literature emerged consistent with Mandelbrot's ideas that incorporated power laws in financial research. Important contributions are, for instance, Gopikrishnan et al. (1999), Jansen and de Vries (1991), Mantegna and Stanley (1995) and Lux (1996). Because power laws are typically one-sided distributions, most studies employed the absolute amount of financial returns (or $|ret|$) to model power law functions.[7] Using the notation $Pr(|ret|\rangle x) \approx x^{-\alpha}$, where *ret* describes a financial return, Lux and Alfarano (2016) inferred from studies on power laws in financial market data over 30 years that researchers gradually converged on an exponent greater than 2 and close to 3. They concluded that the long-standing Levy hypothesis should be rejected due to the more precipitous decay of the outer part of the distribution than allowed by this family of distributions.

Whereas this strand of literature provided strong evidence for power-law behavior across various types of financial market data, Mandelbrot et al.'s (1997b) study was the first addressing the issue that a model must work two ways, forward and backward, as highlighted in Mandelbrot (2008). Indeed, Mandelbrot et al.'s (1997b) proposed MMAR can be used to construct artificial price charts from some fractal seeds and raw price data can be subsequently analyzed by estimating the key parameters that the multifractal model requires. Employing those values, the market behavior can be reconstituted, that is, artificial price series can be generated that differ from the real data but follow the same stochastic pattern. As mentioned earlier, the literature on multifractal models is still in an emerging phase. As pointed out in Mandelbrot (2008), the multiplicative cascade is of fundamental importance for constructing multifractal models. Whereas Mandelbrot et al. (1997b) and Mandelbrot (2008) employed binominal bending of time for time deformation, other approaches to deform time have been intensively discussed in the literature (Calvet and Fisher, 2002; Muzy and Bacry, 2002; Bacry, Kozhemyak, and Muzy, 2008; Calvet, Fisher, and Wu, 2018). However, this study follows Mandelbrot et al. (1997b) and Mandelbrot (2008) in constructing a multiplicative cascade derived from binominal bending. Considering the distribution of commodities, and using gold as an example, the intuition of making use of binominal bending is described in Mandelbrot (2008) as follows:

> Fractals are not about the "things" themselves but about their common property of roughness. This is not a farfetched but an apt idea, because, obviously, gold is not distributed evenly around the world. It clusters here and there–just the way the action in

[4] Mandelbrot (1963a).
[5] Pareto (1897).
[6] Mandelbrot (1963b).
[7] Studies by Gabaix (2009) and Lux and Alfarano (2016) provide excellent surveys of this literature.

> financial markets clusters into different stretches of time. We can mimic that effect mathematically. Pull out a map of gold-rich South Africa, specifically, a cross-section of the earth there along the west-to-east line. Start with a low-resolution map that divides the country into two pieces, one east and one west. About 60 percent of the gold ore lies in the western half, and about 40 percent in the east. Look more closely: Cut each half into halves again. Finer processes concentrated 60 percent of the western gold into the westernmost quarter–or 36 percent of the total gold deposits […] (Mandelbrot, 2008, p. 216)

It becomes evident that the distribution of important natural resources is based on some binominal bending. Here, the multiplicative cascade proposed in Mandelbrot (2008) is extended by accounting for various types of time deformation allowing for either *less* time concentration or *more* time concentration because the way how extreme time stretches may deviate across different financial asset markets.

3. Methodology

The early study by Mandelbrot et al. (1997b) was the first to introduce the multifractal model of asset returns (MMAR). Mandelbrot (2008) discussed a simplified version of the MMAR that uses binominal bending of time to compute the multiplicative cascade serving as multifractal time, or the "multifractal father," and a Brownian motion serving as the "multifractal mother." The "baby theorem" describes the derivation of the "multifractal baby" as the product of the multifractal mother and multifractal father as follows:

$$y(t) = c(t)x(t) \tag{1}$$

where $c(t)$ is the multiplicative cascade at time t and $x(t) \sim \ IIDN(0,1)$. Advocating binominal bending of time, we follow Mandelbrot (2008) and use probability $p = 0.60$ and $(1-p) = 0.40$ for deriving deformed time. Fig. A.1 in the appendix shows the first three iterations of the binominal tree used in the first step. As shown in Fig. A.1, in each iteration, each figure is multiplied with $p = 0.60$ and $(1-p) = 0.40$. Fig. A.2 in the appendix illustrates how the binominal tree illustrated in Fig. A.1 is transformed into trading time by multiplying each figure by the number of elements in each iteration. For instance, considering the second iteration, the vector for the deformed trading time (1.44, 0.96, 0.96, 0.64) is retrieved by multiplying (0.36, 0.24, 0.24, 0.16) with 4. In this study, we use $k = 13$ iterations, giving us $2^{13} = 8192$ observations for vector $\boldsymbol{c}$. Note that for the number of generated observations, $N \in (2^k | k \in \mathbb{N})$ must hold.[8] We use the first 5120 observations of vector $\boldsymbol{c}$ and construct 1000 5120×1 vectors of multifractal asset returns by multiplying elements $c(1), c(2), \ldots, c(5120)$ with drawings from the standard normal distribution. This procedure gives us, in turn, 1000 vectors for $\boldsymbol{y}$, each with the dimension 5120×1. We store the drawings for vectors $\boldsymbol{x}_1, \boldsymbol{x}_2, \ldots, \boldsymbol{x}_{1000}$ and $\boldsymbol{y}_1, \boldsymbol{y}_2, \ldots, \boldsymbol{y}_{1000}$ in matrices $\boldsymbol{X}$ and $\boldsymbol{Y}$, defined as $\boldsymbol{X} = (\boldsymbol{x}_1, \boldsymbol{x}_2, \ldots, \boldsymbol{x}_{1000})$ and $\boldsymbol{Y} = (\boldsymbol{y}_1, \boldsymbol{y}_2, \ldots, \boldsymbol{y}_{1000})$. Note again that all vectors $\boldsymbol{y}_1, \boldsymbol{y}_2, \ldots, \boldsymbol{y}_{1000}$ use the same multiplicative cascade $\boldsymbol{c}$.

Next, we compute the weekly variance by squaring each element in $\boldsymbol{y}_i$ and then summing five consecutive, nonoverlapping elements, such as

$$\boldsymbol{z}_i^W = \left(\sum_{t=1}^{5} y_{t,i}^2, \sum_{t=6}^{10} y_{t,i}^2, \cdots, \sum_{t=5116}^{5120} y_{t,i}^2 \right)' \tag{2}$$

where $\boldsymbol{z}_i^W$ has the dimension 1024×1 and $i = 1, \cdots, 1000$. In the same manner, the monthly variance is calculated by squaring each element in $\boldsymbol{y}_i$ and then summing 20 consecutive, nonoverlapping elements, such as

$$\boldsymbol{z}_i^M = \left(\sum_{t=1}^{20} y_{t,i}^2, \sum_{t=21}^{40} y_{t,i}^2, \cdots, \sum_{t=5101}^{5120} y_{t,i}^2 \right)' \tag{3}$$

where $\boldsymbol{z}_i^M$ has the dimension 256×1 and $i = 1, \cdots, 1000$. Obviously, the approach we choose to compute the variances is based on realized variances. Using realized variance or volatility to model uncertainty in financial markets has some important advantages. Apart from being a highly efficient estimator of the underlying true return variation, as pointed out by Segnon and Lux (2013), Wang and Yang (2009, p. 600) documented that "… a realized-volatility-based approach is able to uncover volatility features (asymmetric volatility in particular) that the conventional GARCH type models fail to reveal."

The realized variances are mainly explored with respect to their two forms of wild variability. As pointed out by Mandelbrot (2008), the first wild trait that financial markets have in common is *abrupt change* or *discontinuity*. A typical example often referred to is the 29.2% market collapse of the U.S. equity market occuring on October 1987, which "arrived without warning or convincing reason; and at the time, it seemed like the end of the financial world" (Mandelbrot, 2008, p. 200). This effect is manifested in a Paretian tail; that is, the tail of financial markets is governed by individual power-law processes measured by the individual power-law exponent. To investigate this effect, which Mandelbrot termed the "Noah-effect," for each vector $\boldsymbol{z}_i^W$ and $\boldsymbol{z}_i^M$, we use the following model:

$$p(z) = Bz^{-\alpha} \tag{4}$$

where $B = (\alpha - 1)z_{MIN}^{\alpha - 1}$ with $\alpha \in \{\mathbb{R}_+ | \alpha > 1\}$, $z \in \{\mathbb{R}_+ | z_{MIN} \leq z < \infty\}$, z_{MIN} is the minimum value of realized-variance observations

[8] The motivation for the choice of 2^{13} will become evident to the reader later. Note that for the number of generated observations, $N \in (2^k | k \in \mathbb{N})$ must hold.

governed by the power law, and α is the magnitude of the tail exponent.[9] Moreover, to ensure better readability, we drop indices in the notation here, so z can be either z_i^W or z_i^M. It can be shown that the conditional first moment, or $E[Z|Z \geq z_{MIN}]$, is given by

$$E[Z|Z \geq z_{MIN}] = \int_{z_{MIN}}^{\infty} zp(z)dz = \frac{(\alpha-1)}{(\alpha-2)} z_{MIN} \tag{5}$$

whereas the conditional second moment, or $E\left[Z^2|Z \geq z_{MIN}\right]$, is defined as

$$E\left[Z^2|Z \geq z_{MIN}\right] = \int_{z_{MIN}}^{\infty} z^2 p(z)dz = \frac{(\alpha-1)}{(\alpha-3)} z_{MIN}^2 \tag{6}$$

and conditional higher moments of order k are analogously defined as

$$E\left[Z^k|Z \geq z_{MIN}\right] = \frac{(\alpha-1)}{(\alpha-1-k)} z_{MIN}^k \tag{7}$$

From Equations (5) or (7), we see that the conditional mean only exists for $\alpha > 2$, whereas the conditional variance only exists for $\alpha > 3$. Following White, Enquist, and Green (2008) and Clauset et al. (2009), we employ maximum likelihood estimation (MLE) and estimate the tail exponent as

$$\widehat{\alpha} = 1 + N\left(\sum_{i=1}^{N} \ln\left(\frac{z_i}{z_{MIN}}\right)\right)^{-1} \tag{8}$$

where $\widehat{\alpha}$ denotes the MLE estimator, and N denotes the number of sample observations exceeding z, that is, $z_i \geq z_{MIN}$. As seen from Equations (4) to (8), minimum value z_{MIN} is essential for the calculation of the power-law exponent. A question concerns which MLE estimator $\widehat{\alpha}$ in association with z_{MIN} is most accurate in describing the data-generating processes for the variances. Following Clauset et al. (2009), we estimate lower threshold z_{MIN} by making use of the Kolmogorov-Smirnov (KS) approach. This statistic is simply the maximum distance, D, between the data and fitted cumulative density functions (CDFs), given by

$$D = MAX_{z \geq z_{MIN}} |S(z) - P(z)| \tag{9}$$

where $S(z)$ is the CDF of the data for the observation with a value of at least z_{MIN}, and $P(z)$ is the CDF for the power-law model that best fits the data in the region of $z \geq z_{MIN}$. The estimate of z_{MIN} is the value of $\widehat{z}_{MIN}$ that minimizes D. The question arises, then, whether the power-law model is reasonable.

To investigate this issue, we follow Clauset et al. (2009) in employing the estimated parameter vector $(\widehat{\alpha}, \widehat{z}_{MIN})$, which is optimal with respect to D in a goodness-of-fit (GoF) test, thereby generating a p-value that quantifies the plausibility of the power-law null hypothesis. Specifically, this test compares D from Equation (9) with distance measurements for comparable synthetic data sets drawn from the hypothesized model. The p-value is defined to be the fraction of synthetic distances that are longer than the empirical distance. Given a significance level of 5%, the power-law null hypothesis is not rejected, as the difference between the empirical data and the model can be attributed to statistical fluctuations alone.[10]

Note that Mandelbrot (2008) highlighted that "… economics is different. It lacks unquestioned mathematical laws to rely upon. Also, time, not space, is the scaling factor" (Mandelbrot, 2008, p. 169). If asset variances were scaled in time, we would expect weekly asset variances and monthly asset variances to exhibit the same scaling factor as measured by power-law exponent α. This phenomenon is often referred to as (scale) invariance. Therefore, to explore the invariance phenomenon, we fit the model defined in Equation (4) to both data frequencies, weekly and monthly.

Furthermore, Mandelbrot (2008) argued that the second wild trait that financial markets have in common is "*long-range dependence* in an otherwise random process – or, put another way, a long-term memory through which the past continues to influence the random fluctuations of the present" (Mandelbrot, 2008, p. 201). To investigate this effect, termed by Mandelbrot the "Joseph effect," we employ detrended fluctuation analysis (DFA) as proposed first by Peng, Buldyrev, Havlin, Simons, Stanley, and Goldberger (1994) which has the principal virtue that, in contrast to many common statistical tests, it makes no assumption about how the original data are organized which is a critical point when studying financial data for which evidence abounds that the conventional assumptions are flatly wrong.

The DFA approach to derive the Hurst exponent can be summarized as follows: First, data series z_t is converted to the mean-centered cumulative sum:

$$\widetilde{z}_t = \sum_{t=1}^{T} z_t \tag{10}$$

[9] We follow the notations of Clauset et al. (2009).
[10] The GoF test is detailed in Clauset et al. (2009).

Then different time scales k are defined, that is, $k \in \{4, 8, 16, 32, 64, 128, 256, 512\}$ for weekly data and $k \in \{4, 8, 16, 32, 64, 128\}$ for monthly data. Depending on the defined time scale, data is split into epochs and for each epoch s, a time series regression is used to detrend the data. For instance, employing $k = 512$ means that weekly data for $\widetilde{z}_t$ is split into two non-overlapping epochs. For each epoch s, the following regression is employed:

$$\widetilde{z}_t = \gamma_0 + \gamma_1 t + e_t \tag{11}$$

where $t = 1, \cdots, 512$ for the first epoch and $t = 513, \cdots, 1024$ for the second epoch. Then for each respective epoch s, the root mean squared error (RMSE) is computed as:

$$RMSE_S = \sqrt{\frac{1}{T_s}\sum_{t}^{T_s} \widehat{e}_t} \tag{12}$$

where $T_s = 512$. Finally, the estimates for $RMSE_S$ are averaged for each time scale k, giving us $\overline{RMSE}_k$. According to the corresponding theory, the following relation holds:

$$\overline{RMSE}_k = ck^H \tag{13}$$

The Hurst exponent is then estimated by computing a linear fit between log-scales and log-$\overline{RMSE}_k$.

If the data were independent, the ratio between numerator and denominator should be, according to the theory, 1:2, corresponding to a Hurst exponent of $H = 0.50$. Moreover, $H > 0.50$ implies long-term dependence, that is, a long memory of the stochastic process in which the data are persistent; on the other hand, $H < 0.50$ implies antipersistence, which is characterized by the tendency to keep back on themselves.[11]

As in the return process, multifractality implies that the variance process exhibits a Paretian tail. The question arises, however: how are those observations for which $z \geq z_{MIN}$ holds distributed across time? In traditional finance, an often-discussed phenomenon is that of volatility clustering, meaning that periods of low and high volatility are persistent. We argue that in a multifractal framework, the presence of volatility clustering is manifested in observations governed by a power-law regime; that is, observations for which $z \geq z_{MIN}$ holds occur in clusters. If $z \geq z_{MIN}$ were independently distributed across the support of z, the observations should be distributed across the sample with respect to the percentage of power-law observations. To test this issue, we code vectors of binary variables. Specifically, vector $\boldsymbol{d}_i^W$ has a value of 1if $z \geq z_{MIN}$ holds for observations in z_i^W and values of 0 otherwise. Likewise, vector $\boldsymbol{d}_i^M$ has a value of 1if $z \geq z_{MIN}$ holds for observations in z_i^M and values of 0 otherwise. Summing the values in $\boldsymbol{d}_i^W$ and $\boldsymbol{d}_i^M$ and dividing the sum by the number of observations (e.g., 1024 or 256) gives us the percentage of power-law observations in a given process z_i^W or z_i^M, respectively. We can interpret this figure as empirical probability and denote it as θ.

Next, we can store the time length of each cluster in vectors $\boldsymbol{d}_i^W$ and $\boldsymbol{d}_i^M$. To provide a concrete illustrative example, binary vector $\boldsymbol{d}_a^W = (0, \cdots 0, 1, 1, 1, 0, \cdots 0, 1, 0, \cdots, 0, 1, 1, 1, 1, 1, 0, \cdots 0, 1, 0, \cdots 0)$ would give us (3,1,5,1), where the maximum time length is equal to 5. Let us define the operator $TL(.)$ that sums consecutive values of 1 in a binary vector and stores them in another vector such as $TL\left(\boldsymbol{d}_a^W\right) = (3, 1, 5, 1)$. In the same manner, for each vector $\boldsymbol{d}_i^W$ or $\boldsymbol{d}_i^M$, we can compute the maximum time lengths of consecutive observations (e.g., clusters) that obey a power-law regime. In the illustrative example mentioned above, we then can ask how likely it is to observe five consecutive observations in a power-law regime given probability θ. Assuming independence under the null hypothesis, we would not reject the null hypothesis if and only if $\theta^{MAX\left(TL\left(\boldsymbol{d}_i^W\right)\right)} > 0.05$. [12] However, a rejection of the null hypothesis implies clustering of power-law observations corresponding to volatility clustering simply because the probability to observe such a long cluster of observations governed by different processes (e.g., a power-law process) in a given distribution governed by two distinct probability distributions purely by chance would be <5%.

Finally, Mandelbrot (2008) highlighted the importance of the multiplicative cascade, which has the purpose to transform clock time into multifractal trading time by many repeated multiplications. Following Mandelbrot (2008), we use as a benchmark model for the binominal bending of time probability $p = 0.60$ and $(1-p) = 0.40$ in association with 13 iterations for deriving deformed time. Mandelbrot (2008) noted the following:

> In fractal analysis, time is flexible. The multifractal model describes markets as deforming time – expanding it here, contracting it there. The more dramatic the time changes, the more the trading time-scale expands. The duller the price chart, the slower runs the market clock. Some researchers have tried linking this concept to trading volume: High volume equals fast trading time.

[11] It becomes evident that $k \in (2^r | r \in \mathbb{N})$ must hold. If we require 1024 weekly observations for the estimation, we would need 5120 daily observations, and hence, the multiplicative cascade used must exhibit ≥ 5120 observations. Therefore, earlier, we require 13 iterations for constructing the multiplicative cascade because $2^{13} = 8192 > 5120$ as opposed to $2^{12} = 4096 < 5120$, which wouldn't provide us with a sufficient number of observations.

[12] As an illustrative example, let us assume that 30% of the overall sample observations are governed by some power-law process. Assuming independence, odds to observe two consecutive observations in the power-law regime are 0.3·0.3=0.09 or 9%, whereas odds to observe three consecutive observations in the power-law regime are 0.3^3=0.027 or 2.7%. Hence, observing more than two consecutive observations in the power-law regime is an indication for some dependency.

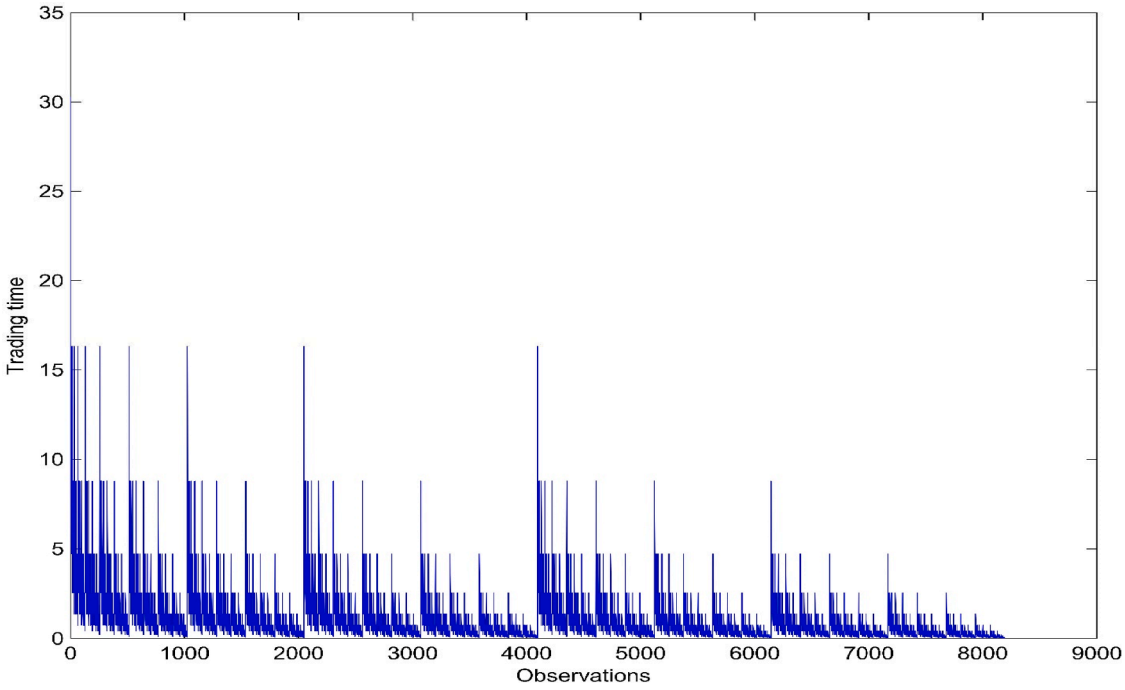

Fig. 1. Binominal multiplicative cascade with $p = 0.60$. This Figure plots the multiplicative cascade using binominal bending of time with probabilities $p = 0.60$ and $(1 - p) = 0.40$ as proposed by Mandelbrot (2008). We employ 13 iterations, giving us $2^{13} = 8192$ observations.

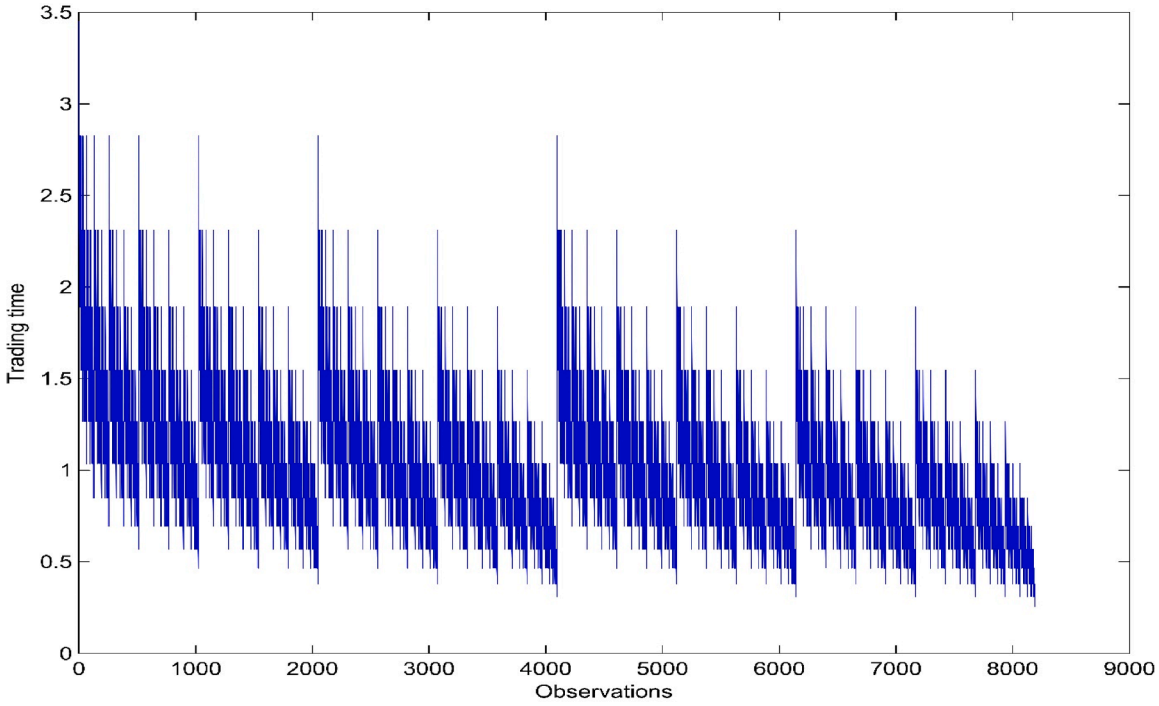

Fig. 2. Binominal multiplicative cascade with $p = 0.55$. This Figure plots the multiplicative cascade using binominal bending of time with probabilities $p = 0.55$ and $(1 - p) = 0.45$. We employ 13 iterations, giving us $2^{13} = 8192$ observations.

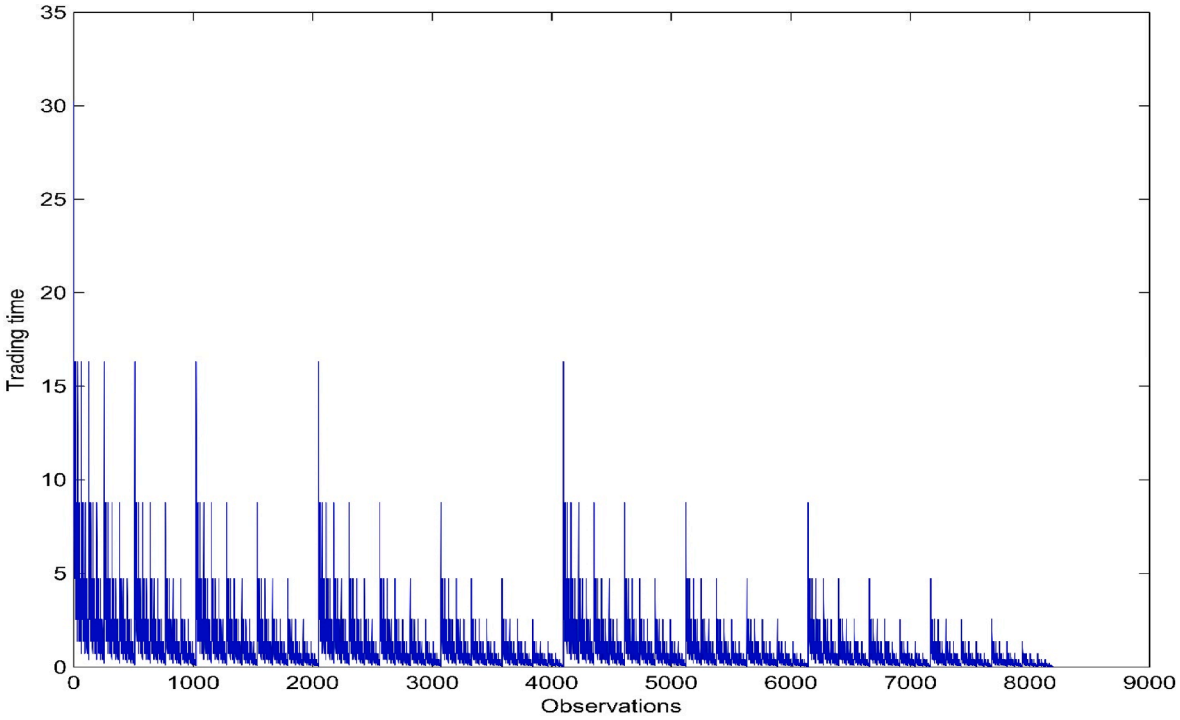

Fig. 3. Binominal multiplicative cascade with $p = 0.65$. This Figure plots the multiplicative cascade using binominal bending of time with probabilities $p = 0.65$ and $(1 - p) = 0.35$. We employ 13 iterations, giving us $2^{13} = 8192$ observations.

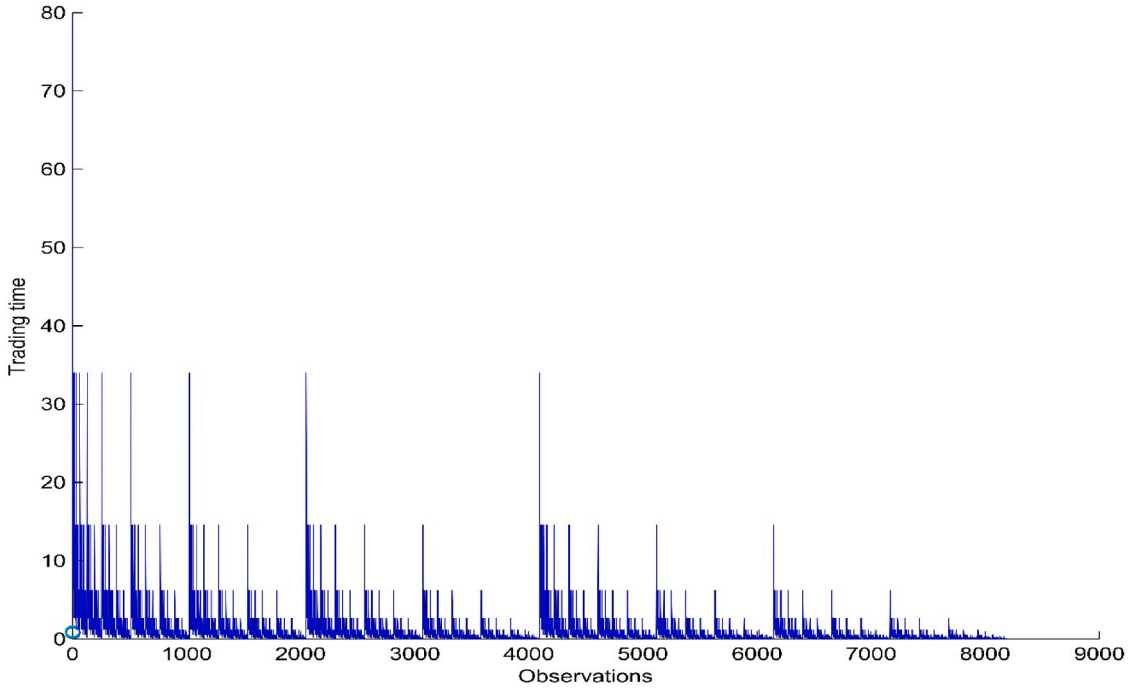

Fig. 4. Binominal multiplicative cascade with $p = 0.70$. This Figure plots the multiplicative cascade using binominal bending of time with probabilities $p = 0.70$ and $(1 - p) = 0.30$. We employ 13 iterations, giving us $2^{13} = 8192$ observations.

Table 1
Multifractal model of realized weekly asset variances using binominal bending with $p = 0.60$.

Distribution	MAX	MIN	Mean	VAR	α	z_{min}	% #PL	*p*-value (GoF)	Hurst	MAX time units in PL
<5%	190.6965	0.0129	10.4257	332.4624	2.0965	7.8201	0.0420	0.0000	0.8503	3
Median	323.7946	0.0373	11.1723	500.0409	2.5578	20.4811	0.1416	0.2000	0.8824	9
>95%	699.3533	0.0760	12.0723	960.6080	3.2911	50.5673	0.3447	0.8900	0.9142	21
Min	135.1928	0.0013	9.7694	244.1521	1.9186	4.4336	0.0156	0.0000	0.8241	2
Max	1761.5106	0.1160	12.8682	3345.2243	4.7167	87.7050	0.5020	1.0000	0.9436	46
Mean	366.2736	0.0401	11.1980	553.8809	2.6112	23.7350	0.1613	0.3008	0.8827	9.8140
Std.Dev	173.3615	0.0193	0.4948	236.6526	0.3812	13.5728	0.0955	0.3066	0.0192	5.5707

Following Mandelbrot (2008), the multifractal process generating asset returns is given as $y(t) = c(t)x(t)$,
where $c(t)$ is the multiplicative cascade at time t and $x(t)$ $IIDN(0,1)$. We use binominal bending of time with probability $p = 0.60$ and $(1-p) = 0.40$ for deriving deformed time. Weekly variance is found by squaring each element in y_i and then summing five consecutive, nonoverlapping elements, such as

$$z_i^W = \left(\sum_{t=1}^{5} y_{t,i}^2, \sum_{t=6}^{10} y_{t,i}^2, \cdots, \sum_{t=5116}^{5120} y_{t,i}^2\right)',$$

where z_i^W has the dimension 1024×1 and $i = 1, \cdots, 1000$. To investigate the tail properties for each vector z_i^W we use the following model:

$$p(z) = Bz^{-\alpha},$$

where $B = (\alpha - 1)z_{MIN}^{\alpha-1}$ with $\alpha \in \{\mathbb{R}_+ | \alpha > 1\}$, $z \in \{\mathbb{R}_+ | z_{MIN} \leq z < \infty\}$, z_{MIN} is the minimum value of realized-variance observations governed by the power law, and α is the magnitude of tail exponent. Following White, Enquist, and Green (2008) and Clauset et al. (2009), we employ MLE and estimate the tail exponent as

$$\widehat{\alpha} = 1 + N\left(\sum_{i=1}^{N} \ln\left(\frac{z_i}{z_{MIN}}\right)\right)^{-1},$$

where $\widehat{\alpha}$ denotes the MLE estimator, and N denotes the number of sample observations exceeding z, that is, $z_i \geq z_{MIN}$. To estimate lower threshold z_{MIN}, we follow Clauset et al. (2009) by applying the KS approach. This statistic is simply the maximum distance, D, between the data and fitted CDFs, given by

$$D = MAX_{z \geq z_{MIN}} |S(z) - P(z)|,$$

where $S(z)$ is the CDF of the data for the observation with a value of at least z_{MIN}, and $P(z)$ is the CDF for the power-law model that best fits the data in the region of $z \geq z_{MIN}$. The estimate of z_{MIN} is the value of $\widehat{z}_{MIN}$ that minimizes D. To test the power-law null hypothesis, we follow Clauset et al. (2009) in employing the estimated parameter vector $(\widehat{\alpha}, \widehat{z}_{MIN})$ that is optimal with respect to D in a GoF test, thereby generating a p-value that quantifies the plausibility of the power-law null hypothesis. Specifically, this test compares D from the equation above with distance measurements for comparable synthetic data sets drawn from the hypothesized model. The p-value is defined as the fraction of synthetic distances that are longer than the empirical distance. Given a significance level of 5%, the power-law null hypothesis is not rejected, as the difference between the empirical data and the model can be attributed to statistical fluctuations alone. Employing detrended fluctuation analysis (DFA) to derive the Hurst exponent we first convert the data series z_t to the mean-centered cumulative sum:

$$\widetilde{z}_t = \sum_{t=1}^{T} z_t.$$

Then different time scales k are defined, that is, $k \in \{4, 8, 16, 32, 64, 128, 256, 512\}$ for weekly data and $k \in \{4, 8, 16, 32, 64, 128\}$ for monthly data. Depending on the defined time scale, data is split into epochs and for each epoch s, a time series regression is used to detrend the data. For instance, if $k = 512$, weekly data for $\widetilde{z}_t$ is split into two non-overlapping epochs. For each epoch s, the following regression is employed:

$$\widetilde{z}_t = \gamma_0 + \gamma_1 t + e_t,$$

where $t = 1, \cdots, 512$ for the first epoch and $t = 513, \cdots, 1024$ for the second epoch. Then for each epoch s, the root mean squared error (RMSE) is computed as:

$$RMSE_S = \sqrt{\frac{1}{T_s}\sum_{t}^{T_s} \widehat{e}_t},$$

where $T_s = 512$. Finally, the estimates for $RMSE_S$ are averaged for each time scale k, giving us $\overline{RMSE}_k$. According to the theory, the following relation holds:

$$\overline{RMSE}_k = ck^H.$$

The Hurst exponent is then estimated by computing a linear fit between log-scales and log-$\overline{RMSE}_k$. If the data were independent, the ratio between numerator and denominator should be, according to the theory, 1:2, corresponding to a Hurst exponent of $H = 0.50$. Moreover, $H > 0.50$ implies long-term dependence, that is, a long memory of the stochastic process in which the data are persistent; on the other hand, $H < 0.50$ implies anti-persistence, which is characterized by the tendency to keep back on themselves. To test the dependency in the power-law regime, we code vectors of binary variables. Specifically, vector $\boldsymbol{d}_i^W$ has a value of 1if $z \geq z_{MIN}$ holds for observations in z_i^W and values of 0 otherwise. Summing the values of $\boldsymbol{d}_i^W$ and dividing the sums by the number of observations (e.g., 1024) gives us the percentage of power-law observations in given processes z_i^W which we can interpret as empirical probability and denote it as θ. Assuming independence under the null hypothesis, defining the operator $TL(.)$ that sums consecutive values of 1 in a binary vector and stores them in another vector and using a significance level of 5%, we would not reject the null hypothesis if and only if $\theta^{MAX(TL(\boldsymbol{d}_i^W))} > 0.05$.

> That is a connection not yet established, and it need not be. Time deformation is a mathematical convenience, handy for analyzing the market; and it happens to fit our subjective experience. Time does not run in a straight line … (Mandelbrot, 2008, p. 240)

Segnon and Lux (2013) provided an overview on various other options to transform clock time into trading time that have been

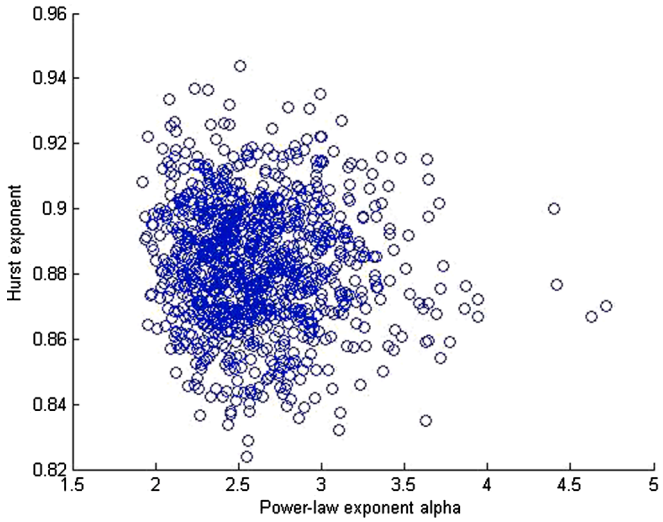

Fig. 5. Power law exponent and Hurst exponent for a model with binominal multiplicative cascade with $p = 0.60$ and weekly data. We construct the multiplicative cascade using binominal bending of time with probabilities $p = 0.60$ and $(1 - p) = 0.40$ as proposed by Mandelbrot (2008). Then we simulate 1000 vectors, each containing 8192 drawings of the standard normal distribution. Multiplying the multiplicative cascade with each drawing in a vector array by array, we retrieve 1000 simulated time-series of asset returns. We use the first 5120 elements in each simulated time-series of asset returns to compute the weekly realized variance by summing five successive elements in each vector in a nonoverlapping manner. This procedure gives us 1000 data vectors, each having 1024 weekly variance observations. For each simulated time series, we estimate the power-law exponent and Hurst exponent as described in section 2. This Figure plots across the simulated data the estimated power-law exponents against the estimated Hurst exponents.

discussed in the literature. Here, however, we follow Mandelbrot et al. (1997b) and Mandelbrot (2008) by using binominal bending of time. The difference between the works of Mandelbrot et al. (1997b) and Mandelbrot (2008) and the current research is first (*i*) that we extend the multifractal model of asset returns (MMAR) to derive realized variances as opposed to asset returns, and second (*ii*) that we provide simulation-based evidence on the distribution of key metrics.

To explore the impact of the multiplicative cascade on the derived variance processes, we also explore multifractal models using binominal bending of time with probability $p = 0.55$ and $(1 - p) = 0.45$ to study a more moderate time deformation relative to the benchmark model and a multifractal model using $p = 0.65$ and $(1 - p) = 0.35$ as well as $p = 0.70$ and $(1 - p) = 0.30$ to study more accelerated time deformations. In doing so, we perform the same analysis as for the benchmark model and use the same matrix $\boldsymbol{X}$, and by controlling for randomness in $\boldsymbol{X}$, any deviation from the benchmark model must be an artifact of its underlying multiplicative cascade.

4. Results

4.1. Multifractal modeling of realized variances: Simulation-based evidence.

As pointed out by Mandelbrot (2008), the multiplicative cascade used for deforming trading time is of fundamental importance for the multifractal model. In Figs. 1 to 4, we plot the multiplicative cascades for using binominal bending of time. In Fig. 1, we use the binominal bending of time with probabilities $p = 0.60$ and $(1 - p) = 0.40$ as proposed by Mandelbrot (2008). We employ 13 iterations, giving us $2^{13} = 8192$ observations. In Figs. 2, 3 and 4, we use the binominal bending of time with probabilities (*i*) $p = 0.55$ and $(1 - p) = 0.45$, (*ii*) $p = 0.65$ and $(1 - p) = 0.35$, and (*iii*) $p = 0.70$ and $(1 - p) = 0.30$, respectively. We observe from Figs. 1 to 4 that the higher the probability (p) chosen, the more extreme the time deformation.

Next, we simulate 1000 vectors, each containing 8192 drawings of the standard normal distribution. Multiplying the multiplicative cascade with each drawing in a vector array by array, we retrieve 1000 simulated time-series of asset returns. In conducting the simulated time-series of asset returns, we use the same set of 1000 simulated vectors from random drawings from the standard normal distribution so that the constructed randomness is determined by the multiplicative cascade only.

We use the first 5120 elements in each simulated time-series of asset returns to compute the weekly realized variance by summing five successive elements in each vector in a nonoverlapping manner. This procedure gives us 1000 data vectors, each having 1024 weekly variance observations for each multiplicative cascade. For illustrative purposes, we plot in Figs. A.3 to A.6 in the appendix the first time-series vector for the simulated asset variances using multiplicative cascades with $p = 0.60$, $p = 0.55$, $p = 0.65$, and $p = 0.70$ respectively. We observe from Figs. A.3 to A.6 that the higher the chosen p, the more extreme events are generated.

In the same manner, we use the first 5120 elements in each simulated time-series of asset returns to compute the monthly realized variance by summing 20 successive elements in each vector in a nonoverlapping manner. This procedure gives us 1000 vectors, each having 256 monthly variance observations for each multiplicative cascade. Again, we plot in Figs. A.7 to A.10 in the appendix the first

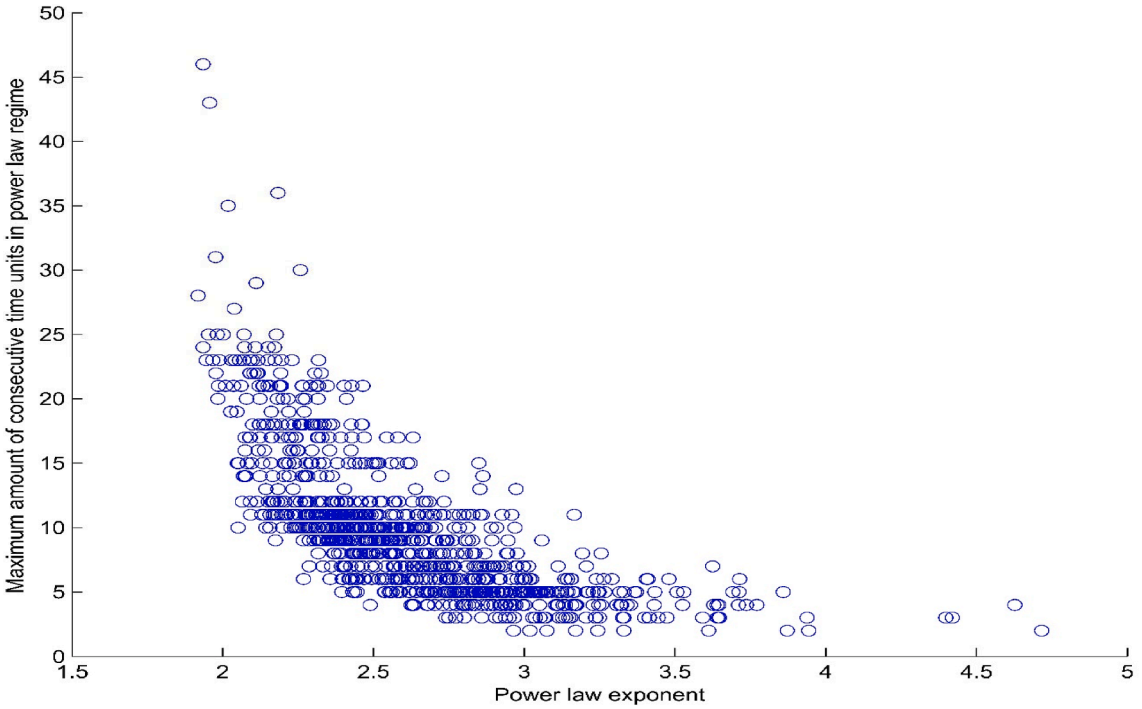

Fig. 6. Power law exponent and maximum length of consecutive time units in power law regime for a model with binominal multiplicative cascade with $p = 0.60$ and weekly data. We construct the multiplicative cascade using binominal bending of time with probabilities $p = 0.60$ and $(1 - p) = 0.40$ as proposed by Mandelbrot (2008). Then we simulate 1000 vectors, each containing 8192 drawings of the standard normal distribution. Multiplying the multiplicative cascade with each drawing in a vector array by array, we retrieve 1000 simulated time-series of asset returns. We use the first 5120 elements in each simulated time-series of asset returns to compute the weekly realized variance by summing five successive elements in each vector in a nonoverlapping manner. This procedure gives us 1000 data vectors, each having 1024 weekly variance observations. For each simulated time series, we estimate the power-law exponent and the maximum time length of subsequent observations that a process is in power-law regime as detailed in section 2. This Figure plots across the simulated data the estimated power-law exponents against the estimated maximum time lengths of observations being in a power-law regime.

time-series vector for the simulated asset variances using multiplicative cascades with $p = 0.60$, $p = 0.55$, $p = 0.65$, and $p = 0.70$, respectively. For comparison reasons, we also plot the monthly realized variance for the S&P 500 over the period of March 1957 to March 2021 in Fig. A.11. Visual inspection shows that the simulated monthly variance using a multiplicative cascade with $p = 0.60$ closely resembles the monthly realized variance for the S&P 500. To highlight this issue, we mirror-invert the last 256 observations of the monthly realized variance for the S&P 500 and plot in Fig. A.12 those data series against the data series of Fig. A.7. It becomes evident that the simulated data resemble the factual data so closely that without any table descriptions, the real-life and synthetic data are indistinguishable.

4.2. Commonalities and differences across multifractal models depending on multifractal cascade.

We continue to evaluate potential commonalities among those 1000 simulated realized-variance data series using this multifractal model framework. We start with the weekly realized variance using the binominal multiplicative cascade with $p = 0.60$, as proposed by Mandelbrot (2008). In evaluating the model, we differentiate the results with respect to the estimated power-law exponents. The results are summarized in Table 1. Based on the simulation experiment, we observe from Table 1 that the expected mean of the power-law exponents across those 1000 simulations is $E[\alpha] = \overline{\widehat{\alpha}} = 2.6112$ with a standard deviation of $\sigma_{\overline{\widehat{\alpha}}} = 0.3812$. The average, respectively, expected Hurst exponent across the 1000 simulated multifractal time-series is $E[H] = \overline{\widehat{H}} = 0.8827$ with an average standard deviation of $\sigma_{\overline{\widehat{H}}} = 0.0192$. Fig. 5 plots the estimated power-law exponents against the estimated Hurst exponents. Fig. 5 does not show any evidence for linear dependency. In fact, the correlation between those two exponents is as low as –0.0677.

Next, the GoF test suggests that the average *p*-value across our 1000 simulated time-series is 30.08%. Moreover, in 671 out of 1000 simulated series, we cannot reject the power-law null hypothesis because the *p*-values exceed 0.05. [13] The maximum time length of the processes being in power-law regimes is, on average, 9.81 time units, suggesting a high level of persistence. Assuming that the power-

[13] Unreported results indicate no clear evidence for any linear dependency between the power-law exponent and the *p*-value of the GoF test.

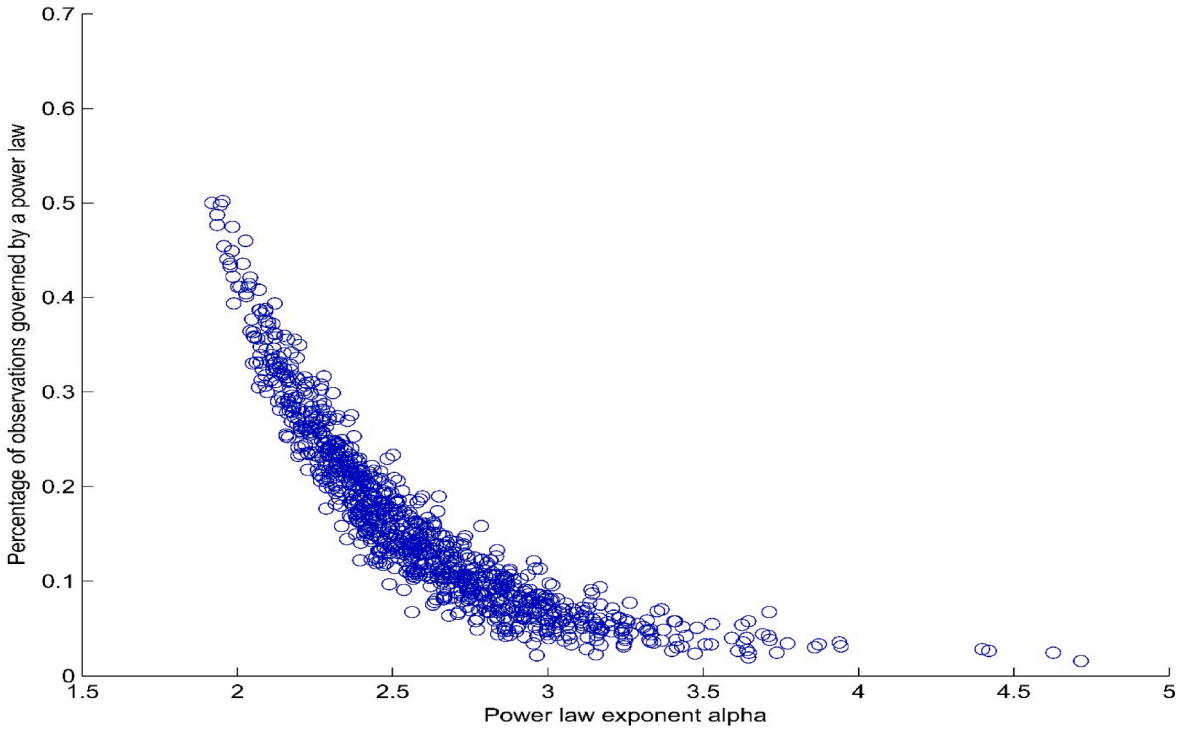

Fig. 7. Power law exponent and percentage of observations governed by a power law for a model with binominal multiplicative cascade with $p = 0.60$ and weekly data, We construct the multiplicative cascade using binominal bending of time with probabilities $p = 0.60$ and $(1 - p) = 0.40$ as proposed by Mandelbrot (2008). Then we simulate 1000 vectors, each containing 8192 drawings of the standard normal distribution. Multiplying the multiplicative cascade with each drawing in a vector array by array, we retrieve 1000 simulated time-series of asset returns. We use the first 5120 elements in each simulated time-series of asset returns to compute the weekly realized variance by summing five successive elements in each vector in a nonoverlapping manner. This procedure gives us 1000 data vectors, each having 1024 weekly variance observations. For each simulated time series, we estimate the power-law exponent and the percentage of observations that a process is in power-law regime as detailed in section 2. This Figure plots across the simulated data the estimated power-law exponents against the estimated percentage of observations that a process is in a power-law regime.

law regimes are evenly distributed across each data series, the probability of that happening is virtually zero. In Fig. 6, we plot the estimated power-law exponent against the maximum length of consecutive time units in a power-law regime. From the results, the model suggests that the lower the absolute value of the power-law exponent, the higher the maximum value of consecutive time units that a process remains in the power-law regime.

Further, we find that, on average, 16.13% of sample observations are governed by a power-law process and that the z_{min} is, on average, 23.7350, implying that, on average, weekly variances exceeding 23.7350 are governed by a power-law process. In Figs. 7 and 8, we plot the estimated power-law exponents against the percentage of sample observations governed by a power-law process and the estimated power-law exponents against z_{min}. From Figs. 7 and 8, it becomes evident that the model suggests a negative link for the former and a positive link for the latter; that is, the lower the economic magnitude of the power-law exponent, the more observations governed by a power-law process. Moreover, the higher the economic magnitude of the power-law exponent, the higher the z_{min}.

The mean of sample means across the 1000 simulated models is 11.1980 with a standard deviation of 0.4948, and the mean of sample variances across the 1000 simulated models is 553.8809 with a standard deviation of 236.6526. In Figs. 9 and 10, we plot the estimated power-law exponents against the sample means and sample variances. We see no strong evidence for any linear dependency between either of them. Moreover, no strong evidence exists for linear dependency between the power-law exponent and the minimum or maximum value.[14] Overall, the multifractal model suggests three links between the power-law exponent and other metrics: a higher absolute economic magnitude of the power-law exponent is associated with (*i*) a lower maximum number of consecutive units of time spent in the power-law regime (negative association), (*ii*) a lower percentage of observations governed by the power-law process (negative association), and (*iii*) a higher value for z_{min} (positive association). Applying multifractal models using a binominal multiplicative cascade with $p = 0.55$, $p = 0.65$, or $p = 0.70$ shows very similar commonalities.[15] However, there are also some differences. Tables 2–4 report the results for the multifractal models using binominal multiplicative cascades with $p = 0.55$, $p = 0.65$, and $p =$

[14] The scatterplots look very similar to those in Fig. 10 and are available upon request.
[15] The corresponding figures look similar to those reported here and are available upon request.

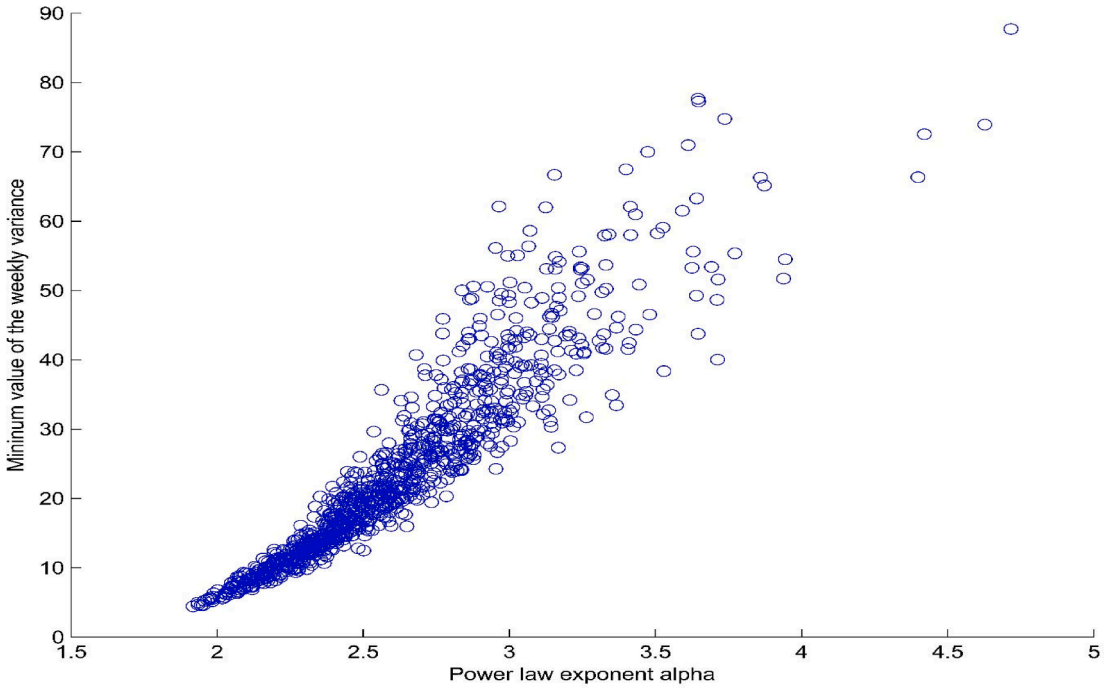

Fig. 8. Power law exponent and corresponding cutoffs derived from a model with binominal multiplicative cascade with $p = 0.60$ and weekly data, We construct the multiplicative cascade using binominal bending of time with probabilities $p = 0.60$ and $(1 - p) = 0.40$ as proposed by Mandelbrot (2008). Then we simulate 1000 vectors, each containing 8192 drawings of the standard normal distribution. Multiplying the multiplicative cascade with each drawing in a vector array by array, we retrieve 1000 simulated time-series of asset returns. We use the first 5120 elements in each simulated time-series of asset returns to compute the weekly realized variance by summing five successive elements in each vector in a nonoverlapping manner. This procedure gives us 1000 data vectors, each having 1024 weekly variance observations. For each simulated time series, we estimate the power-law exponent and the corresponding cutoff (z_{min}) as detailed in section 2. This Figure plots across the simulated data the estimated power-law exponents against the estimated cutoffs.

0.70, respectively.

A key finding from Table 2 is that that the 1000 simulated weekly variance series using a binominal multiplicative cascade with $p = 0.55$ generate an average power-law exponent of $\overline{\widehat{\alpha}} = 3.7216$ with a standard deviation of $\sigma_{\overline{\widehat{\alpha}}} = 0.6658$. From Table 1, we see that in 95% of the estimated exponents for variance processes based on a binominal multiplicative cascade with $p = 0.60$, $\widehat{\alpha} < 3.2911$. Therefore, we can reject on a 5% level the hypothesis that those two models would produce, on average, the same stochastic tail properties. Comparing the results from Table 1 with those of Table 2, another interesting finding is that the average Hurst exponent from variance processes based on a binominal multiplicative cascade with $p = 0.55$ has a lower economic magnitude compared to the average Hurst exponent from variance processes based on a binominal multiplicative cascade with $p = 0.60$. In fact, point estimate $\overline{\widehat{H}} = 0.7979$ is almost four standard deviations lower as $\overline{\widehat{H}} = 0.8827$. As a result, the multifractal model using variance processes based on a binominal multiplicative cascade with $p = 0.55$ produces, on average, variance processes that exhibit less persistence as opposed to those based on a binominal multiplicative cascade with $p = 0.60$. This issue is also manifested in the maximum time lengths of the processes being in power-law regimes. Specifically, the multifractal model using variance processes based on a binominal multiplicative cascade with $p = 0.55$ is, on average, 6.2520 consecutive time units in a power-law regime, whereas the corresponding figure is 9.8140 for the benchmark model. Again, the hypothesis that the power-law regimes are, on average, evenly distributed across time is rejected on any level, suggesting that the part of the distributions governed by power laws occurs in clusters. The fact that the average maximum time length of the processes being in power-law regimes is shorter for the multifractal model of variance processes based on a binominal multiplicative cascade with $p = 0.55$ nicely coincides with the results discussed earlier for the multifractal model of variance processes based on a binominal multiplicative cascade with $p = 0.60$ because that model evidences a negative association between the power-law exponent and maximum time length of the processes being in power-law regimes (see Fig. 6). That is, the within-model result holds in an across-model comparison as well.

A key finding from Table 3 is that that the 1000 simulated weekly variance series using a binominal multiplicative cascade with $p = 0.65$ generate an average power-law exponent of $\overline{\widehat{\alpha}} = 2.1253$ with a standard deviation of $\sigma_{\overline{\widehat{\alpha}}} = 0.2863$. From Table 1, we see that in 95% of the estimated exponents for variance processes based on a binominal multiplicative cascade with $p = 0.60$, $\widehat{\alpha} > 2.0965$. On a 5% significance level, the hypothesis that those two models would produce, on average, the same stochastic tail properties cannot be rejected with respect to the alpha. Next, comparing the results from Table 1 with those of Table 3, another key finding is that the average Hurst exponent from variance processes based on a binominal multiplicative cascade with $p = 0.65$ is higher in its economic

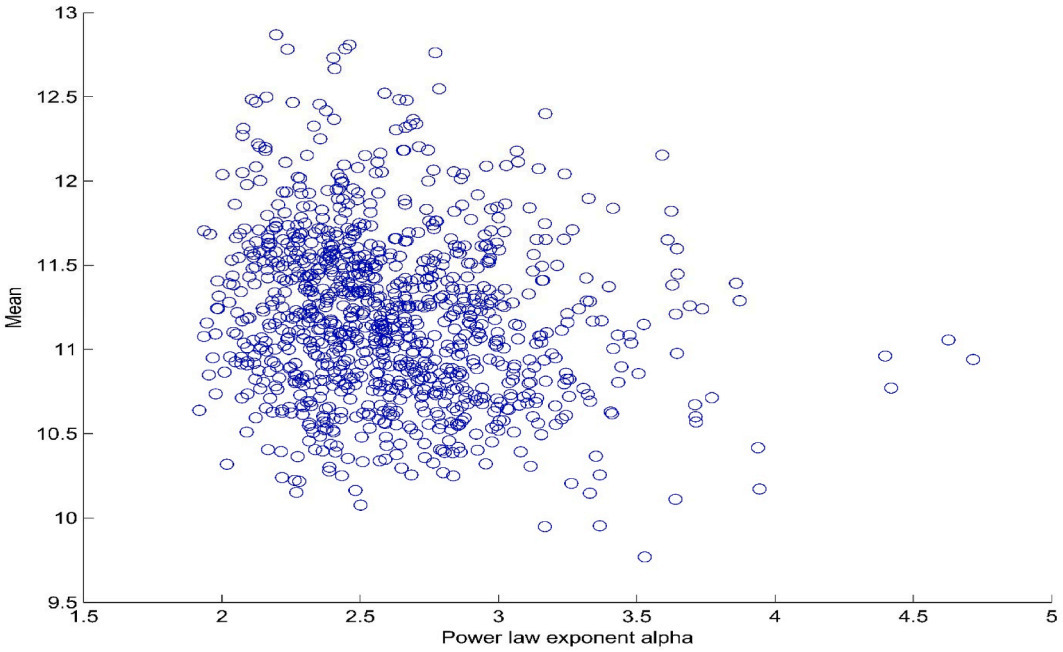

Fig. 9. Power law exponent and sample mean for a model with binominal multiplicative cascade with $p = 0.60$ and weekly data, We construct the multiplicative cascade using binominal bending of time with probabilities $p = 0.60$ and $(1 - p) = 0.40$ as proposed by Mandelbrot (2008). Then we simulate 1000 vectors, each containing 8192 drawings of the standard normal distribution. Multiplying the multiplicative cascade with each drawing in a vector array by array, we retrieve 1000 simulated time-series of asset returns. We use the first 5120 elements in each simulated time-series of asset returns to compute the weekly realized variance by summing five successive elements in each vector in a nonoverlapping manner. This procedure gives us 1000 data vectors, each having 1024 weekly variance observations. For each simulated time series, we estimate the power-law exponent and the sample means as detailed in section 2. This Figure plots across the simulated data the estimated power-law exponents against the estimated sample means.

magnitude compared to the average Hurst exponent from variance processes based on a binominal multiplicative cascade with $p = 0.60$. Point estimate $\widehat{\overline{H}} = 0.9044$ is more than one standard deviation higher than $\widehat{\overline{H}} = 0.8827$. As a result, the multifractal model using variance processes based on a binominal multiplicative cascade with $p = 0.65$ produces variance processes exhibiting a slightly higher level of persistence as opposed to those based on a binominal multiplicative cascade with $p = 0.60$. Furthermore, the maximum time length of the processes being in power-law regimes is, on average, 11.64 time units, confirming the evidence derived from the Hurst exponents.

Furthermore, and again, the hypothesis that the power-law regimes are, on average, evenly distributed across time is rejected on any level, suggesting that the part of the distributions governed by power laws occurs in clusters. The fact that the average maximum time length of the processes being in power-law regimes is higher for the multifractal model of variance processes using a binominal multiplicative cascade with $p = 0.65$, again, nicely coincides with the results discussed earlier for the multifractal model of variance processes employing a binominal multiplicative cascade with $p = 0.60$ because it predicts that processes with lower power-law exponents are associated with longer maximum time units of the processes being in power-law regimes (see Fig. 6).

In Fig. 4 we report the results derived from a model employing 1000 simulated weekly variance series using a binominal multiplicative cascade with $p = 0.70$. A key finding from Table 4 is that that the 1000 simulated weekly variance series using a binominal multiplicative cascade with $p = 0.70$ generate an average power-law exponent of $\widehat{\overline{\alpha}} = 1.8362$ with a standard deviation of $\sigma_{\widehat{\overline{\alpha}}} = 0.2121$. This implies that the processes are expected to exhibit no defined first moment. From Table 3, we observe that in 95% of the estimated exponents for variance processes based on a binominal multiplicative cascade with $p = 0.65$, $\widehat{\alpha} > 1.7809$. Hence, on a 5% significance level, the hypothesis that those two models would produce, on average, the same stochastic tail properties cannot be rejected with respect to the tail exponent. Comparing the multifractal model of variance processes using a binominal multiplicative cascade with $p = 0.65$ with the counterpart model (e.g., the model using a binominal multiplicative cascade with $p = 0.70$), it becomes evident that the averages are very close to each other (viz., 0.9044 and 0.9056). Like evidenced in earlier model comparisons, the slightly higher level of persistence for the multifractal model of variance processes using a binominal multiplicative cascade with $p = 0.70$ is also manifested in the maximum length of time units spent in the power-law regime which is higher for that model than for the model using a binominal multiplicative cascade with $p = 0.65$.

Overall, the key findings are that the more extreme trading time is deformed, the lower is the expected power-law exponent and the higher is the expected Hurst exponent. This simulation-based evidence lines up nicely with the dual relationship between power-law exponent and Hurst exponent:

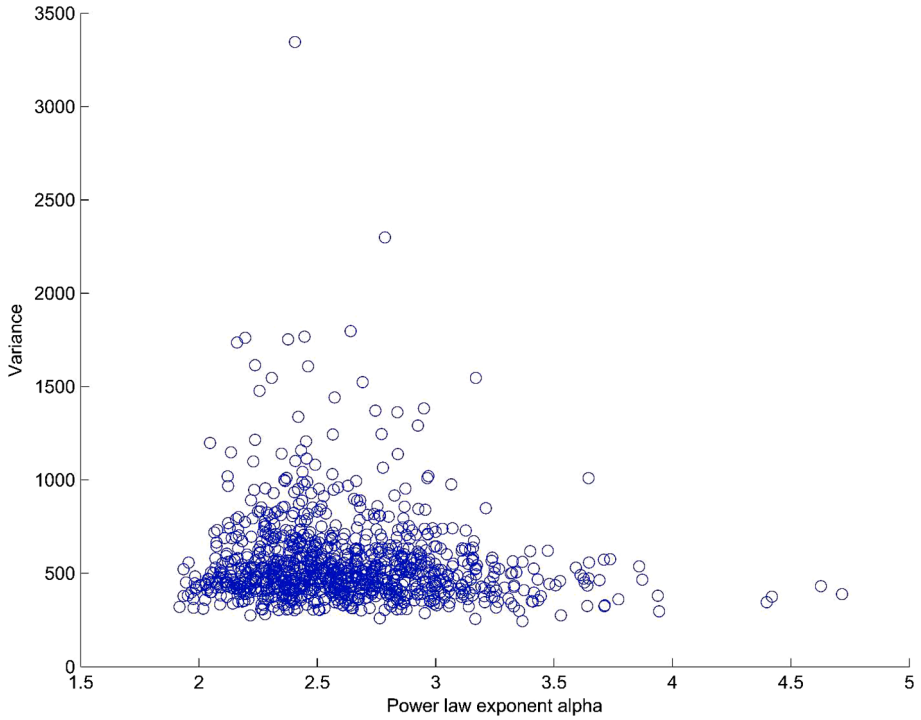

Fig. 10. Power law exponent and sample variance for a model with binominal multiplicative cascade with $p = 0.60$ and weekly data, We construct the multiplicative cascade using binominal bending of time with probabilities $p = 0.60$ and $(1 - p) = 0.40$ as proposed by Mandelbrot (2008). Then we simulate 1000 vectors, each containing 8192 drawings of the standard normal distribution. Multiplying the multiplicative cascade with each drawing in a vector array by array, we retrieve 1000 simulated time-series of asset returns. We use the first 5120 elements in each simulated time-series of asset returns to compute the weekly realized variance by summing five successive elements in each vector in a nonoverlapping manner. This procedure gives us 1000 data vectors, each having 1024 weekly variance observations. For each simulated time series, we estimate the power-law exponent and the sample variance as detailed in section 2. This Figure plots across the simulated data the estimated power-law exponents against the estimated sample variances.

Specifically, Mandelbrot (2008) argues that power-law exponent and Hurst exponent are in a dual relationship manifested in a negative correlation between Hurst exponent and power-law exponent.[16] To illustrate this issue, in Fig. 11, we plot the power-law exponents and the corresponding Hurst exponents for all multifractal models investigated here. Strikingly, we observe four clear clusters. We also see from Fig. 11 that the distributions of power-law exponents are clearly concentrated around different means. Note that the turquoise, red, green, and blue clusters of estimated power-law and Hurst exponents correspond to the estimates derived from various multifractal models based on binominal multiplicative cascades with $p = 0.70, p = 0.65, p = 0.60$, and $p = 0.55$, respectively. Strikingly, the correlation between average power-law exponents and average Hurst exponents is -0.9781. We interpret this as strong evidence for different multiplicative cascades indeed producing very distinct stochastic processes as defined in terms of their discontinuities and dependency structures.

Next, we explore the characteristics of the model using simulated monthly variance data. The results are reported in Tables 5 to 8. Comparing the results of Table 5 with those of Table 1 where the binominal multiplicative cascade with $p = 0.60$ is used to generate the monthly and weekly, respectively, variance data, we observe that the average power-law exponent is slightly higher in its economic magnitude for monthly as opposed to weekly data. However, 95% of the weekly estimates for $\widehat{\alpha}$ are below 3.2911 in economic magnitude, implying that on a 5% significance level, we cannot reject the null hypothesis that the $\overline{\widehat{\alpha}}$ for monthly and weekly data are statistically the same. We consider this result a strong indication for (scale) invariance across different time frequencies. Similar evidence can be documented for the binominal multiplicative cascades with $p = 0.55, p = 0.65$, and $p = 0.70$; that is, we cannot reject the null hypothesis that monthly data exhibit statistically the same tail characteristics as the corresponding weekly data. Also, the estimated average Hurst exponents based on monthly data are very close to corresponding estimates for weekly data, indicating that the memory of the processes does not change across time scales. As an example, the point estimate for the average Hurst exponent $\overline{\widehat{H}}$ derived from a model employing 1000 simulated monthly variance series using a binominal multiplicative cascade with $p = 0.60$ is 0.9106 which is less than one standard deviation higher than 0.8827 which is the corresponding figure for the counterpart model based on weekly data.

[16] The dual relationship between power-law exponent and Hurst exponent is detailed in Mandelbrot (2008, p. 200–206).

Table 2
Multifractal model of realized weekly asset variances using binominal bending with $p = 0.55$.

Distribution	MAX	MIN	Mean	VAR	α	z_{min}	% #PL	*p*-value (GoF)	Hurst	MAX time units in PL
<5%	45.4955	0.0452	6.4951	37.5460	2.8678	7.4141	0.0410	0.0000	0.7616	3
Median	63.7457	0.1314	6.7682	45.1255	3.6315	12.7490	0.1328	0.2000	0.7977	5
>95%	104.2574	0.2506	7.0551	57.1513	4.9739	21.7829	0.3086	0.8800	0.8333	12
Min	36.6981	0.0065	6.3297	32.7363	2.5070	4.8053	0.0156	0.0000	0.7350	1
Max	214.5671	0.4050	7.2668	81.5879	6.9149	30.2283	0.5059	1.0000	0.8593	24
Mean	67.7768	0.1377	6.7715	45.9518	3.7216	13.3932	0.1509	0.3066	0.7979	6.2520
Std.Dev	19.0406	0.0632	0.1661	6.2397	0.6658	4.4436	0.0872	0.3065	0.0218	3.2381

Following Mandelbrot (2008), the multifractal process generating asset returns is given as
$y(t) = c(t)x(t)$,
where $c(t)$ is the multiplicative cascade at time t and $x(t)$ $IIDN(0,1)$. We use binominal bending of time with probability $p = 0.55$ and $(1-p) = 0.45$ for deriving deformed time. Weekly variance is found by squaring each element in y_i and then summing five consecutive, nonoverlapping elements, such as

$$z_i^W = \left(\sum_{t=1}^{5} y_{t,i}^2, \sum_{t=6}^{10} y_{t,i}^2, \cdots, \sum_{t=5116}^{5120} y_{t,i}^2\right)',$$

where z_i^W has the dimension 1024×1 and $i = 1, \cdots, 1000$. To investigate the tail properties for each vector z_i^W we use the following model:
$p(z) = Bz^{-\alpha}$,
where $B = (\alpha - 1)z_{MIN}^{\alpha-1}$ with $\alpha \in \{\mathbb{R}_+ | \alpha > 1\}$, $z \in \{\mathbb{R}_+ | z_{MIN} \leq z < \infty\}$, z_{MIN} is the minimum value of realized-variance observations governed by the power law, and α is the magnitude of tail exponent. Following White, Enquist, and Green (2008) and Clauset et al. (2009), we employ MLE and estimate the tail exponent as

$$\widehat{\alpha} = 1 + N\left(\sum_{i=1}^{N} \ln\left(\frac{z_i}{z_{MIN}}\right)\right)^{-1},$$

where $\widehat{\alpha}$ denotes the MLE estimator, and N denotes the number of sample observations exceeding z, that is, $z_i \geq z_{MIN}$. To estimate lower threshold z_{MIN}, we follow Clauset et al. (2009) by applying the KS approach. This statistic is simply the maximum distance, D, between the data and fitted CDFs, given by
$D = MAX_{z \geq z_{MIN}} |S(z) - P(z)|$,
where $S(z)$ is the CDF of the data for the observation with a value of at least z_{MIN}, and $P(z)$ is the CDF for the power-law model that best fits the data in the region of $z \geq z_{MIN}$. The estimate of z_{MIN} is the value of $\widehat{z}_{MIN}$ that minimizes D. To test the power-law null hypothesis, we follow Clauset et al. (2009) in employing the estimated parameter vector $(\widehat{\alpha}, \widehat{z}_{MIN})$ that is optimal with respect to D in a GoF test, thereby generating a p-value that quantifies the plausibility of the power-law null hypothesis. Specifically, this test compares D from the equation above with distance measurements for comparable synthetic data sets drawn from the hypothesized model. The p-value is defined as the fraction of synthetic distances that are longer than the empirical distance. Given a significance level of 5%, the power-law null hypothesis is not rejected, as the difference between the empirical data and the model can be attributed to statistical fluctuations alone. Employing detrended fluctuation analysis (DFA) to derive the Hurst exponent we first convert the data series z_t to the mean-centered cumulative sum:
$\widetilde{z}_t = \sum_{t=1}^{T} z_t$.
Then different time scales k are defined, that is, $k \in \{4, 8, 16, 32, 64, 128, 256, 512\}$ for weekly data and $k \in \{4, 8, 16, 32, 64, 128\}$ for monthly data. Depending on the defined time scale, data is split into epochs and for each epoch s, a time series regression is used to detrend the data. For instance, if $k = 512$, weekly data for $\widetilde{z}_t$ is split into two non-overlapping epochs. For each epoch s, the following regression is employed:
$\widetilde{z}_t = \gamma_0 + \gamma_1 t + e_t$,
where $t = 1, \cdots, 512$ for the first epoch and $t = 513, \cdots, 1024$ for the second epoch. Then for each epoch s, the root mean squared error (RMSE) is computed as:

$$RMSE_S = \sqrt{\frac{1}{T_s}\sum_{t}^{T_s} \widehat{e}_t},$$

where $T_s = 512$. Finally, the estimates for $RMSE_S$ are averaged for each time scale k, giving us $\overline{RMSE}_k$. According to the theory, the following relation holds:
$\overline{RMSE}_k = ck^H$.
The Hurst exponent is then estimated by computing a linear fit between log-scales and log-$\overline{RMSE}_k$. If the data were independent, the ratio between numerator and denominator should be, according to the theory, 1:2, corresponding to a Hurst exponent of $H = 0.50$. Moreover, $H > 0.50$ implies long-term dependence, that is, a long memory of the stochastic process in which the data are persistent; on the other hand, $H < 0.50$ implies anti-persistence, which is characterized by the tendency to keep back on themselves. To test the dependency in the power-law regime, we code vectors of binary variables. Specifically, vector d_i^W has a value of 1if $z \geq z_{MIN}$ holds for observations in z_i^W and values of 0 otherwise. Summing the values of d_i^W and dividing the sums by the number of observations (e.g., 1024) gives us the percentage of power-law observations in given processes z_i^W which we can interpret as empirical probability and denote it as θ. Assuming independence under the null hypothesis, defining the operator $TL(.)$ that sums consecutive values of 1 in a binary vector and stores them in another vector and using a significance level of 5%, we would not reject the null hypothesis if and only if $\theta^{MAX(TL(d_i^W))} > 0.05$.

4.3. How well does the model explain realized asset variances in real life?

To explore how well the multifractal models explain real-life data, we download daily price data on the GBP/USD exchange rate, Bitcoin, crude oil, and the S&P 500. To have some degree of comparability, all data series end on the same day—April 19, 2022.

Table 3
Multifractal model of realized weekly asset variances using binominal bending with $p = 0.65$.

Distribution	MAX	MIN	Mean	VAR	α	z_{min}	% #PL	*p*-value (GoF)	Hurst	MAX time units in PL
<5%	799.5418	0.0016	19.3973	3557.7144	1.7809	8.5514	0.0381	0.0000	0.8659	4
Median	1685.7156	0.0051	22.0847	7363.0592	2.0601	29.0518	0.1475	0.1700	0.9045	11
>95%	4475.0750	0.0112	26.2533	24991.1179	2.6639	121.2373	0.3262	0.8900	0.9407	23
Min	522.8358	0.0002	17.2574	1921.0971	1.6258	3.0708	0.0127	0.0000	0.8355	2
Max	12554.5332	0.0159	31.8135	157086.4876	4.3895	268.4269	0.5166	1.0000	0.9745	47
Mean	2034.6503	0.0056	22.3433	10152.9781	2.1253	42.7085	0.1603	0.2956	0.9044	11.6410
Std.Dev	1310.8141	0.0030	2.1237	10821.7698	0.2863	38.3628	0.0920	0.3095	0.0226	6.4848

Following Mandelbrot (2008), the multifractal process generating asset returns is given as
$y(t) = c(t)x(t)$,
where $c(t)$ is the multiplicative cascade at time t and $x(t)$ $IIDN(0,1)$. We use binominal bending of time with probability $p = 0.65$ and $(1-p) = 0.35$ for deriving deformed time. Weekly variance is found by squaring each element in y_i and then summing five consecutive, nonoverlapping elements, such as

$$z_i^W = \left(\sum_{t=1}^{5} y_{t,i}^2, \sum_{t=6}^{10} y_{t,i}^2, \cdots, \sum_{t=5116}^{5120} y_{t,i}^2\right)',$$

where z_i^W has the dimension 1024×1 and $i = 1, \cdots, 1000$. To investigate the tail properties for each vector z_i^W we use the following model:
$p(z) = Bz^{-\alpha}$,
where $B = (\alpha - 1)z_{MIN}^{\alpha-1}$ with $\alpha \in \{\mathbb{R}_+ | \alpha > 1\}$, $z \in \{\mathbb{R}_+ | z_{MIN} \leq z < \infty\}$, z_{MIN} is the minimum value of realized-variance observations governed by the power law, and α is the magnitude of tail exponent. Following White, Enquist, and Green (2008) and Clauset et al. (2009), we employ MLE and estimate the tail exponent as

$$\widehat{\alpha} = 1 + N\left(\sum_{i=1}^{N} \ln\left(\frac{z_i}{z_{MIN}}\right)\right)^{-1},$$

where $\widehat{\alpha}$ denotes the MLE estimator, and N denotes the number of sample observations exceeding z, that is, $z_i \geq z_{MIN}$. To estimate lower threshold z_{MIN}, we follow Clauset et al. (2009) by applying the KS approach. This statistic is simply the maximum distance, D, between the data and fitted CDFs, given by
$D = MAX_{z \geq z_{MIN}} |S(z) - P(z)|$,
where $S(z)$ is the CDF of the data for the observation with a value of at least z_{MIN}, and $P(z)$ is the CDF for the power-law model that best fits the data in the region of $z \geq z_{MIN}$. The estimate of z_{MIN} is the value of $\widehat{z}_{MIN}$ that minimizes D. To test the power-law null hypothesis, we follow Clauset et al. (2009) in employing the estimated parameter vector $(\widehat{\alpha}, \widehat{z}_{MIN})$ that is optimal with respect to D in a GoF test, thereby generating a p-value that quantifies the plausibility of the power-law null hypothesis. Specifically, this test compares D from the equation above with distance measurements for comparable synthetic data sets drawn from the hypothesized model. The p-value is defined as the fraction of synthetic distances that are longer than the empirical distance. Given a significance level of 5%, the power-law null hypothesis is not rejected, as the difference between the empirical data and the model can be attributed to statistical fluctuations alone. Employing detrended fluctuation analysis (DFA) to derive the Hurst exponent we first convert the data series z_t to the mean-centered cumulative sum:
$\widetilde{z}_t = \sum_{t=1}^{T} z_t$.
Then different time scales k are defined, that is, $k \in \{4, 8, 16, 32, 64, 128, 256, 512\}$ for weekly data and $k \in \{4, 8, 16, 32, 64, 128\}$ for monthly data. Depending on the defined time scale, data is split into epochs and for each epoch s, a time series regression is used to detrend the data. For instance, if $k = 512$, weekly data for $\widetilde{z}_t$ is split into two non-overlapping epochs. For each epoch s, the following regression is employed:
$\widetilde{z}_t = \gamma_0 + \gamma_1 t + e_t$,
where $t = 1, \cdots, 512$ for the first epoch and $t = 513, \cdots, 1024$ for the second epoch. Then for each epoch s, the root mean squared error (RMSE) is computed as:

$$RMSE_S = \sqrt{\frac{1}{T_s}\sum_{t}^{T_s} \widehat{e}_t},$$

where $T_s = 512$. Finally, the estimates for $RMSE_S$ are averaged for each time scale k, giving us $\overline{RMSE}_k$. According to the theory, the following relation holds:
$\overline{RMSE}_k = ck^H$.
The Hurst exponent is then estimated by computing a linear fit between log-scales and log-$\overline{RMSE}_k$. If the data were independent, the ratio between numerator and denominator should be, according to the theory, 1:2, corresponding to a Hurst exponent of $H = 0.50$. Moreover, $H > 0.50$ implies long-term dependence, that is, a long memory of the stochastic process in which the data are persistent; on the other hand, $H < 0.50$ implies anti-persistence, which is characterized by the tendency to keep back on themselves. To test the dependency in the power-law regime, we code vectors of binary variables. Specifically, vector d_i^W has a value of 1if $z \geq z_{MIN}$ holds for observations in z_i^W and values of 0 otherwise. Summing the values of d_i^W and dividing the sums by the number of observations (e.g., 1024) gives us the percentage of power-law observations in given processes z_i^W which we can interpret as empirical probability and denote it as θ. Assuming independence under the null hypothesis, defining the operator $TL(.)$ that sums consecutive values of 1 in a binary vector and stores them in another vector and using a significance level of 5%, we would not reject the null hypothesis if and only if $\theta^{MAX(TL(d_i^W))} > 0.05$.

Retrieving 2561 daily observations, the starting dates for the GBP/USD exchange rate, Bitcoin, crude oil, and the S&P 500 are April 17, 2015, June 27, 2012, February 17, 2012, and February 15, 2012, respectively. Computing the daily returns for each data set gives us 2560 daily returns, and using the sum of 5 and 20 consecutive and squared daily observations provides us with 512 weekly and 128 monthly realized-variance observations. For both weekly and monthly realized variances and each data set, we compute the power-law

Table 4
Multifractal model of realized weekly asset variances using binominal bending with $p = 0.70$.

Distribution	MAX	MIN	Mean	VAR	α	z_{min}	% #PL	*p*-value (GoF)	Hurst	MAX time units in PL
<5%	3210.1842	0.0001	39.8463	37991.6864	1.5796	6.1489	0.0420	0.0000	0.9277	4
Median	7898.9031	0.0004	50.4720	119270.3981	1.7841	32.5899	0.1563	0.1500	0.9068	11
>95%	27627.5740	0.0009	71.2348	807832.9982	2.2343	211.3543	0.3408	0.8900	0.9269	24
Min	1704.4902	0.0000	32.5517	17784.8228	1.5047	2.8381	0.0117	0.0000	0.8056	2
Max	79049.4142	0.0016	116.6765	6135148.2228	3.5754	775.8109	0.4600	1.0000	0.9819	49
Mean	10592.7700	0.0004	52.5146	234990.8534	1.8362	67.6387	0.1644	0.2901	0.9056	13.1760
Std.Dev	8703.1464	0.0003	10.6116	434933.8487	0.2121	87.1992	0.0945	0.3126	0.0281	7.5437

Following Mandelbrot (2008), the multifractal process generating asset returns is given as
$y(t) = c(t)x(t)$,
where $c(t)$ is the multiplicative cascade at time t and $x(t)$ $IIDN(0,1)$. We use binominal bending of time with probability $p = 0.70$ and $(1-p) = 0.30$ for deriving deformed time. Weekly variance is found by squaring each element in y_i and then summing five consecutive, nonoverlapping elements, such as
$z_i^W = \left(\sum_{t=1}^{5} y_{t,i}^2, \sum_{t=6}^{10} y_{t,i}^2, \cdots, \sum_{t=5116}^{5120} y_{t,i}^2\right)'$,
where z_i^W has the dimension 1024×1 and $i = 1, \cdots, 1000$. To investigate the tail properties for each vector z_i^W we use the following model:
$p(z) = Bz^{-\alpha}$,
where $B = (\alpha - 1)z_{MIN}^{\alpha-1}$ with $\alpha \in \{\mathbb{R}_+ | \alpha > 1\}$, $z \in \{\mathbb{R}_+ | z_{MIN} \leq z < \infty\}$, z_{MIN} is the minimum value of realized-variance observations governed by the power law, and α is the magnitude of tail exponent. Following White, Enquist, and Green (2008) and Clauset et al. (2009), we employ MLE and estimate the tail exponent as
$\widehat{\alpha} = 1 + N\left(\sum_{i=1}^{N} \ln\left(\frac{z_i}{z_{MIN}}\right)\right)^{-1}$,
where $\widehat{\alpha}$ denotes the MLE estimator, and N denotes the number of sample observations exceeding z, that is, $z_i \geq z_{MIN}$. To estimate lower threshold z_{MIN}, we follow Clauset et al. (2009) by applying the KS approach. This statistic is simply the maximum distance, D, between the data and fitted CDFs, given by
$D = MAX_{z \geq z_{MIN}} |S(z) - P(z)|$,
where $S(z)$ is the CDF of the data for the observation with a value of at least z_{MIN}, and $P(z)$ is the CDF for the power-law model that best fits the data in the region of $z \geq z_{MIN}$. The estimate of z_{MIN} is the value of $\widehat{z}_{MIN}$ that minimizes D. To test the power-law null hypothesis, we follow Clauset et al. (2009) in employing the estimated parameter vector $(\widehat{\alpha}, \widehat{z}_{MIN})$ that is optimal with respect to D in a GoF test, thereby generating a p-value that quantifies the plausibility of the power-law null hypothesis. Specifically, this test compares D from the equation above with distance measurements for comparable synthetic data sets drawn from the hypothesized model. The p-value is defined as the fraction of synthetic distances that are longer than the empirical distance. Given a significance level of 5%, the power-law null hypothesis is not rejected, as the difference between the empirical data and the model can be attributed to statistical fluctuations alone. Employing detrended fluctuation analysis (DFA) to derive the Hurst exponent we first convert the data series z_t to the mean-centered cumulative sum:
$\widetilde{z}_t = \sum_{t=1}^{T} z_t$.
Then different time scales k are defined, that is, $k \in \{4, 8, 16, 32, 64, 128, 256, 512\}$ for weekly data and $k \in \{4, 8, 16, 32, 64, 128\}$ for monthly data. Depending on the defined time scale, data is split into epochs and for each epoch s, a time series regression is used to detrend the data. For instance, if $k = 512$, weekly data for $\widetilde{z}_t$ is split into two non-overlapping epochs. For each epoch s, the following regression is employed:
$\widetilde{z}_t = \gamma_0 + \gamma_1 t + e_t$,
where $t = 1, \cdots, 512$ for the first epoch and $t = 513, \cdots, 1024$ for the second epoch. Then for each epoch s, the root mean squared error (RMSE) is computed as:
$RMSE_S = \sqrt{\frac{1}{T_s}\sum_{t}^{T_s} \widehat{e}_t}$,
where $T_s = 512$. Finally, the estimates for $RMSE_S$ are averaged for each time scale k, giving us $\overline{RMSE}_k$. According to the theory, the following relation holds:
$\overline{RMSE}_k = ck^H$.
The Hurst exponent is then estimated by computing a linear fit between log-scales and log-$\overline{RMSE}_k$. If the data were independent, the ratio between numerator and denominator should be, according to the theory, 1:2, corresponding to a Hurst exponent of $H = 0.50$. Moreover, $H > 0.50$ implies long-term dependence, that is, a long memory of the stochastic process in which the data are persistent; on the other hand, $H < 0.50$ implies anti-persistence, which is characterized by the tendency to keep back on themselves. To test the dependency in the power-law regime, we code vectors of binary variables. Specifically, vector d_i^W has a value of 1if $z \geq z_{MIN}$ holds for observations in z_i^W and values of 0 otherwise. Summing the values of d_i^W and dividing the sums by the number of observations (e.g., 1024) gives us the percentage of power-law observations in given processes z_i^W which we can interpret as empirical probability and denote it as θ. Assuming independence under the null hypothesis, defining the operator $TL(.)$ that sums consecutive values of 1 in a binary vector and stores them in another vector and using a significance level of 5%, we would not reject the null hypothesis if and only if $\theta^{MAX(TL(d_i^W))} > 0.05$.

exponent and Hurst exponent and test the power-law null hypothesis using Clauset et al.'s (2009) GoF test. The results are reported in Tables 9 and 10.

Considering weekly data, we observe from Table 9 that the estimated power-law exponents vary between $\widehat{\alpha} = 2.1746$ for the S&P 500 and $\widehat{\alpha} = 2.9474$ for Bitcoin, implying that the weekly realized variance for Bitcoin is less exposed to extreme events than the

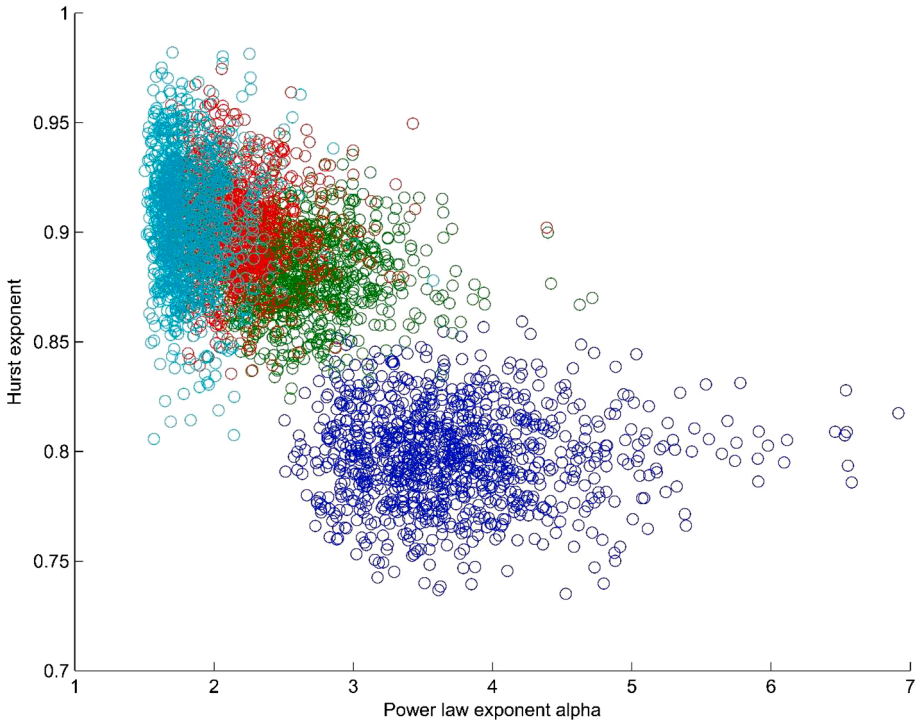

Fig. 11. Clusters of Power law exponents and Hurst exponents. This Figure plots the estimated power-law exponents against the corresponding estimated Hurst exponents for all multifractal models. Each model builds one of the four clusters. The turquoise, red, green, and blue clusters of estimated power-law and Hurst exponents correspond to the multifractal models derived from binominal multiplicative cascades with $p = 0.70$, $p = 0.65$, $p = 0.60$, and $p = 0.55$, respectively. The correlation between average power-law exponents and average Hurst exponents is -0.9781. (For interpretation of the references to colour in this figure legend, the reader is referred to the web version of this article.)

weekly realized variance for the S&P 500. This result is in line with the work of Grobys (2021), who used daily data to compute realized variances and documented power-law exponents for the S&P 500 and Bitcoin corresponding to $\widehat{\alpha} = 2.58$ and $\widehat{\alpha} = 3.02$, respectively. The Hurst exponents vary between 0.8394 for the weekly realized GBP/USD exchange rate variance and 1.1777 for the weekly realized crude oil variance. The null hypothesis that $H = 0.50$ is clearly rejected for all weekly realized variances. It is noteworthy that because $\widehat{H} > 1$ for crude oil and the S&P 500 weekly realized variances, the uncertainty in those asset markets is non-stationary, respectively, unbounded. This is in line with Sun and Zhou (2014) who fitted GARCH models to S&P 500 data. Their estimated models' coefficients indicated that the fitted GARCH models are Near-IGARCH.

Next, using Tables 1, we can test the weekly realized GBP/USD exchange-rate and Bitcoin variances for whether the estimated power-law exponents are statistically significantly larger than $\alpha = 2.6112$, which is the implied value for $E[\alpha]$ for the corresponding multifractal model used as benchmark model here. Because for 95% of the simulated values for α the model predicts $\alpha < 3.2911$, we cannot reject the model with respect to the power-law exponent. Further, as the estimated power-law exponents for the weekly realized variances for crude oil and the S&P 500 are below the implied value for $E[\alpha] = 2.6112$ generated by the multifractal benchmark model, we can test whether the estimated power-law exponents for crude oil and the S&P 500 are significantly lower than $E[\alpha] = 2.6112$. From Table 1, we observe that 95% of simulated values for α by the multifractal model exceed $\alpha = 2.0965$. Again, we cannot reject our multifractal benchmark model with respect to the generated *implied discontinuities*.

We can test the Hurst exponents in the same manner. The benchmark model implies that 95% of the Hurst exponents are either above $\widehat{H} = 0.8503$ or below $\widehat{H} = 0.9142$. Whereas the estimated Hurst exponents for the weekly realized Bitcoin variance is clearly within the boundaries, we observe from Table 1 that the estimated Hurst exponents for the weekly realized crude oil variance is still in the range of possible outcomes because the minimum value for Hurst exponents produced from the multifractal model is $\widehat{H} = 0.8241$ which is clearly lower than the estimated Hurst exponent for weekly realized crude oil variance (viz., $\widehat{H} = 0.8394$). Moreover, it is worth noting that the estimated lower and upper bounds for the multifractal model reported in Tables 1–4 are based on 1024 observations, whereas the estimates for weekly realized variances for the GBP/USD exchange rate, Bitcoin, crude oil, and the S&P 500 incorporate only 512 observations. Accounting for less observations will widen the range of discontinuities and dependencies allowed for by the multifractal models. Overall, the evidence suggests that the multifractal benchmark model is indeed capable of describing the discontinuity and dependency structure we observe for weekly realized variances for the GBP/USD exchange rate and Bitcoin.

However, the estimated Hurst exponents for both crude oil's weekly realized variance and the S&P 500's weekly realized variance (viz., $\widehat{H} = 1.1777$ and $\widehat{H} = 1.1165$) are clearly outside the range of possible Hurst exponents produced from the benchmark model.

Table 5
Multifractal model of realized monthly asset variances using binominal bending with $p = 0.60$.

Distribution	MAX	MIN	Mean	VAR	α	z_{min}	% #PL	*p*-value (GoF)	Hurst	MAX time units in PL
<5%	343.9031	0.7249	41.7545	2659.9105	2.1465	23.5203	0.0703	0.0000	0.8539	1
Median	573.5962	1.2296	44.6836	3897.9596	2.7364	58.5107	0.2383	0.3100	0.9097	3
>95%	1060.2399	1.8406	48.2892	7160.7704	3.9909	136.4062	0.5352	0.9500	0.9657	9
Min	244.8299	0.4736	39.0774	1926.0629	1.9008	14.1641	0.0313	0.0000	0.8071	0
Max	2116.5679	2.4709	51.4730	19010.4331	7.9932	219.1731	0.7188	1.0000	1.0076	22
Mean	622.1480	1.2563	44.7919	4262.7881	2.8697	66.6449	0.2615	0.3824	0.9106	3.9300
Std.Dev	233.8105	0.3337	1.9793	1579.0514	0.6232	35.2948	0.1460	0.3266	0.0341	2.5277

Following Mandelbrot (2008), the multifractal process generating asset returns is given as
$y(t) = c(t)x(t)$,
where $c(t)$ is the multiplicative cascade at time t and $x(t)$ $IIDN(0,1)$. We use binominal bending of time with probability $p = 0.60$ and $(1-p) = 0.40$ for deriving deformed time. Monthly variance is found by squaring each element in y_i and then summing five consecutive, nonoverlapping elements, such as
$z_i^M = \left(\sum_{t=1}^{20} y_{t,i}^2, \sum_{t=21}^{40} y_{t,i}^2, \cdots, \sum_{t=5101}^{5120} y_{t,i}^2\right)'$,
where z_i^M has the dimension 256×1 and $i = 1, \cdots, 1000$. To investigate the tail properties for each vector z_i^M, we use the following model:
$p(z) = Bz^{-\alpha}$,
where $B = (\alpha - 1)z_{MIN}^{\alpha-1}$ with $\alpha \in \{\mathbb{R}_+ | \alpha > 1\}$, $z \in \{\mathbb{R}_+ | z_{MIN} \leq z < \infty\}$, z_{MIN} is the minimum value of realized-variance observations governed by the power law, and α is the magnitude of tail exponent. Following White, Enquist, and Green (2008) and Clauset et al. (2009), we employ MLE and estimate the tail exponent as
$\widehat{\alpha} = 1 + N\left(\sum_{i=1}^{N} \ln\left(\frac{z_i}{z_{MIN}}\right)\right)^{-1}$,
where $\widehat{\alpha}$ denotes the MLE estimator, and N denotes the number of sample observations exceeding z, that is, $z_i \geq z_{MIN}$. To estimate lower threshold z_{MIN}, we follow Clauset et al. (2009) by applying the KS approach. This statistic is simply the maximum distance, D, between the data and fitted CDFs, given by
$D = MAX_{z \geq z_{MIN}} |S(z) - P(z)|$,
where $S(z)$ is the CDF of the data for the observation with a value of at least z_{MIN}, and $P(z)$ is the CDF for the power-law model that best fits the data in the region of $z \geq z_{MIN}$. The estimate of z_{MIN} is the value of $\widehat{z}_{MIN}$ that minimizes D. To test the power-law null hypothesis, we follow Clauset et al. (2009) in employing the estimated parameter vector $(\widehat{\alpha}, \widehat{z}_{MIN})$ that is optimal with respect to D in a GoF test, thereby generating a p-value that quantifies the plausibility of the power-law null hypothesis. Specifically, this test compares D from the equation above with distance measurements for comparable synthetic data sets drawn from the hypothesized model. The p-value is defined to be the fraction of synthetic distances that are longer than the empirical distance. Given a significance level of 5%, the power-law null hypothesis is not rejected, as the difference between the empirical data and the model can be attributed to statistical fluctuations alone. Employing detrended fluctuation analysis (DFA) to derive the Hurst exponent we first convert the data series z_t to the mean-centered cumulative sum:
$\widetilde{z}_t = \sum_{t=1}^{T} z_t$.
Then different time scales k are defined, that is, $k \in \{4, 8, 16, 32, 64, 128, 256, 512\}$ for weekly data and $k \in \{4, 8, 16, 32, 64, 128\}$ for monthly data. Depending on the defined time scale, data is split into epochs and for each epoch s, a time series regression is used to detrend the data. For instance, if $k = 512$, weekly data for $\widetilde{z}_t$ is split into two non-overlapping epochs. For each epoch s, the following regression is employed:
$\widetilde{z}_t = \gamma_0 + \gamma_1 t + e_t$,
where $t = 1, \cdots, 512$ for the first epoch and $t = 513, \cdots, 1024$ for the second epoch. Then for each epoch s, the root mean squared error (RMSE) is computed as:
$RMSE_S = \sqrt{\frac{1}{T_s}\sum_{t}^{T_s} \widehat{e}_t}$,
where $T_s = 512$. Finally, the estimates for $RMSE_S$ are averaged for each time scale k, giving us $\overline{RMSE}_k$. According to the theory, the following relation holds:
$\overline{RMSE}_k = ck^H$.
The Hurst exponent is then estimated by computing a linear fit between log-scales and log-$\overline{RMSE}_k$. If the data were independent, the ratio between numerator and denominator should be, according to the theory, 1:2, corresponding to a Hurst exponent of $H = 0.50$. Moreover, $H > 0.50$ implies long-term dependence, that is, a long memory of the stochastic process in which the data are persistent; on the other hand, $H < 0.50$ implies anti-persistence, which is characterized by the tendency to keep back on themselves. To test the dependency in the power-law regime, we code vectors of binary variables. Specifically, vector d_i^M has a value of 1if $z \geq z_{MIN}$ holds for observations in z_i^M and values of 0 otherwise. Summing the values of d_i^M, and dividing the sum by the number of observations (e.g., 256) gives us the percentage of power-law observations in given processes z_i^M which we can interpret as empirical probability and denote it as θ. Assuming independence under the null hypothesis, defining the operator $TL(.)$ that sums consecutive values of 1 in a binary vector and stores them in another vector and using a significance level of 5%, we would not reject the null hypothesis if and only if $\theta^{MAX(TL(d_i^M))} > 0.05$.

From Table 1 we see that $\widehat{H} = 0.9436$ is the maximum for estimated Hurst exponents produced from the benchmark model. Noting moreover that the estimated power-law exponents for the weekly realized variances for crude oil and the S&P 500 are considerably lower than the estimates for weekly realized variances for the GBP/USD exchange or Bitcoin, it may be obvious that the underlying multifractal model is required to produce both a higher level of discontinuity and a higher level of persistence. From Tables 1–4 it

Table 6
Multifractal model of realized monthly asset variances using binominal bending with $p = 0.55$.

Distribution	MAX	MIN	Mean	VAR	α	z_{min}	% #PL	*p*-value (GoF)	Hurst	Time units in PL
<5%	91.3696	2.6447	25.9803	250.9106	3.0603	21.7855	0.0820	0.0000	0.7847	1
Median	120.6268	4.1031	27.0728	314.7829	4.1067	34.9599	0.2539	0.3400	0.8490	1
>95%	189.4988	5.4393	28.2205	407.2549	6.1781	54.6598	0.5352	0.9400	0.9083	3
Min	73.7550	1.6406	25.3189	202.2815	2.5043	14.7438	0.0391	0.0000	0.7404	0
Max	293.4821	6.6686	29.0673	584.3071	8.7385	68.8414	0.8008	1.0000	0.9462	8
Mean	128.0125	4.0820	27.0859	319.1622	4.3002	36.4299	0.2728	0.3916	0.8480	1.6150
Std.Dev	30.7539	0.8466	0.6644	49.4064	1.0090	10.2067	0.1413	0.3238	0.0365	0.9443

Following Mandelbrot (2008), the multifractal process generating asset returns is given as
$y(t) = c(t)x(t)$,
where $c(t)$ is the multiplicative cascade at time t and $x(t)$ $IIDN(0,1)$. We use binominal bending of time with probability $p = 0.55$ and $(1-p) = 0.45$ for deriving deformed time. Monthly variance is found by squaring each element in y_i and then summing five consecutive, nonoverlapping elements, such as
$z_i^M = \left(\sum_{t=1}^{20} y_{t,i}^2, \sum_{t=21}^{40} y_{t,i}^2, \cdots, \sum_{t=5101}^{5120} y_{t,i}^2\right)'$,
where z_i^M has the dimension 256×1 and $i = 1, \cdots, 1000$. To investigate the tail properties for each vector z_i^M, we use the following model:
$p(z) = Bz^{-\alpha}$,
where $B = (\alpha - 1)z_{MIN}^{\alpha-1}$ with $\alpha \in \{\mathbb{R}_+ | \alpha > 1\}$, $z \in \{\mathbb{R}_+ | z_{MIN} \leq z < \infty\}$, z_{MIN} is the minimum value of realized-variance observations governed by the power law, and α is the magnitude of tail exponent. Following White, Enquist, and Green (2008) and Clauset et al. (2009), we employ MLE and estimate the tail exponent as
$$\widehat{\alpha} = 1 + N\left(\sum_{i=1}^{N} \ln\left(\frac{z_i}{z_{MIN}}\right)\right)^{-1},$$
where $\widehat{\alpha}$ denotes the MLE estimator, and N denotes the number of sample observations exceeding z, that is, $z_i \geq z_{MIN}$. To estimate lower threshold z_{MIN}, we follow Clauset et al. (2009) by applying the KS approach. This statistic is simply the maximum distance, D, between the data and fitted CDFs, given by
$D = MAX_{z \geq z_{MIN}} |S(z) - P(z)|$,
where $S(z)$ is the CDF of the data for the observation with a value of at least z_{MIN}, and $P(z)$ is the CDF for the power-law model that best fits the data in the region of $z \geq z_{MIN}$. The estimate of z_{MIN} is the value of $\widehat{z}_{MIN}$ that minimizes D. To test the power-law null hypothesis, we follow Clauset et al. (2009) in employing the estimated parameter vector $(\widehat{\alpha}, \widehat{z}_{MIN})$ that is optimal with respect to D in a GoF test, thereby generating a p-value that quantifies the plausibility of the power-law null hypothesis. Specifically, this test compares D from the equation above with distance measurements for comparable synthetic data sets drawn from the hypothesized model. The p-value is defined to be the fraction of synthetic distances that are longer than the empirical distance. Given a significance level of 5%, the power-law null hypothesis is not rejected, as the difference between the empirical data and the model can be attributed to statistical fluctuations alone. Employing detrended fluctuation analysis (DFA) to derive the Hurst exponent we first convert the data series z_t to the mean-centered cumulative sum:
$\widetilde{z}_t = \sum_{t=1}^{T} z_t$.
Then different time scales k are defined, that is, $k \in \{4, 8, 16, 32, 64, 128, 256, 512\}$ for weekly data and $k \in \{4, 8, 16, 32, 64, 128\}$ for monthly data. Depending on the defined time scale, data is split into epochs and for each epoch s, a time series regression is used to detrend the data. For instance, if $k = 512$, weekly data for $\widetilde{z}_t$ is split into two non-overlapping epochs. For each epoch s, the following regression is employed:
$\widetilde{z}_t = \gamma_0 + \gamma_1 t + e_t$,
where $t = 1, \cdots, 512$ for the first epoch and $t = 513, \cdots, 1024$ for the second epoch. Then for each epoch s, the root mean squared error (RMSE) is computed as:
$$RMSE_S = \sqrt{\frac{1}{T_s}\sum_{t}^{T_s} \widehat{e}_t},$$
where $T_s = 512$. Finally, the estimates for $RMSE_S$ are averaged for each time scale k, giving us $\overline{RMSE}_k$. According to the theory, the following relation holds:
$\overline{RMSE}_k = ck^H$.
The Hurst exponent is then estimated by computing a linear fit between log-scales and log-$\overline{RMSE}_k$. If the data were independent, the ratio between numerator and denominator should be, according to the theory, 1:2, corresponding to a Hurst exponent of $H = 0.50$. Moreover, $H > 0.50$ implies long-term dependence, that is, a long memory of the stochastic process in which the data are persistent; on the other hand, $H < 0.50$ implies anti-persistence, which is characterized by the tendency to keep back on themselves. To test the dependency in the power-law regime, we code vectors of binary variables. Specifically, vector d_i^M has a value of 1if $z \geq z_{MIN}$ holds for observations in z_i^M and values of 0 otherwise. Summing the values of d_i^M, and dividing the sum by the number of observations (e.g., 256) gives us the percentage of power-law observations in given processes z_i^M which we can interpret as empirical probability and denote it as θ. Assuming independence under the null hypothesis, defining the operator $TL(.)$ that sums consecutive values of 1 in a binary vector and stores them in another vector and using a significance level of 5%, we would not reject the null hypothesis if and only if $\theta^{MAX(TL(d_i^M))} > 0.05$.

becomes evident that the model derived from a multiplicative cascade with $p = 0.70$ could be a potential candidate. We observe from Table 4 that this model predicts that 95% of the simulated values for α, it holds that $\alpha < 2.2343$. Since $\widehat{\alpha}$ for the weekly realized variances for crude oil and the S&P 500 (viz., $\widehat{\alpha} = 2.1959$ and $\widehat{\alpha} = 2.1746$) $\widehat{\alpha} < 2.2343$ holds, we cannot reject the model with respect to the power-law exponent. On the other hand, even though this model produces the highest level of persistence in weekly realized

Table 7
Multifractal model of realized monthly asset variances using binominal bending with $p = 0.65$.

Distribution	MAX	MIN	Mean	VAR	α	z_{min}	% #PL	*p*-value (GoF)	Hurst	MAX time units in PL
<5%	1377.2700	0.1492	77.5893	26650.5987	1.7571	21.4816	0.0625	0.0000	0.8526	3
Median	2686.8215	0.2782	88.3389	53639.4745	2.1902	96.3357	0.2188	0.3300	0.9184	10
>95%	5766.3069	0.4604	105.0133	154094.2047	3.0244	329.2078	0.5469	0.9500	0.9901	23
Min	818.0499	0.0692	69.0296	15397.5732	1.6168	11.4208	0.0352	0.0000	0.7891	2
Max	13966.4253	0.6734	127.2540	771240.3391	4.3112	520.5462	0.6836	1.0000	1.0271	47
Mean	3020.7764	0.2871	89.3733	68991.7444	2.2684	125.2794	0.2533	0.4000	0.9197	11.9840
Std.Dev	1523.7510	0.0943	8.4947	57880.0493	0.4125	97.9644	0.1498	0.3400	0.0426	7.1031

Following Mandelbrot (2008), the multifractal process generating asset returns is given as
$y(t) = c(t)x(t)$,
where $c(t)$ is the multiplicative cascade at time t and $x(t)$ $IIDN(0,1)$. We use binominal bending of time with probability $p = 0.65$ and $(1-p) = 0.35$ for deriving deformed time. Monthly variance is found by squaring each element in y_i and then summing five consecutive, nonoverlapping elements, such as
$z_i^M = \left(\sum_{t=1}^{20} y_{t,i}^2, \sum_{t=21}^{40} y_{t,i}^2, \cdots, \sum_{t=5101}^{5120} y_{t,i}^2\right)'$,
where z_i^M has the dimension 256×1 and $i = 1, \cdots, 1000$. To investigate the tail properties for each vector z_i^M, we use the following model:
$p(z) = Bz^{-\alpha}$,
where $B = (\alpha - 1)z_{MIN}^{\alpha-1}$ with $\alpha \in \{\mathbb{R}_+ | \alpha > 1\}$, $z \in \{\mathbb{R}_+ | z_{MIN} \leq z < \infty\}$, z_{MIN} is the minimum value of realized-variance observations governed by the power law, and α is the magnitude of tail exponent. Following White, Enquist, and Green (2008) and Clauset et al. (2009), we employ MLE and estimate the tail exponent as
$\widehat{\alpha} = 1 + N\left(\sum_{i=1}^{N} \ln\left(\frac{z_i}{z_{MIN}}\right)\right)^{-1}$,
where $\widehat{\alpha}$ denotes the MLE estimator, and N denotes the number of sample observations exceeding z, that is, $z_i \geq z_{MIN}$. To estimate lower threshold z_{MIN}, we follow Clauset et al. (2009) by applying the KS approach. This statistic is simply the maximum distance, D, between the data and fitted CDFs, given by
$D = MAX_{z \geq z_{MIN}} |S(z) - P(z)|$,
where $S(z)$ is the CDF of the data for the observation with a value of at least z_{MIN}, and $P(z)$ is the CDF for the power-law model that best fits the data in the region of $z \geq z_{MIN}$. The estimate of z_{MIN} is the value of $\widehat{z}_{MIN}$ that minimizes D. To test the power-law null hypothesis, we follow Clauset et al. (2009) in employing the estimated parameter vector $(\widehat{\alpha}, \widehat{z}_{MIN})$ that is optimal with respect to D in a GoF test, thereby generating a p-value that quantifies the plausibility of the power-law null hypothesis. Specifically, this test compares D from the equation above with distance measurements for comparable synthetic data sets drawn from the hypothesized model. The p-value is defined to be the fraction of synthetic distances that are longer than the empirical distance. Given a significance level of 5%, the power-law null hypothesis is not rejected, as the difference between the empirical data and the model can be attributed to statistical fluctuations alone. Employing detrended fluctuation analysis (DFA) to derive the Hurst exponent we first convert the data series z_t to the mean-centered cumulative sum:
$\widetilde{z}_t = \sum_{t=1}^{T} z_t$.
Then different time scales k are defined, that is, $k \in \{4, 8, 16, 32, 64, 128, 256, 512\}$ for weekly data and $k \in \{4, 8, 16, 32, 64, 128\}$ for monthly data. Depending on the defined time scale, data is split into epochs and for each epoch s, a time series regression is used to detrend the data. For instance, if $k = 512$, weekly data for $\widetilde{z}_t$ is split into two non-overlapping epochs. For each epoch s, the following regression is employed:
$\widetilde{z}_t = \gamma_0 + \gamma_1 t + e_t$,
where $t = 1, \cdots, 512$ for the first epoch and $t = 513, \cdots, 1024$ for the second epoch. Then for each epoch s, the root mean squared error (RMSE) is computed as:
$RMSE_S = \sqrt{\frac{1}{T_s}\sum_{t}^{T_s} \widehat{e}_t}$,
where $T_s = 512$. Finally, the estimates for $RMSE_S$ are averaged for each time scale k, giving us $\overline{RMSE}_k$. According to the theory, the following relation holds:
$\overline{RMSE}_k = ck^H$.
The Hurst exponent is then estimated by computing a linear fit between log-scales and log-$\overline{RMSE}_k$. If the data were independent, the ratio between numerator and denominator should be, according to the theory, 1:2, corresponding to a Hurst exponent of $H = 0.50$. Moreover, $H > 0.50$ implies long-term dependence, that is, a long memory of the stochastic process in which the data are persistent; on the other hand, $H < 0.50$ implies anti-persistence, which is characterized by the tendency to keep back on themselves. To test the dependency in the power-law regime, we code vectors of binary variables. Specifically, vector d_i^M has a value of 1if $z \geq z_{MIN}$ holds for observations in z_i^M and values of 0 otherwise. Summing the values of d_i^M, and dividing the sum by the number of observations (e.g., 256) gives us the percentage of power-law observations in given processes z_i^M which we can interpret as empirical probability and denote it as θ. Assuming independence under the null hypothesis, defining the operator $TL(.)$ that sums consecutive values of 1 in a binary vector and stores them in another vector and using a significance level of 5%, we would not reject the null hypothesis if and only if $\theta^{MAX(TL(d_i^M))} > 0.05$.

variances, we see that 95% of the simulated values for H, it holds that $H < 0.9269$. These results imply apparently that this model is not either capable of describing the dependency structures we observe for weekly realized variances for the crude oil and the S&P 500. In Fig. 12, we extend Fig. 11 by identifying the locations for $(\widehat{H}, \widehat{\alpha})$ for the weekly realized variance for the GBP/USD exchange rate, Bitcoin, crude oil, and the S&P 500. Whereas $(\widehat{H}, \widehat{\alpha})$ for the weekly realized variances for the GBP/USD exchange rate and Bitcoin are

Table 8
Multifractal model of realized monthly asset variances using binominal bending with $p = 0.70$.

Distribution	MAX	MIN	Mean	VAR	α	z_{min}	% #PL	*p*-value (GoF)	Hurst	MAX time units in PL
<5%	5130.8344	0.0213	159.3852	265986.3603	1.5549	17.0792	0.0703	0.0000	0.8339	2
Median	11305.3606	0.0455	201.8881	772563.1391	1.8752	134.4935	0.2109	0.3100	0.9160	5
>95%	31969.8684	0.0840	284.9393	4178034.3577	2.4646	645.0536	0.5313	0.9500	1.0110	18
Min	2667.1790	0.0076	130.2070	126829.9017	1.4697	8.3098	0.0391	0.0000	0.7589	1
Max	84030.9219	0.1415	466.7060	27626735.0963	3.3163	1305.4364	0.6680	1.0000	1.0987	31
Mean	13974.2582	0.0482	210.0583	1338032.5012	1.9187	204.9380	0.2533	0.3701	0.9176	7.4640
Std.Dev	9349.9590	0.0196	42.4462	2029000.8881	0.2916	211.1264	0.1464	0.3277	0.0557	5.0040

Following Mandelbrot (2008), the multifractal process generating asset returns is given as
$y(t) = c(t)x(t)$,
where $c(t)$ is the multiplicative cascade at time t and $x(t)$ $IIDN(0,1)$. We use binominal bending of time with probability $p = 0.65$ and $(1-p) = 0.35$ for deriving deformed time. Monthly variance is found by squaring each element in y_i and then summing five consecutive, nonoverlapping elements, such as

$$z_i^M = \left(\sum_{t=1}^{20} y_{t,i}^2, \sum_{t=21}^{40} y_{t,i}^2, \cdots, \sum_{t=5101}^{5120} y_{t,i}^2\right)',$$

where z_i^M has the dimension 256×1 and $i = 1, \cdots, 1000$. To investigate the tail properties for each vector z_i^M, we use the following model:
$p(z) = Bz^{-\alpha}$,
where $B = (\alpha - 1)z_{MIN}^{\alpha-1}$ with $\alpha \in \{\mathbb{R}_+ | \alpha > 1\}$, $z \in \{\mathbb{R}_+ | z_{MIN} \leq z < \infty\}$, z_{MIN} is the minimum value of realized-variance observations governed by the power law, and α is the magnitude of tail exponent. Following White, Enquist, and Green (2008) and Clauset et al. (2009), we employ MLE and estimate the tail exponent as

$$\widehat{\alpha} = 1 + N\left(\sum_{i=1}^{N} \ln\left(\frac{z_i}{z_{MIN}}\right)\right)^{-1},$$

where $\widehat{\alpha}$ denotes the MLE estimator, and N denotes the number of sample observations exceeding z, that is, $z_i \geq z_{MIN}$. To estimate lower threshold z_{MIN}, we follow Clauset et al. (2009) by applying the KS approach. This statistic is simply the maximum distance, D, between the data and fitted CDFs, given by
$D = MAX_{z \geq z_{MIN}} |S(z) - P(z)|$,
where $S(z)$ is the CDF of the data for the observation with a value of at least z_{MIN}, and $P(z)$ is the CDF for the power-law model that best fits the data in the region of $z \geq z_{MIN}$. The estimate of z_{MIN} is the value of $\widehat{z}_{MIN}$ that minimizes D. To test the power-law null hypothesis, we follow Clauset et al. (2009) in employing the estimated parameter vector $(\widehat{\alpha}, \widehat{z}_{MIN})$ that is optimal with respect to D in a GoF test, thereby generating a p-value that quantifies the plausibility of the power-law null hypothesis. Specifically, this test compares D from the equation above with distance measurements for comparable synthetic data sets drawn from the hypothesized model. The p-value is defined to be the fraction of synthetic distances that are longer than the empirical distance. Given a significance level of 5%, the power-law null hypothesis is not rejected, as the difference between the empirical data and the model can be attributed to statistical fluctuations alone. Employing detrended fluctuation analysis (DFA) to derive the Hurst exponent we first convert the data series z_t to the mean-centered cumulative sum:
$\widetilde{z}_t = \sum_{t=1}^{T} z_t$.
Then different time scales k are defined, that is, $k \in \{4, 8, 16, 32, 64, 128, 256, 512\}$ for weekly data and $k \in \{4, 8, 16, 32, 64, 128\}$ for monthly data. Depending on the defined time scale, data is split into epochs and for each epoch s, a time series regression is used to detrend the data. For instance, if $k = 512$, weekly data for $\widetilde{z}_t$ is split into two non-overlapping epochs. For each epoch s, the following regression is employed:
$\widetilde{z}_t = \gamma_0 + \gamma_1 t + e_t$,
where $t = 1, \cdots, 512$ for the first epoch and $t = 513, \cdots, 1024$ for the second epoch. Then for each epoch s, the root mean squared error (RMSE) is computed as:

$$RMSE_S = \sqrt{\frac{1}{T_s}\sum_{t}^{T_s} \widehat{e}_t},$$

where $T_s = 512$. Finally, the estimates for $RMSE_S$ are averaged for each time scale k, giving us $\overline{RMSE}_k$. According to the theory, the following relation holds:
$\overline{RMSE}_k = ck^H$.
The Hurst exponent is then estimated by computing a linear fit between log-scales and log-$\overline{RMSE}_k$. If the data were independent, the ratio between numerator and denominator should be, according to the theory, 1:2, corresponding to a Hurst exponent of $H = 0.50$. Moreover, $H > 0.50$ implies long-term dependence, that is, a long memory of the stochastic process in which the data are persistent; on the other hand, $H < 0.50$ implies anti-persistence, which is characterized by the tendency to keep back on themselves. To test the dependency in the power-law regime, we code vectors of binary variables. Specifically, vector $\boldsymbol{d}_i^M$ has a value of 1if $z \geq z_{MIN}$ holds for observations in z_i^M and values of 0 otherwise. Summing the values of $\boldsymbol{d}_i^M$, and dividing the sum by the number of observations (e.g., 256) gives us the percentage of power-law observations in given processes z_i^M which we can interpret as empirical probability and denote it as θ. Assuming independence under the null hypothesis, defining the operator $TL(.)$ that sums consecutive values of 1 in a binary vector and stores them in another vector and using a significance level of 5%, we would not reject the null hypothesis if and only if $\theta^{MAX\left(TL\left(d_i^W\right)\right)} > 0.05$.

well-located in the scatter of estimates produced from the benchmark model, the estimates for $\widehat{H}$ for the weekly realized variances for crude oil and the S&P 500 are outside the range of estimates produced from the multifractal model based on a multiplicative cascade with $p = 0.70$.

Table 9
Weekly realized asset market variances.

Asset market	MAX	MIN	VAR	α	z_{min}	%#PL	*p*-value (GoF)	Hurst (Std.Dev)	MAX time units in PL
GBP/USD	61.3011	0.0302	9.3941	2.8424	1.4554	32.81%	0.7450	0.8394 (0.0260)	7
Bitcoin	1566.5330	0.2240	15470.7900	2.9474	143.3561	15.04%	0.2220	0.8955 (0.0196)	10
Crude oil	833.2175	0.0959	9016.5020	2.1959	23.3077	34.38%	0.8420	1.1777 (0.0331)	18
S&P 500	380.1593	0.0186	380.4374	2.1746	2.8107	48.44%	0.0320	1.1165 (0.0431)	23

We download daily data on the GBP/USD exchange rate, Bitcoin, crude oil, and the S&P 500. All data series end on the same day—April 19, 2022. Retrieving 2561 daily observations, the starting dates for the GBP/USD exchange rate, Bitcoin, crude oil, and the S&P 500 are April 17, 2015, June 27, 2012, February 17, 2012, and February 15, 2012, respectively. Computing the daily returns from price data for each data gives us 2560 daily returns, and using the sum of five consecutive and squared daily observations provides us with 512 weekly realized-variance observations. This table reports the same statistical metrics as for the simulated models.

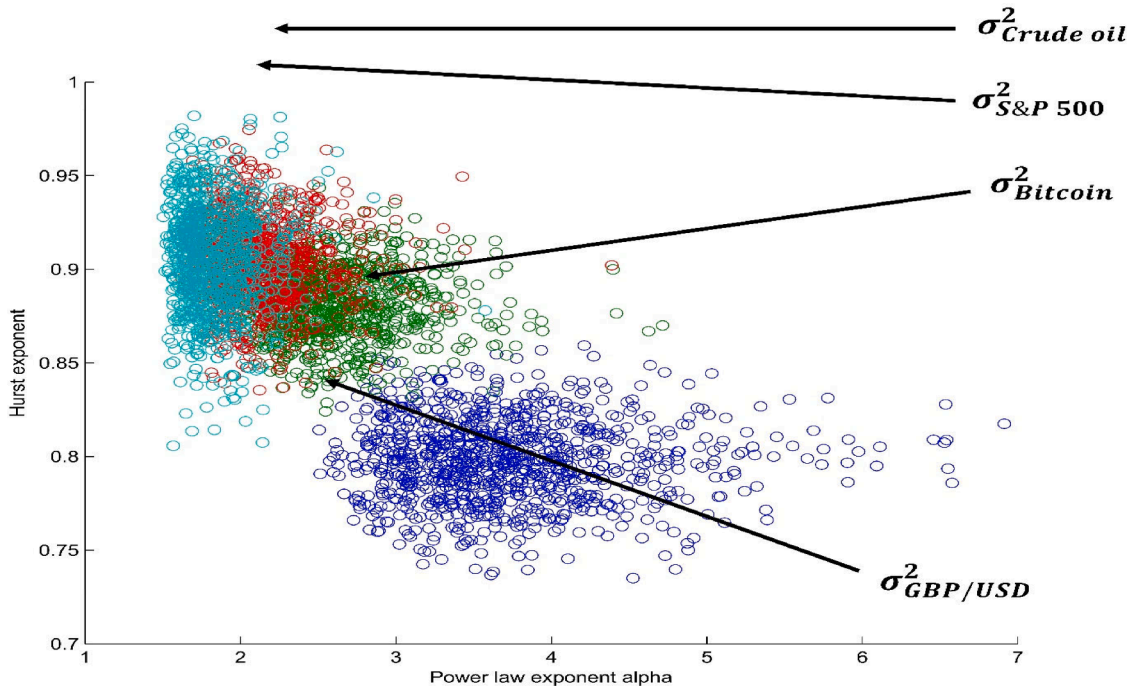

Fig. 12. Testing the Multifractal Model using real life data. This Figure plots the estimated power-law exponents against the corresponding estimated Hurst exponents for all multifractal models. Each model builds one of the four clusters. The turquoise, red, green, and blue clusters of estimated power-law and Hurst exponents correspond to the multifractal models derived from binominal multiplicative cascades with $p = 0.70$, $p = 0.65$, $p = 0.60$, and $p = 0.55$, respectively. The correlation between average power-law exponents and average Hurst exponents is −0.9781. Additionally, daily data on the GBP/USD exchange rate, Bitcoin, crude oil, and the S&P 500 is downloaded. All data series end on the same day—April 19, 2022. Retrieving 2561 daily observations, the starting dates for the GBP/USD exchange rate, Bitcoin, crude oil, and the S&P 500 are April 17, 2015, June 27, 2012, February 17, 2012, and February 15, 2012, respectively. Computing the daily returns from price data for each data gives us 2560 daily returns, and using the sum of five consecutive and squared daily observations provides us with 512 weekly realized-variance observations for $\sigma^2_{GBP/USD}$, $\sigma^2_{Bitcoin}$, $\sigma^2_{Crudeoil}$, and $\sigma^2_{S\&P500}$. Then for each data, the specific power-law exponent (α) and Hurst exponent (H) are estimated. The specific locations for $\sigma^2_{GBP/USD}$, $\sigma^2_{Bitcoin}$, $\sigma^2_{Crudeoil}$, and $\sigma^2_{S\&P500}$ in H/α – diagram are marked via arrows. (For interpretation of the references to colour in this figure legend, the reader is referred to the web version of this article.)

However, as mentioned earlier, the estimates for the models reported in Tables 1–4 are derived from 1024 simulated sample observations. If less observations are included, the range for possible values for $\widehat{\alpha}$ and $\widehat{H}$ will inevitably widen. To illustrate this issue, in Fig. A.13 we plot the estimated power-law exponents against the corresponding estimated Hurst exponents for the multifractal model derived from a binominal multiplicative cascade with $p = 0.70$. Whereas the estimates for the Hurst exponents illustrated by the green cluster incorporate 1024 simulated sample observations, the estimates for the Hurst exponents illustrated by the blue cluster incorporate only 256 simulated sample observations. To make the results comparable, for both clusters, the estimated power-law exponents

are based on the same model incorporating all simulated sample observations (viz., 1024 observations). We observe from Fig. A.13 that as we account for less observations, the estimates for $\widehat{H}$ for both the weekly variance for crude oil (viz., $\widehat{H} = 1.1777$) and the weekly variance for the S&P 500 (viz., $\widehat{H} = 1.1165$) are clearly covered from the multifractal model derived from a multiplicative cascade with $p = 0.70$.

Overall, whereas the evidence suggests that the multifractal benchmark model derived from a multiplicative cascade with $p = 0.60$ is capable of describing the discontinuity and dependency structure we observe for weekly realized variances for the GBP/USD exchange rate and Bitcoin, pricing the weekly realized variances for crude oil and the S&P 500 requires more extreme bending of time manifested in a multiplicative cascade with $p = 0.70$. In the same manner, we can test the properties of the realized asset variances based on monthly data as reported in Table A.1 in the appendix. The main results do not change.

5. Discussion

5.1. Computation and usage of realized variances in finance research

This paper uses the MMAR in the spirit of Mandelbrot et al. (1997b) to model realized variance processes. In doing so, we note that realized variance or volatility, as proposed first from Andersen et al. (2001), is an alternative measure of the variability of asset prices which is considered a consistent and highly efficient nonparametric estimator. We note that the approach in our study requires to interpret the output of the MMAR as daily returns of some financial assets. Summing squared daily returns to obtain weekly or monthly variances seems to be common practice in the finance literature. For instance, Moreira and Muir (2017) construct asset portfolios that scale monthly returns by the inverse of their previous month's realized variance, decreasing risk exposure when variance was recently high and vice versa. They estimate the realized monthly portfolio variance by summing up the squared daily returns over the past 22 trading days. In the same manner, Grobys, Ruotsalainen and Äijö (2018) and Grobys and Vähämaa (2020) use the exact number of trading days for each month varying from 15 to 27 to compute monthly realized variances for industrial momentum strategies, the stock price momentum factor and the value factor. Our approach is in line with this literature as we use the sum of 20 (5) consecutive nonoverlapping squared observations to compute the monthly (weekly) realized variance. On the one hand, one could argue that using intraday data would perhaps result in less noisy estimates for the realized variances. On the other hand, one could have the view that high frequency data could be polluted with a substantially higher degree of noise. In this regard, Mandelbrot (2008) points out that high frequency data may suffer from microstructure issues. For instance, foreign exchange rate data having a higher frequency than two hours or a lower frequency that 180 days are subject to crossovers: points where the mathematical relation takes a hold. In addition, Mandelbrot (2008) highlights that crossovers are common for real as opposed to theoretical fractal data. While the current research follows this view of the literature, future research could extend our proposed model framework to the usage of higher frequented financial data.

5.2. Commonalities of realized asset market variances

Next, a stream of recent literature explores the power-law properties of realized variances/volatilities (Grobys et al., 2021; Grobys, 2021, 2023; Grobys and Kolari, 2022). The current study proposes that the realized variances for the GBP/USD exchange rate and Bitcoin share the same underlying "uncertainty generator." On the other hand, the realized variances for crude oil and the S&P 500 share another common "uncertainty generator." Time deformation in the latter two asset markets appears to be much more extreme than in the former two and requires a multiplicative cascade using $p = 0.70$ as opposed $p = 0.60$. However, both models share a commonality manifested in multiplicative cascade derived from binominal bending of time as proposed first by Mandelbrot et al. (1997b). This is indeed a novel finding. There is no other such model available in the literature that would exhibit such properties. Future research is still needed to explore whether our proposed model is capable of describing the variance evolutions for single assets such as stocks or cryptocurrencies exhibiting lower market capitalizations than Bitcoin which is the market leader and perhaps lacks representativeness for the cryptocurrency asset market.

5.3. Other multifractal model frameworks

Segnon and Lux (2013) point out that in its original setting, the multifractal set in line with Mandelbrot et al. (1997b) results from operations performed on probability measures. The creation of a multifractal cascade is initiated by assigning uniform probability to a bounded interval. However, many variations of the above generating mechanism have been discussed in the literature such as the grid-free Poisson multifractal measure (Calvet and Fisher, 2001) or Lognormal, Poisson and Gamma distributions (Calvet and Fisher, 2002), among others. Interestingly, Segnon and Lux (2013) argue that the MMAR in its original setting has not been pursued further in subsequent literature despite the attractiveness of its stochastic properties. The main drawback is according to the authors that its practical applicability suffers from the combinatorial nature of the subordinator and its non-stationarity due to the restriction of this measure to a bounded interval. While the authors highlight that these potential limitations have been overcome by the analogous iterative time series models introduced by Calvet and Fisher (2001, 2004), the current research argues that using modern bootstrapping techniques such as blocks bootstraps with randomly chosen block lengths, as proposed in Grobys and Junttila (2021), ensures stationary of the subordinator as any bounded interval could be arbitrarily extended to any desired sample length without altering the original stochastic properties. While the current research extends Mandelbrot's (2008) proposed multifractal setting,

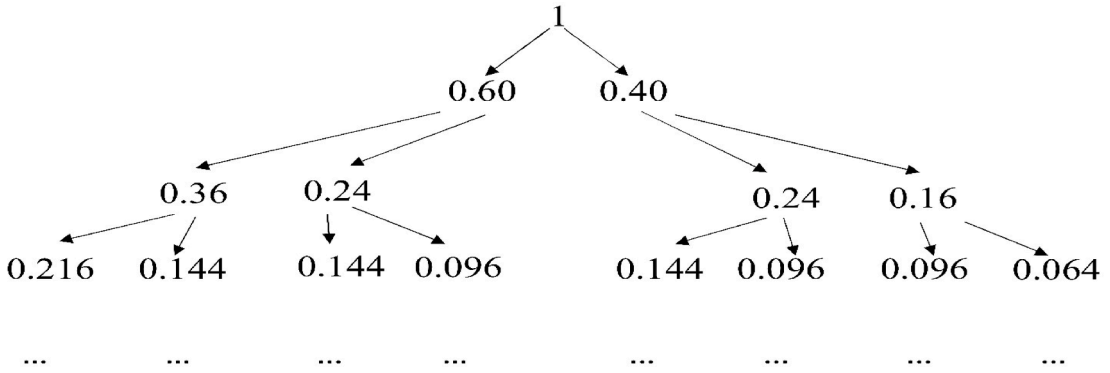

Fig. A1. Binominal tree. This figure illustrates the binominal tree used for constructing the deformed trading time. Following Mandelbrot (2008), the probabilities $p = 0.60$ and $(1-p) = 0.40$ are used. This figure shows the first three iterations of the binominal tree. In each iteration, each figure is multiplied with $p = 0.60$ and $(1-p) = 0.40$.

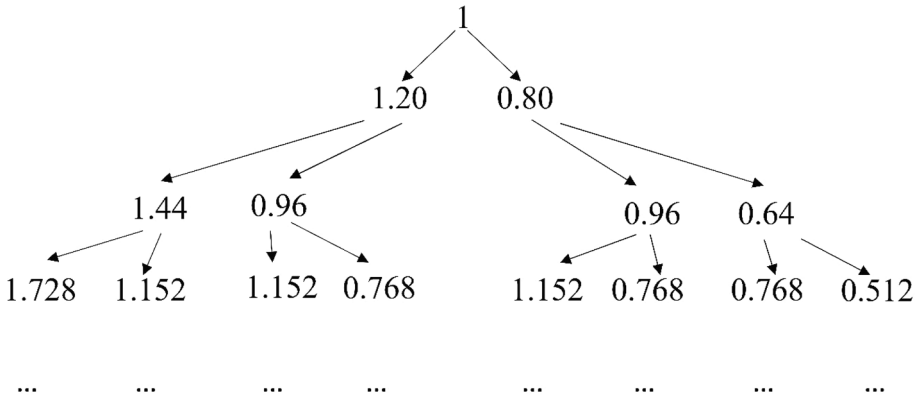

Fig. A2. Deformed trading time. This figure illustrates how the binominal tree illustrated in Fig. A.1 is transformed into trading time by multiplying each figure by the number of elements in each iteration. For instance, considering the second iteration the vector for the deformed trading time (1.44, 0.96, 0.96, 0.64) is retrieved by multiplying (0.36, 0.24, 0.24, 0.16) with 4.

future research is encouraged to compare the performance of our model with multifractal models using other frameworks such as those discussed in Calvet and Fisher (2001; 2002; 2004). Since this exceeds the scope of the current study by a substantial margin, this is left for future research.

5.4. Detrended fluctuation analysis or rescaled range analysis?

This study employed detrended fluctuation analysis (DFA) to estimate Hurst exponent, whereas Mandelbrot (2008) suggested using rescale range (R/S) analysis. The R/S statistic was derived and detailed by Mandelbrot (1969, 1971, 1972) and Mandelbrot and Wallis (1969) and can be, according to Mandelbrot (2008, p. 298–299), summarized as

$$R/S_k = \frac{MAX_{1\le k\le T}\sum_{j=1}^{k}\left(z_j-\bar{z}_T\right) - MIN_{1\le k\le T}\sum_{j=1}^{k}\left(z_j-\bar{z}_T\right)}{\left[\frac{1}{T}\sum_j\left(z_j-\bar{z}_T\right)^2\right]^{1/2}}$$

where average variance $\bar{z}_T$ is calculated for each cluster of size k. For each subsample cluster k, the difference between variance z_j over that period and average variance $\bar{z}_T$ is calculated while keeping a running total of all the differences as the time period lengthens up to period k. This has to be done for $k \in \{4, 8, 16, 32, 64, 128, 256, 512\}$ for weekly data and $k \in \{4, 8, 16, 32, 64, 128\}$ for monthly data and then the maximum (*MAX*) and minimum (*MIN*) of all those differences are taken. The estimate of the range from peak to through in the accumulated deviations is simply computed by the differences between the corresponding maximum and minimum, which is the numerator of Equation (10). The denominator is simply the standard deviation of the respective data. If the data were independent, the ratio between numerator and denominator should be, according to Mandelbrot, 1:2, corresponding to a Hurst exponent of $H = 0.50$. Moreover, $H > 0.50$ implies long-term dependence, that is, a long memory of the stochastic process in which the data are persistent; on the other hand, $H < 0.50$ implies antipersistence, which is characterized by the tendency to keep back on themselves. According to the theory,

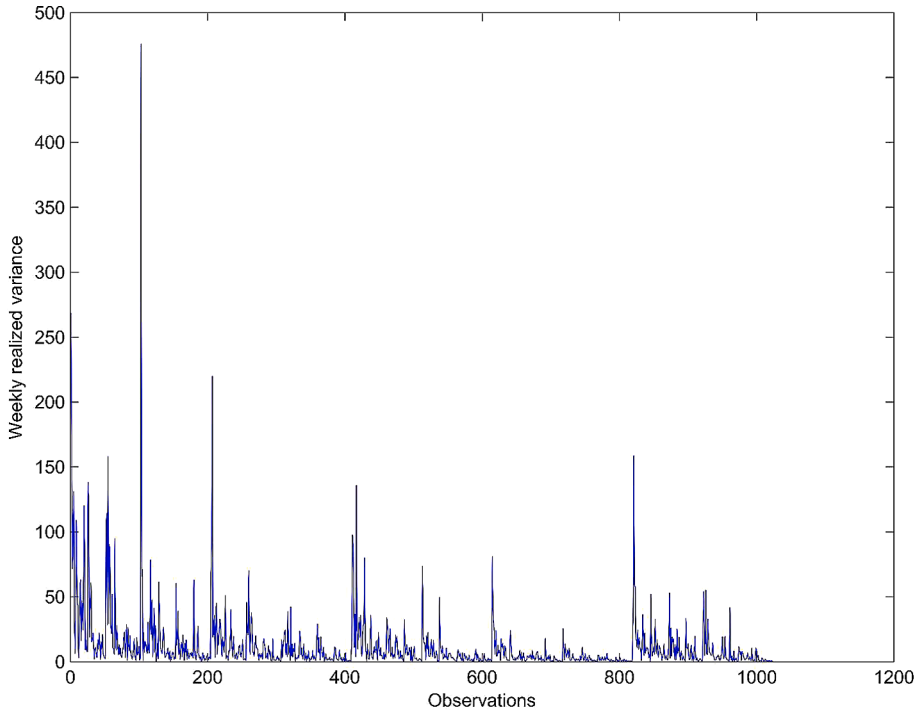

Fig. A3. Weekly realized variance using a binominal multiplicative cascade with $p = 0.60$. This Figure plots the first time-series vector for the simulated weekly asset variances using a multiplicative cascade with $p = 0.60$.

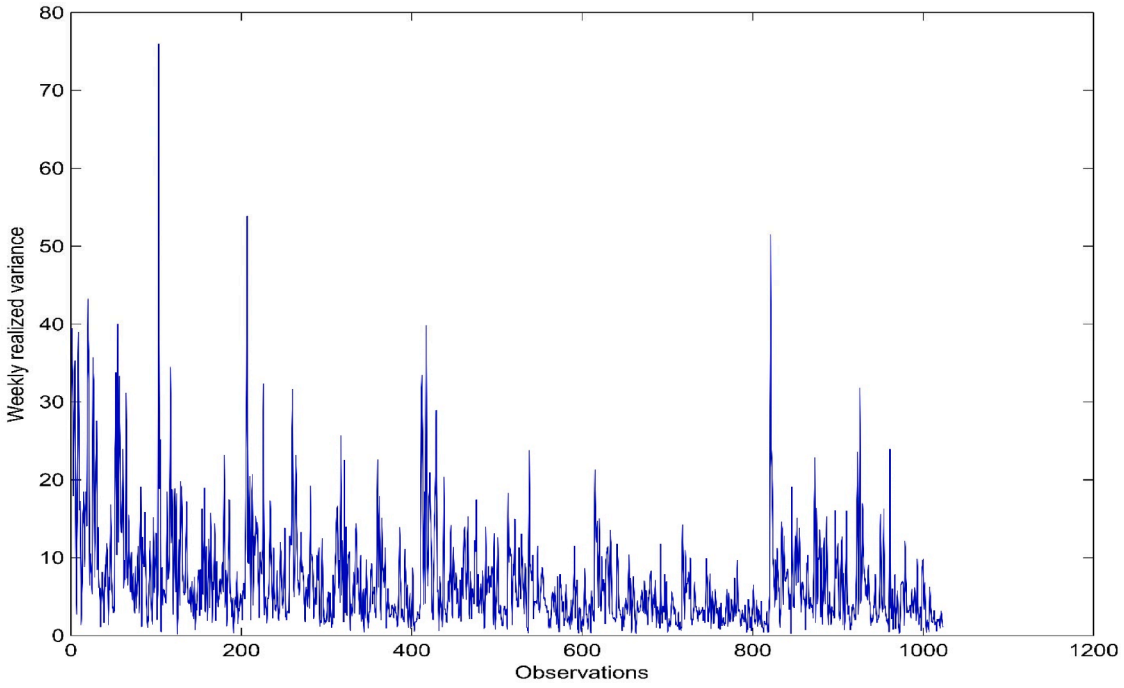

Fig. A4. Weekly realized variance using a binominal multiplicative cascade with $p = 0.55$. This Figure plots the first time-series vector for the simulated weekly asset variances using a multiplicative cascade with $p = 0.55$.

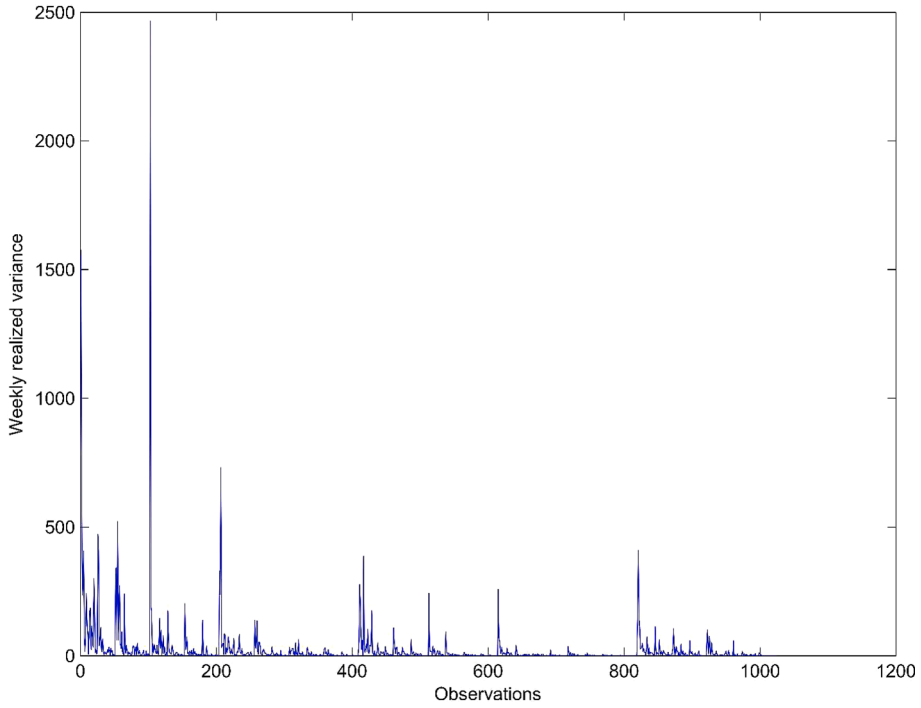

Fig. A5. Weekly realized variance using a binominal multiplicative cascade with $p = 0.65$. This Figure plots the first time-series vector for the simulated weekly asset variances using a multiplicative cascade with $p = 0.65$.

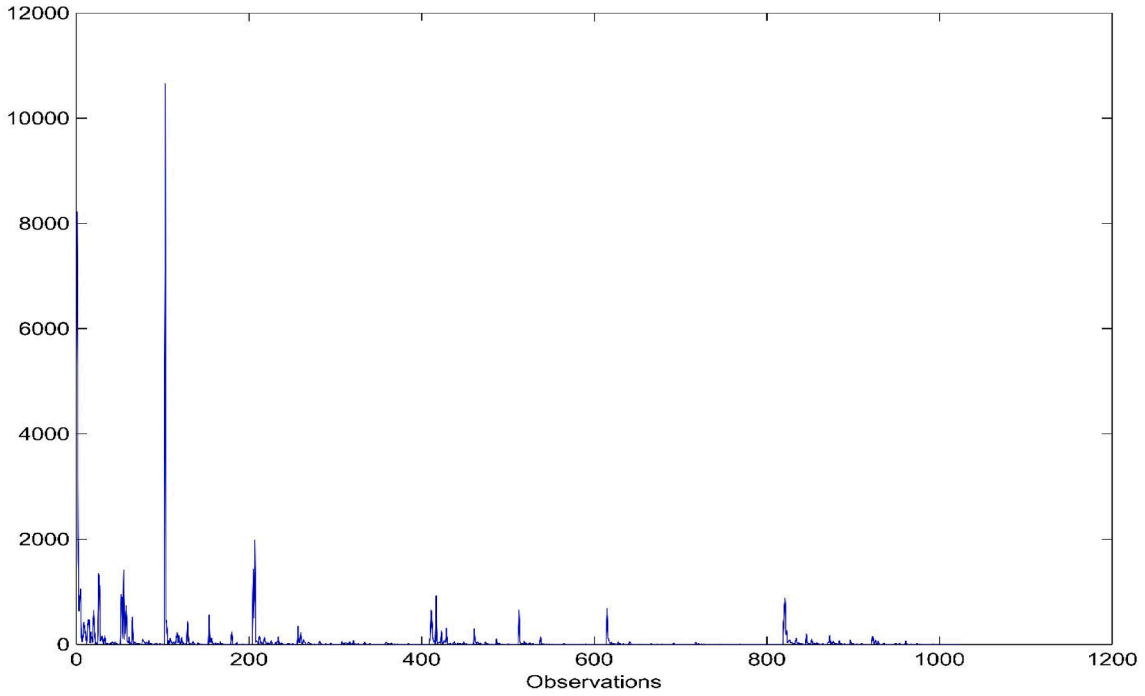

Fig. A6. Weekly realized variance using a binominal multiplicative cascade with $p = 0.70$. This Figure plots the first time-series vector for the simulated weekly asset variances using a multiplicative cascade with $p = 0.70$.

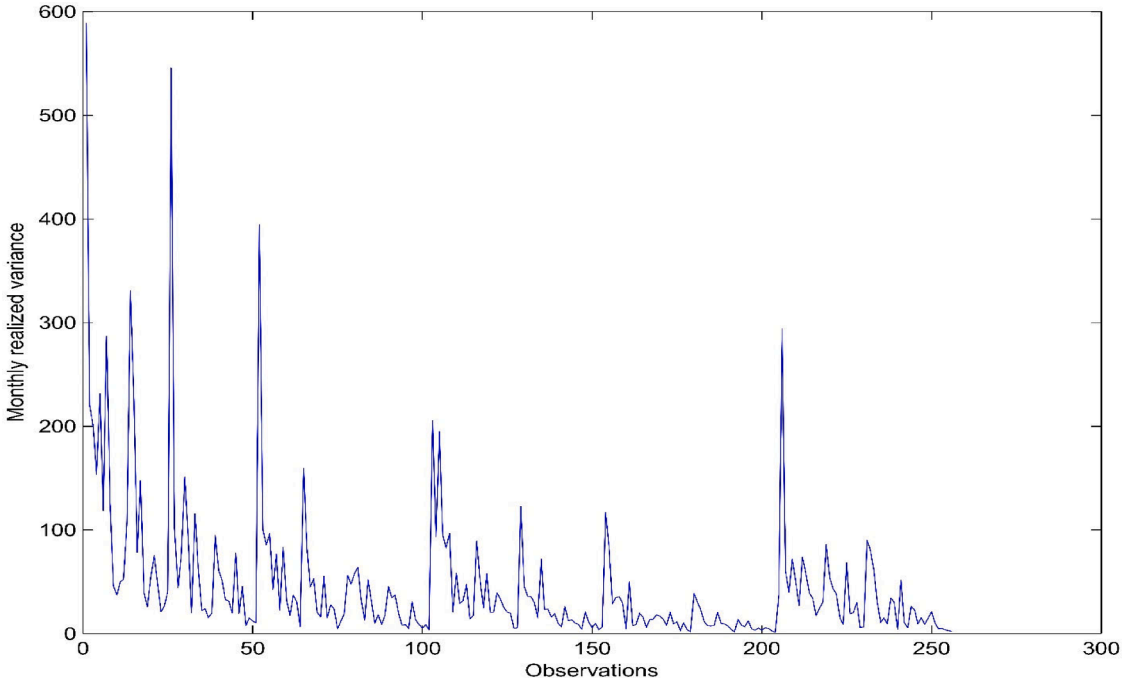

Fig. A7. Monthly realized variance using a binominal multiplicative cascade with $p = 0.60$. This Figure plots the first time-series vector for the simulated monthly asset variances using a multiplicative cascade with $p = 0.60$.

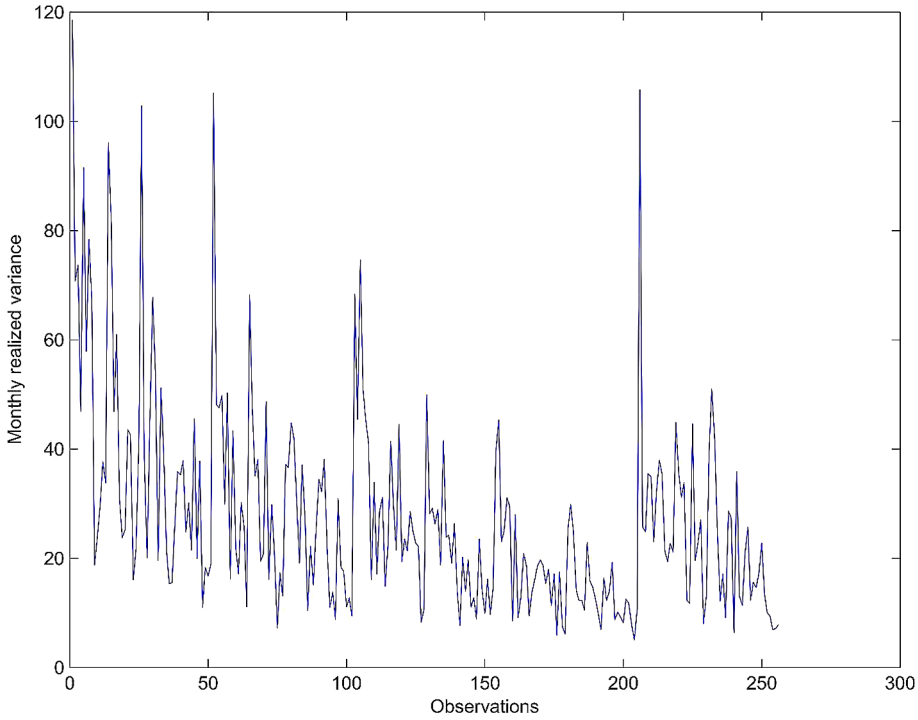

Fig. A8. Monthly realized variance using a binominal multiplicative cascade with $p = 0.55$. This Figure plots the first time-series vector for the simulated monthly asset variances using a multiplicative cascade with $p = 0.55$.

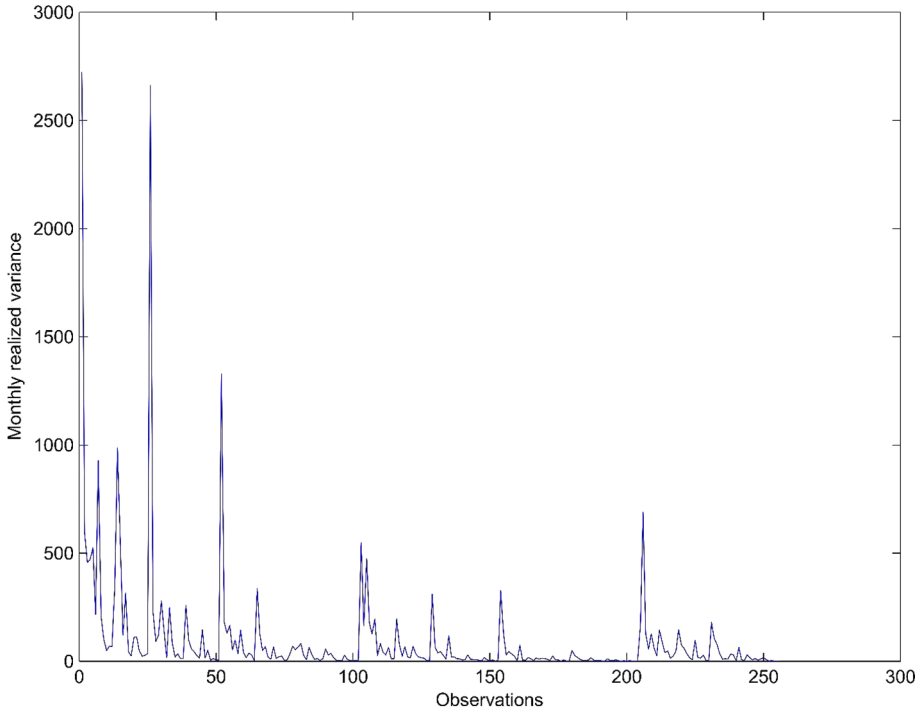

Fig. A9. Monthly realized variance using a binominal multiplicative cascade with $p = 0.65$. This Figure plots the first time-series vector for the simulated monthly asset variances using a multiplicative cascade with $p = 0.65$.

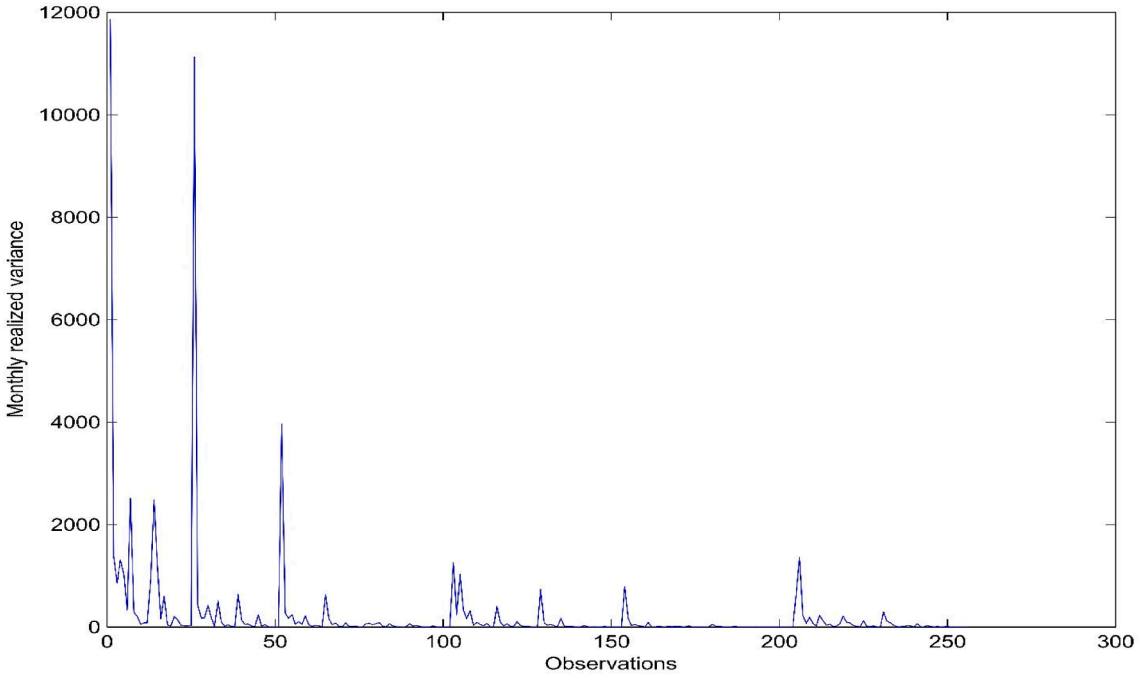

Fig. A10. Monthly realized variance using a binominal multiplicative cascade with $p = 0.70$. This Figure plots the first time-series vector for the simulated monthly asset variances using a multiplicative cascade with $p = 0.70$.

$$\ln\left(\frac{R}{S}\right)_k = \ln(C) + H\ln(k) + u$$

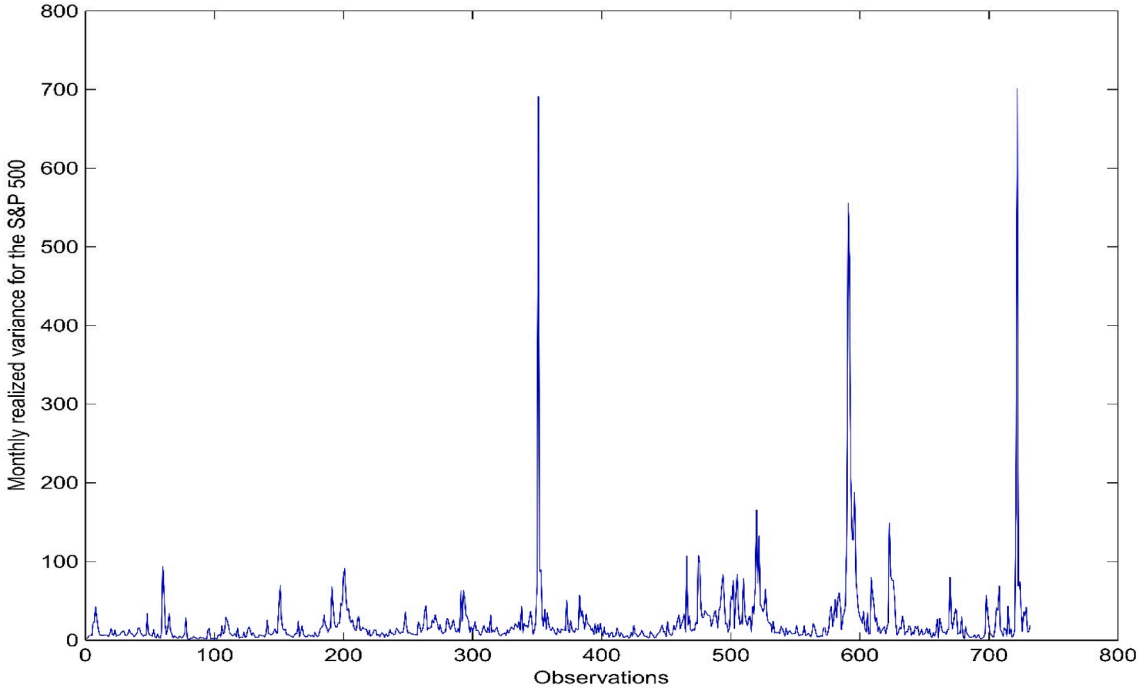

Fig. A11. Monthly realized variance of the S&P 500, Daily data for the S&P 500 are retrieved covering the period from March 4, 1957, when the original S&P 500 companies were added to the index, until March 31, 2021. Realized monthly variances are computed as $\sum_{j=1}^{22} R_{j,t}^2$, where $R_{j,t}$ denotes the daily return of the S&P 500 in month t. Assuming 22 trading days per month, the realized monthly variances are computed as nonoverlapping observations. Fig. A.1. plots the evolution of 732 realized monthly S&P variance covering the March 1957 to March 2021 period.

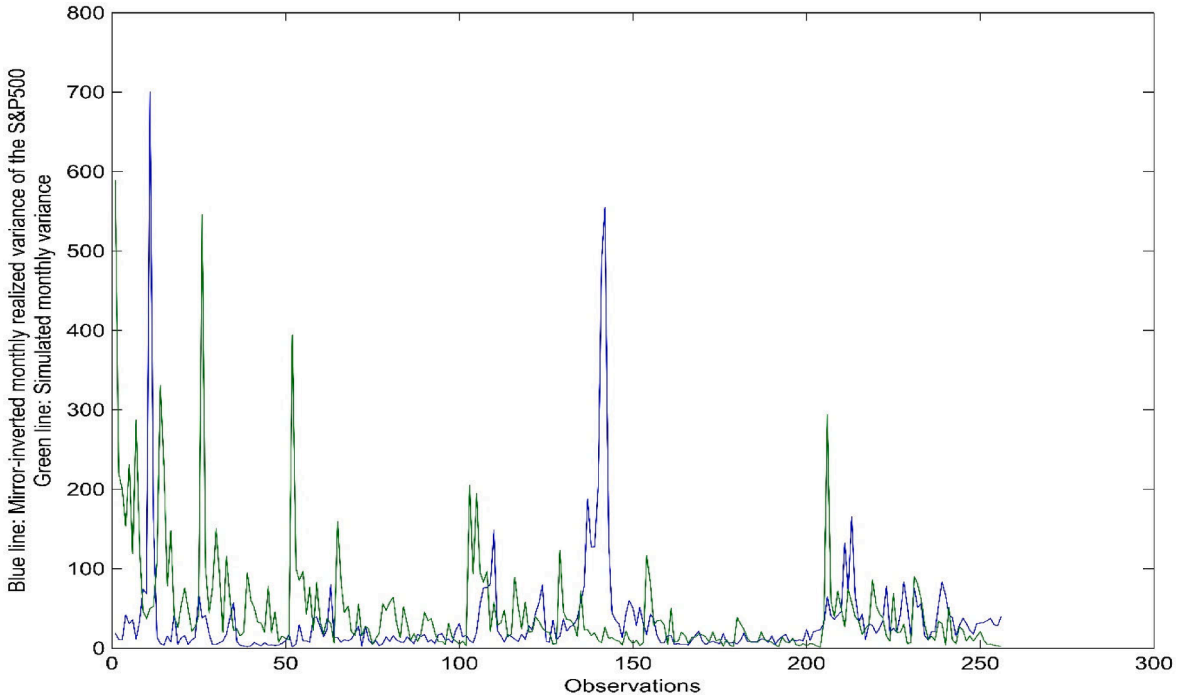

Fig. A12. Comparison between realized variance of the S&P 500 and simulated realized variance, The blue graph in this Figure shows the mirror-inverted last 256 observations of the realized monthly S&P variance from Fig. A.11, whereas the green graph shows the evolution of the simulated monthly realized variance using a multiplicative cascade with $p = 0.60$ as shown in Fig. A.7. (For interpretation of the references to colour in this figure legend, the reader is referred to the web version of this article.)

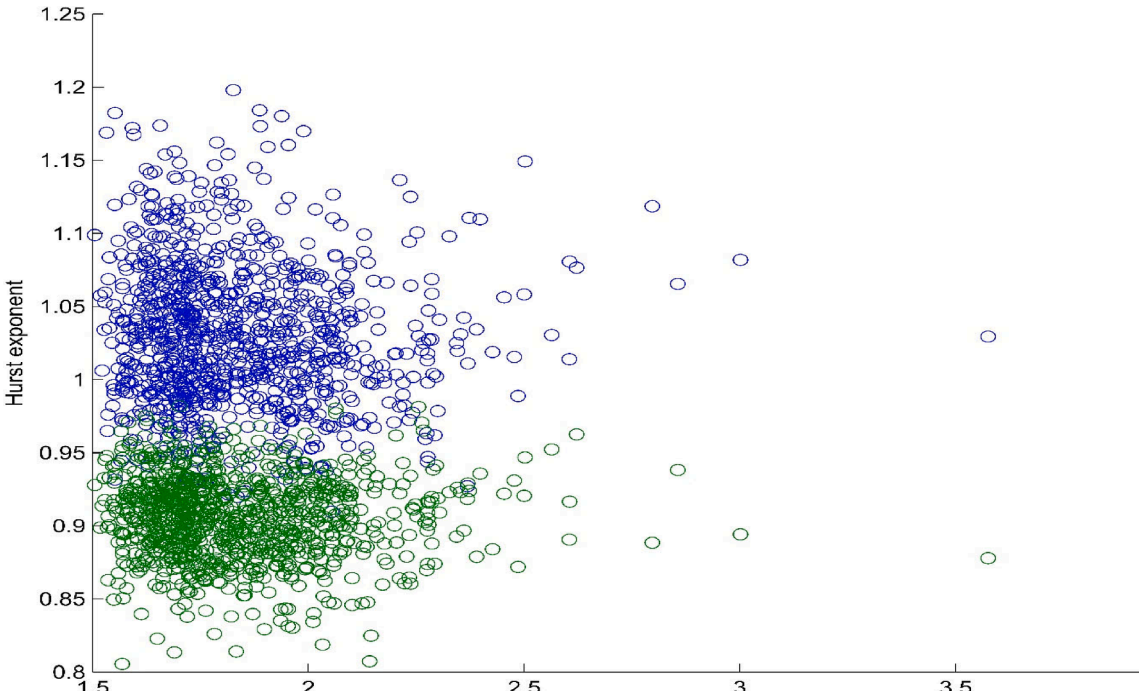

Fig. A13. Clusters of Power law exponents and Hurst exponents depending on sample lengths. This Figure plots the estimated power-law exponents against the corresponding estimated Hurst exponents for the multifractal model derived from a binominal multiplicative cascade with $p = 0.70$. Whereas the estimates for the Hurst exponents illustrated by the green cluster incorporate 1024 simulated sample observations, the estimates for the Hurst exponents illustrated by the blue cluster incorporate only 256 simulated sample observations. For both clusters, the estimated power-law exponents are based on the model incorporating all simulated sample observations (viz., 1024 observations). (For interpretation of the references to colour in this figure legend, the reader is referred to the web version of this article.)

where u $IID(0, \sigma_u)$. Hence, the estimated Hurst exponent $\widehat{H}$ is obtained via log–log regression. The rationale for choosing DFA as opposed to R/S analysis is that research has shown that R/S analysis is subject to some bias. For instance, Bassingthwaighte and Raymond (1994) document that R/S tends to give biased estimates of the Hurst exponent, too low for $H > 0.72$, and too high for $H < 0.72$. On the other hand, a more recent study of Bryce and Sprague (2012) highlights that even though DFA has become the preferred option for estimating the Hurst exponent, it introduces (*i*) uncontrolled bias, (*ii*) is computationally more expensive than the R/S statistic, and (*iii*) cannot provide generic or useful protection against nonstationaries.

Hence, to evaluate the association between DFA and R/S analysis, we use weekly data and estimate the Hurst exponents using R/S analysis and examine the correlation between Hurst exponents derived from DFA and R/S analysis. The scatter plot shown in Fig. A.14 in the appendix shows the estimated Hurst exponents derived from R/S analysis against the corresponding estimated Hurst exponents derived from detrended fluctuation analysis in four different clouds. The estimates are based on weekly data (e.g., 1024 observations). The turquoise, red, green, and blue clusters of estimated Hurst exponent clouds correspond to the multifractal models derived from binominal multiplicative cascades with $p = 0.70$, $p = 0.65$, $p = 0.60$, and $p = 0.55$, respectively. Strikingly, the correlation between the estimated Hurst exponents decrease as we move from low level of time deformation (viz., $p = 0.55$) to a high level of time deformation (viz., $p = 0.70$). Specifically, the estimated correlations for $p = 0.55$, $p = 0.60$, $p = 0.65$, and $p = 0.70$ are 0.8113, 0.4606, 0.2393, and 0.0925. The strong correlation between the estimated Hurst exponents derived from DFA and R/S analysis for the multifractal model derived from a multiplicative cascade with $p = 0.55$ is manifested in a linear trend visualized by the blue cloud in Fig. A.14. The more the range for estimated Hurst exponents departs from $\approx$0.80 the less the estimated Hurst exponents retrieved from applying those two methodologies are correlated which, in turn, supports the study of Bassingthwaighte and Raymond (1994). Other methodologies to estimate the persistence of some data have been proposed in the literature. For instance, Alessio, Carbone, Castelli, and Frappietro (2002) propose the detrending moving average analysis (DMA) to measure long-term dependency structures of some data. While the current research followed earlier studies in using DFA, future studies are encouraged to evaluate other metrics to measure the persistence.

6. Conclusion

This study extends the literature on multifractal models in finance for modeling realized asset market variances. In doing so, weekly and monthly frequencies of realized variance are considered. The benchmark model used in this study employs binominal bending with $p = 0.60$ and $(1 - p) = 0.40$ to compute the multifractal cascade. This study also explores the impact of both more moderate and

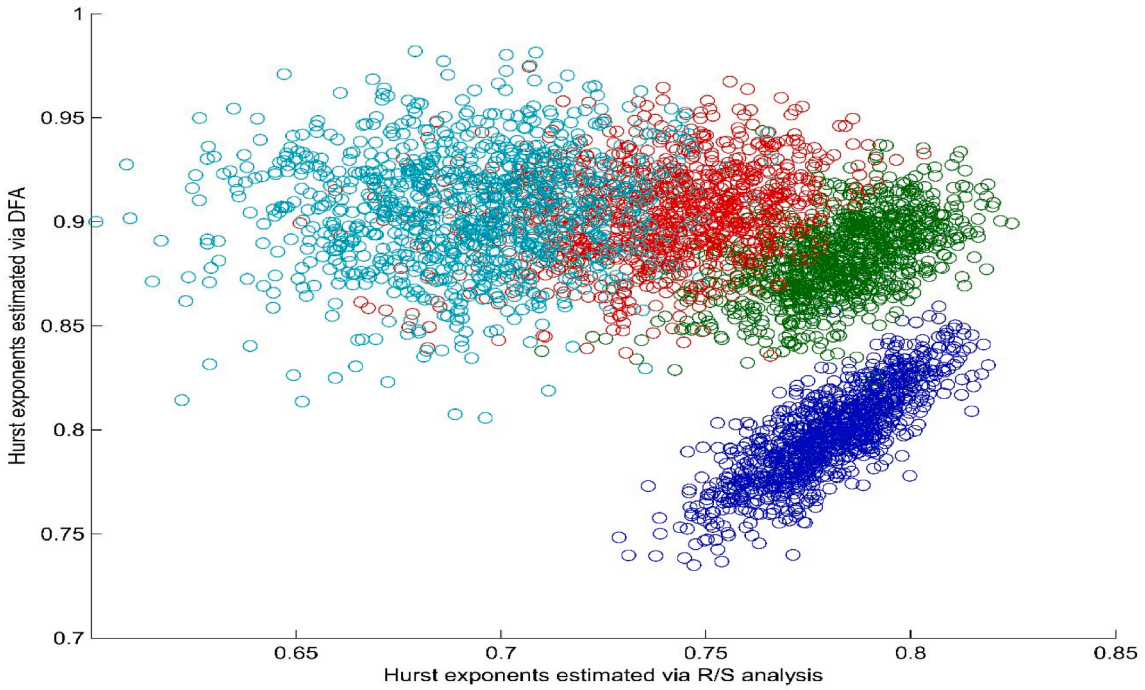

Fig. A14. Hurst exponents derived from detrended fluctuation analysis and rescaled/range analysis. This Figure plots the estimated Hurst exponents derived from rescaled/range analysis (R/S analysis) against the corresponding estimated Hurst exponents derived from detrended fluctuation analysis (DFA). The estimates are based on weekly data (1024 observations). The turquoise, red, green, and blue clusters of estimated Hurst exponent clouds correspond to the multifractal models derived from binominal multiplicative cascades with $p = 0.70$, $p = 0.65$, $p = 0.60$, and $p = 0.55$, respectively. (For interpretation of the references to colour in this figure legend, the reader is referred to the web version of this article.)

Table A1
Monthly realized asset market variances.

Asset market	MAX	MIN	VAR	α	z_{min}	%#PL	*p*-value (GoF)	Hurst (Std.Dev)	MAX time units in PL
GBP/USD	76.1442	0.6302	58.7064	3.5802	6.7974	25.00%	0.1810	0.8227 (0.0447)	5
Bitcoin	2189.5770	7.3561	99079.2000	3.3878	443.1134	24.21%	0.2350	0.9467 (0.0435)	7
Crude oil	932.9301	12.1197	21376.1900	3.0756	144.6281	26.56%	0.7510	1.0935 (0.0548)	5
S&P 500	664.5742	1.2036	3629.0380	2.7229	28.0938	20.31%	0.9550	1.2946 (0.0679)	5

We download daily data on the GBP/USD exchange rate, Bitcoin, crude oil, and the S&P 500. All data series end on the same day—April 19, 2022. Retrieving 2561 daily observations, the starting dates for the GBP/USD exchange rate, Bitcoin, crude oil, and the S&P 500 are April 17, 2015, June 27, 2012, February 17, 2012, and February 15, 2012, respectively. Computing the daily returns from price data for each data set gives us 2560 daily returns, and using the sum of 20 consecutive and squared daily observations provides us with 128 monthly realized-variance observations. This table reports the same statistical metrics as for the simulated models.

more extreme time deformations as opposed to the benchmark model. The models are mainly evaluated with respect to their tail characteristics and dependency structures as measured by their power-law exponent and Hurst exponent, respectively. The benchmark model generates asset variances exhibiting, on average, a power-law exponent and Hurst exponent of $\overline{\widehat{\alpha}} = 2.6112$ and $\overline{\widehat{H}} = 0.8827$, respectively. Moreover, 90% of the generated power-law exponents and Hurst exponents are between $\widehat{\alpha} = 2.0965$ and $\widehat{\alpha} = 3.2911$ and $\widehat{H} = 0.8503$ and $\widehat{H} = 0.9142$, respectively. Given that according to our simulation experiment $E[\alpha] = 2.6112$, an interesting implication of the benchmark model is that the variance of variance is undefined as $E[\alpha] < 3$, which means that we are not in an environment allowing us to work with the variance because we do not observe the true value in finite samples; even if an empirically observed realized variance exhibits $\widehat{\alpha} \leq 3.2911$, one cannot rule out that the variance of variance does not exist.

Testing realized weekly variances for the GBP/USD exchange rate and Bitcoin shows that the benchmark model is capable of explaining their properties as measured by those two key metrics. Testing the benchmark model based on monthly data supports this evidence. On the other hand, testing realized weekly variances for crude oil and the S&P 500 shows that the underlying multifractal model is required to incorporate more extreme bending of time manifested in a common multiplicative cascade with $p = 0.70$. Our

study suggests that some realized variances of otherwise unrelated asset markets are indeed driven by the same underlying "driving force," which is manifested in multifractal-behavior driven by a common multiplicative cascade. The question arises what is the underlying mechanism that could explain these findings? First, Grobys et al. (2018) point out that investors in foreign exchange rate markets are relatively sophisticated and face no short-selling constraints. Moreover, the authors highlight that foreign exchange rate markets are more liquid than equity markets and feature large transaction volumes with relatively low transaction costs. While foreign exchange rate markets certainly form one extreme in the spectrum of asset markets market participants (viz., highly sophisticated market participants), Bitcoin – as a representative for the market for cryptocurrencies – might form the other extreme in the spectrum of asset markets participants: Specifically, recent research shows that the market for cryptocurrencies is driven to a large extent by retail investors engaging in speculation (Grobys and Junttila, 2021), or criminals engaging in money laundry (Foley et al., 2019) which are here termed less sophisticated market participants. The uncertainty in these two distinct asset markets measured in terms of their realized variances exhibits, however, the *same* fractal-behavior manifested in power-law exponents and Hurst exponents produced by the same multifractal model derived from a multiplicative cascade with $p = 0.60$.

On the other hand, in commodity markets or equity markets – which form the middle section in the spectrum of asset market participants – time is more concentrated as both highly sophisticated and less sophisticated market participants interact with each other. Heterogenous market participants' interactions may, in turn, result in feedback loops manifested in a higher level of discontinuity and a higher level of persistence. Similarly, the uncertainty in these two distinct asset markets measured in terms of their realized variances exhibits the *same* fractal-behavior manifested in power-law exponents and Hurst exponents produced by the same multifractal model derived from a multiplicative cascade with $p = 0.70$ as opposed to $p = 0.60$. Future research is, however, encouraged to elaborate more in this issue.

CRediT authorship contribution statement

Klaus Grobys: Conceptualization, Data curation, Formal analysis, Funding acquisition, Investigation, Methodology, Project administration, Resources, Software, Supervision, Validation, Visualization, Writing – original draft, Writing – review & editing.

Declaration of Competing Interest

The authors declare that they have no known competing financial interests or personal relationships that could have appeared to influence the work reported in this paper.

Data availability

Data was simulated and the empirical data is available for free in the internet.

Acknowledgement

This research article was presented at the 2022 Finance Research Seminar organized from the Chair of Monetary Economics and International Finance, Christian-Albrechts-University (CAU) of Kiel. The author is thankful for having received valuable comments from Thomas Lux, Cristina Sattarhoff, and Lutz Honvehlmann. The author is thankful for having received valuable comments from two anonymous reviewers.

Appendix A

Figs. A1–A14, Table A1

References

Alessio, E., Carbone, A., Castelli, G., Frappietro, V., 2002. Second-order moving average and scaling of stochastic time series. Eur. Phys. J. B 27, 197–200.
Andersen, T., Bollerslev, T., Diebold, F., Labys, P., 2001. The distribution of realized stock return volatility. J. Financ. Economet. 63, 43–76.
Bacry, E., Kozhemyak, A., Muzy, J.-F., 2008. Continuous cascade model for asset returns. J. Econ. Dyn. Control 32, 156–199.
Bassingthwaighte, J.B., Raymond, G.M., 1994. Evaluating rescaled range analysis for time series. Ann. Biomed. Eng. 22, 432–444.
Bollerslev, T., 1986. Generalized autoregressive conditional heteroskedasticity. J. Econ. 31 (3), 307–327.
Bryce, R.M., Sprague, K.B., 2012. Revisiting detrended fluctuation analysis. Sci. Rep. 2, 315.
Cai, J., 1994. A Markov model of switching-regime ARCH. J. Bus. 12, 309–316.
Calvet, L., Fisher, A., 2001. Forecasting multifractal volatility. J. Econ. 105, 27–58.
Calvet, L., Fisher, A., 2002. Multifractality in asset returns: Theory and evidence. Rev. Econ. Stat. 83, 381–406.
Calvet, L., Fisher, A., 2004. Regime-switching and the estimation of multifractal processes. J. Financ. Economet. 2, 44–83.
Calvet, L., Fisher, A., Wu, L., 2018. Staying on Top of the Curve: A Cascade Model of Term Structure Dynamics. J. Financ. Quant. Anal. 53, 937–963.
Chalissery, N., Anagreh, S., Nishad T., M., Tabash, M.I., 2022. Mapping the Trend, Application and Forecasting Performance of Asymmetric GARCH Models: A Review Based on Bibliometric Analysis, *J. Risk Finan. Manage.* 15, 406.
Chu, C.-S.-J., 1995. Detecting parameter shift in GARCH models. Econ. Rev. 14 (2), 241–266.
Clauset, A., Shalizi, C.R., Newman, M.E.J., 2009. Power law distributions in empirical data. SIAM Rev. 51, 661–703.

Drost, F.C., Werker, B.J.M., 1996. Closing the GARCH gap: Continuous time GARCH modeling. J. Econ. 74, 31–57.
Engle, R.F., 1982. Autoregressive conditional heteroscedasticity with estimates of the variance of United Kingdom inflation. Econometrica 50, 987–1007.
Engle, R.F., Bollerslev, T., 1986. Modelling the persistence of conditional variances. Econ. Rev. 5, 1–50.
Fama, E.F., 1963. Mandelbrot and the stable Paretian hypothesis. J. Bus. 36, 420–429.
Foley, S., Karlsen, J.R., Putniņš, T.J., 2019. Sex, Drugs, and Bitcoin: How Much Illegal Activity Is Financed Through Cryptocurrencies? Rev. Financ. Stud. 32 (5), 1798–1853.
Gabaix, X., 2009. Power laws in economics and finance. Ann. Rev. Econ. Finance 1, 255–294.
Glosten, L.R., Jagannathan, R., Runkle, D.E., 1993. On the relation between the expected value and the volatility of the nominal excess return on stocks. J. Financ. 48 (5), 1779–1801.
Gopikrishnan, P., Plerou, V., Amaral, L., Meyer, M., Stanley, H.E., 1999. Scaling of the distribution of fluctuations of financial market indices. Phys. Rev. E 60, 5305–5316.
Grobys, K., 2021. What do we know about the second moment of financial markets? Int. Rev. Financ. Anal. 78, 101891.
Grobys, K., 2023. Correlation versus co-fractality: evidence from foreign exchange rate variances. Int. Rev. Financ. Anal. 86, 102531.
Grobys, K., J. Kolari, 2022. Why Benoit Mandelbrot was right: Fractality and realized foreign exchange rate variances, working paper, available at: https://www.researchgate.net/publication/358901267_Why_Benoit_Mandelbrot_was_right_Fractality_and_realized_foreign_exchange_rate_variances.
Grobys, K., Junttila, J.-P., 2021. Speculation and Lottery-Like Demand in Cryptocurrency Markets. J. Int. Financ. Markets Inst. Money 71, 101289.
Grobys, K., Ruotsalainen, J., Äijö, J., 2018. Risk-managed industry momentum and momentum crashes. Quantitative Finance 18, 1715–1733.
Grobys, K., Heinonen, J.-P., Kolari, J., 2018. Return Dispersion Risk in FX and Global Equity Markets: Does It Explain Currency Momentum? Int. Rev. Financial Analysis 56, 264–280.
Grobys, K., Vähämaa, S., 2020. Another Look at Value and Momentum: Volatility Spillovers. Rev. Quant. Finan. Acc. 55, 1459–1479.
Grobys, K., Kolari, J.W., Junttila, J.-P., Sapkota, N., 2021. On the stability of stablecoins. J. Empir. Financ. 64, 207–223.
Hsiao, C., Li, Q., 2001. A Consistent Test for Conditional Heteroskedasticity in Time-Series Regression Models. Economet. Theor. 17, 188–221.
Jansen, D., de Vries, C., 1991. On the frequency of large stock returns: Putting booms and busts into perspective. Rev. Econ. Stat. 73, 18–24.
Lundbergh, S., Teräsvirta, T., 2002. Evaluating GARCH models. J. Econ. 110 (2), 417–435.
Lux, T., 1996. The stable Paretian hypothesis and the frequency of large returns: An examination of major German stocks. Appl. Financ. Econ. 5, 463–475.
Lux, T., Alfarano, S., 2016. Financial power laws: Empirical evidence, models, and mechanisms. Chaos Solitons Fractals 88, 3–18.
Mandelbrot, B., 1963a. New methods in statistical economics. J. Polit. Econ. 71, 421–440.
Mandelbrot, B.B., 1963b. The variation of certain speculative prices. J. Bus. 36, 394–419.
Mandelbrot, B.B., 1969. Long-run linearity, locally Gaussian process, H-Spectra and infinite variances. Int. Econ. Rev. 10, 82–111.
Mandelbrot, B.B., 1971. When Can Price be Arbitraged Efficiently? A Limit to the Validity of the Random Walk and Martingale Models. Rev. Econ. Stat. 53, 225.
Mandelbrot, B.B., 1972. Statistical Methodology for Nonperiodic Cycles from Covariance to R/S Analysis. Ann. Econ. Soc. Meas. 1, 259–290.
Mandelbrot, B.B., 1997a. Fractals and Scaling in Finance: Discontinuity, Concentration, Risk. Springer Verlag, New York.
Mandelbrot, B., 2008. The (Mis)Behavior of Markets. Profile Books.
Mandelbrot, B., Fisher, A., Calvet, L., 1997b. A Multifractal Model of Asset Returns, Cowles Foundation Discussion Paper No 1164. Yale University, New Haven, CT, USA, pp. 1–33.
Mandelbrot, B.B., Wallis, J.R., 1969. Robustness of the rescaled range R/S in the measurement of noncyclic long run Statistical dependence. Water Resour. Res. 5, 967–988.
Mantegna, R., Stanley, H.E., 1995. Scaling behavior in the dynamics of an economic index. Nature 376, 46–49.
Moreira, A., Muir, T., 2017. Volatility-Managed Portfolios. J. Financ. 72, 1611–1643.
Muzy, J.-F., Bacry, E., 2002. Multifractal stationary random measures and multifractal random walks with log infinitely divisible scaling laws. Phys. Rev. E 66, 056121.
Nelson, D.B., 1990. ARCH models as diffusion approximations. J. Econ. 45, 7–38.
Nelson, D.B., 1991. Conditional heteroskedasticity in asset returns: a new approach. Econometrica 59, 347–370.
Pareto, V., 1897. The new theories of economics. J. Polit. Econ. 5, 485–502.
Peng, C.K., Buldyrev, S.V., Havlin, S., Simons, M., Stanley, H.E., Goldberger, A.L., 1994. Mosaic organization of DNA nucleotides. Phys. Rev. E 49 (2), 1685–1689.
Rabemananjara, R., Zakoian, J., 1993. Threshold ARCH models and asymmetries in volatility. J. Appl. Economet. 8, 31–49.
Segnon M., Lux T., 2013. Multifractal models in finance: their origin, properties, and applications. Kiel Working Paper No. 1860, Kiel Institute for the World Economy.
Sornette, D., 2017. Why Stock Markets Crash: Critical Events in Complex Financial Systems. Princeton University Press, New Jersey.
Sun, P., Zhou, C., 2014. Diagnosing the distribution of GARCH innovations. J. Empir. Financ. 29, 287–303.
Wang, J., Yang, M., 2009. Asymmetric volatility in the foreign exchange markets. J. Int. Finan. Markets. Inst. Money 19, 597–615.
West, G., 2017. Scale: Universal Laws of Life, Growth, and Death in Organisms, Cities, and Companies. Penguin Books, New York.
White, E., Enquist, B., Green, J.L., 2008. On estimating the exponent of power law frequency distributions. Ecology 89, 905–912.